National Library of Canada
Bibliothèque nationale du Canada

Canadian Theses Service
Services des thèses canadiennes

Ottawa, Canada
K1A 0N4

# CANADIAN THESES

# THÈSES CANADIENNES

## NOTICE

The quality of this microfiche is heavily dependent upon the quality of the original thesis submitted for microfilming. Every effort has been made to ensure the highest quality of reproduction possible.

If pages are missing, contact the university which granted the degree.

Some pages may have indistinct print especially if the original pages were typed with a poor typewriter ribbon or if the university sent us an inferior photocopy.

Previously copyrighted materials (journal articles, published tests, etc.) are not filmed.

Reproduction in full or in part of this film is governed by the Canadian Copyright Act, R.S.C. 1970, c. C-30. Please read the authorization forms which accompany this thesis.

## AVIS

La qualité de cette microfiche dépend grandement de la qualité de la thèse soumise au microfilmage. Nous avons tout fait pour assurer une qualité supérieure de reproduction.

S'il manque des pages, veuillez communiquer avec l'université qui a conféré le grade.

La qualité d'impression de certaines pages peut laisser à désirer, surtout si les pages originales ont été dactylographiées à l'aide d'un ruban usé ou si l'université nous a fait parvenir une photocopie de qualité inférieure.

Les documents qui font déjà l'objet d'un droit d'auteur (articles de revue, examens publiés, etc.) ne sont pas microfilmés.

La reproduction, même partielle, de ce microfilm est soumise à la Loi canadienne sur le droit d'auteur, SRC 1970, c. C-30. Veuillez prendre connaissance des formules d'autorisation qui accompagnent cette thèse.

THIS DISSERTATION
HAS BEEN MICROFILMED
EXACTLY AS RECEIVED

LA THÈSE A ÉTÉ
MICROFILMÉE TELLE QUE
NOUS L'AVONS REÇUE

NL 339 (r. 86/01)

Canada

National Library of Canada / Bibliothèque nationale du Canada

Ottawa, Canada
K1A 0N4

1/5

TC –

ISBN 0-315-23312-5

CANADIAN THESES ON MICROFICHE SERVICE – SERVICE DES THÈSES CANADIENNES SUR MICROFICHE

## PERMISION TO MICROFILM – AUTORISATION DE MICROFILMER

• Please print or type – Écrire en lettres moulées ou dactylographier

### AUTHOR – AUTEUR

Full Name of Author – Nom complet de l'auteur

MARGARET ROSARII SMART

| Date of Birth – Date de naissance | Canadian Citizen – Citoyen canadien |
|---|---|
| FEB 21, 1959 | ☒ Yes Oui ☐ No Non |
| **Country of Birth – Lieu de naissance** | **Permanent Address – Résidence fixe** |
| CANADA | 6215 LACOMBE WAY SW<br>CALGARY, AB<br>T3E 5T4 |

### THESIS – THÈSE

Title of Thesis – Titre de la thèse

SIMULATION AND CONTROL OF A POLYETHYLENE REACTOR

| Degree for which thesis was presented<br>Grade pour lequel cette thèse fut présentée | Year this degree conferred<br>Année d'obtention de ce grade |
|---|---|
| M. Sc. | 1985 |
| **University – Université** | **Name of Supervisor – Nom du directeur de thèse** |
| UNIVERSITY OF ALBERTA | D.G. FISHER / D.T. LYNCH |

### AUTHORIZATION – AUTORISATION

Permission is hereby granted to the NATIONAL LIBRARY OF CANADA to **microfilm** this thesis and to **lend** or **sell copies of the film.**

The author reserves other publication rights, and neither the thesis nor extensive extracts from it may be printed or otherwise reproduced without the author's written permission.

L'autorisation est, par la présente, accordée à la BIBLIOTHÈQUE NATIONALE DU CANADA de **microfilmer** cette thèse et de **prêter** ou de **vendre des exemplaires du film.**

L'auteur se réserve les autres droits de publication, ni la thèse ni de longs extraits de celle-ci ne doivent être imprimés ou autrement reproduits sans l'autorisation écrite de l'auteur.

ATTACH FORM TO THESIS – VEUILLEZ JOINDRE CE FORMULAIRE À LA THÈSE

| Signature | Date |
|---|---|
| M Smart | OCT 12, 1985 |

NL-91 (r. 84/03)

Canada

THE UNIVERSITY OF ALBERTA

# SIMULATION AND CONTROL OF A POLYETHYLENE REACTOR

by

MARGARET ROSARII SMART

(C)

A THESIS

SUBMITTED TO THE FACULTY OF GRADUATE STUDIES AND RESEARCH

IN PARTIAL FULFILMENT OF THE REQUIREMENTS FOR THE DEGREE

OF MASTER OF SCIENCE

IN

PROCESS CONTROL

DEPARTMENT OF CHEMICAL ENGINEERING

EDMONTON, ALBERTA

FALL 1985

THE UNIVERSITY OF ALBERTA

RELEASE FORM

NAME OF AUTHOR: Margaret Rosarii Smart

TITLE OF THESIS: SIMULATION AND CONTROL OF A POLYETHYLENE REACTOR

DEGREE FOR WHICH THESIS WAS PRESENTED: M.Sc.

YEAR THIS DEGREE GRANTED: Fall 1985

Permission is hereby granted to THE UNIVERSITY OF ALBERTA LIBRARY to reproduce single copies of this thesis and to lend or sell such copies for private, scholarly or scientific research purposes only.

The author reserves other publication rights, and neither the thesis nor extensive extracts from it may be printed or otherwise reproduced without the author's written permission.

(Signed) M Smart

PERMANENT ADDRESS:

6215 Lacombe Way S.W.
Calgary, Alberta
Canada
T3E 5T4

DATED: Oct 7, 1985

THE UNIVERSITY OF ALBERTA

FACULTY OF GRADUATE STUDIES AND RESEARCH

The undersigned certify that they have read, and recommend to the Faculty of Graduate Studies and Research for acceptance, a thesis entitled "SIMULATION AND CONTROL OF A POLYETHYLENE REACTOR" submitted by MARGARET ROSARII SMART in partial fulfilment of the requirements for the degree of Master of Science in Process Control.

(Supervisor)

(Supervisor)

Date: October 1, 1985

## ABSTRACT

A simulation and control optimization of a steady state, high pressure, tubular polyethylene reactor is presented in this thesis. A kinetic model is developed based on published models in the literature.

Simulation studies for constant jacket temperature and isothermal reactors are presented. Molecular weights and conversion decrease with increases in jacket temperature. Conversion increases and molecular weights decrease with increases in inlet initiator concentration. Optimal operating conditions, determined by desired product qualities, are investigated. The sensitivities of product qualities with respect to control variables and kinetic parameters are examined. The product properties are very sensitive to the values of the kinetic parameters.

Reactor control schemes to improve product conversion are presented. Multiple injections of initiator are used to increase conversion and polydispersity. The relationship between reactor temperature profiles and molecular weights is investigated using temperature moments. Changes in the temperature moments indicate changes in the product molecular weights. Online control using these calculated temperature moments is suggested.

TABLE OF CONTENTS


| | | Page |
|---|---|---|
| 1. | INTRODUCTION | 1 |
| | 1.1 Background on Polyethylene | 1 |
| | 1.2 Objectives | 3 |
| 2. | POLYETHYLENE REACTOR MODEL DEVELOPMENT | 6 |
| | 2.1 Literature Survey | 6 |
| | 2.2 Description of the Reaction Mechanism | 11 |
| | 2.3 Derivation of Kinetic Equations | 14 |
| | 2.4 Parameter Estimates | 20 |
| 3. | MODEL EVALUATION | 31 |
| | 3.1 Base Case Simulation | 31 |
| | 3.2 Effect of Jacket Temperature | 37 |
| | 3.3 Effect of Initiator Concentration | 45 |
| | 3.4 Effect of Initial Temperature | 48 |
| | 3.5 Isothermal Reaction Zone Reactor | 53 |
| | 3.6 Model Features Observed in the Simulations | 68 |
| 4. | SENSITIVITY ANALYSIS | 71 |
| | 4.1 Mathematical Sensitivity Coefficients | 71 |
| | 4.1.1 Jacket Temperature Sensitivities | 72 |
| | 4.1.2 Inlet Initiator Concentration Sensitivities | 76 |
| | 4.2 Numerical Sensitivities | 81 |
| | 4.2.1 Jacket Temperature Sensitivities | 82 |
| | 4.2.2 Inlet Initiator Concentration Sensitivities | 84 |
| | 4.3 Choice of Control Variable Based on Sensitivity Analysis | 86 |
| | 4.4 Sensitivity of Model Outputs to Rate Constants | 87 |

Table of Contents (continued)


| | | Page |
|---|---|---|
| 5. | OPTIMIZATION STUDIES | 91 |
| | 5.1 Definition of the Optimization Problem | 91 |
| | 5.2 Jacket Temperature as the Control Variable | 94 |
| | 5.3 Inlet Initiator Concentration as the Control Variable | 98 |
| | 5.4 Combination of Jacket Temperature and Inlet Initiator Concentration as the Control Variables | 101 |
| | 5.5 Multiple Jacket Temperature Zones as the Control Variable | 104 |
| | 5.5.1 Zone Temperatures | 104 |
| | 5.5.2 Zone Lengths | 106 |
| | 5.6 Multiple Initiator Injection Points as the Control Variables | 109 |
| | 5.6.1 Initiator Concentrations | 109 |
| | 5.6.2 Injection Point Locations | 114 |
| | 5.7 Multiple Initiator Types as the Control Variables | 117 |
| | 5.8 Significance of Optimization Results | 123 |
| 6. | REACTOR CONTROL TO IMPROVE CONVERSION | 125 |
| | 6.1 Overall Control Objective | 125 |
| | 6.2 Conversion Improvement Schemes | 127 |
| | 6.3 Recommendations for Reactor Control to Improve Conversion | 141 |
| 7. | RELATIONSHIPS BETWEEN TEMPERATURE PROFILES AND MOLECULAR WEIGHTS | 143 |
| | 7.1 Definition of Moments of a Temperature Profile | 143 |
| | 7.2 Effect of Jacket Temperature on Temperature Moments | 148 |

Table of Contents (continued)


| | Page |
|---|---|
| 7.3 Effect of Inlet Initiator Concentration on Moments | 148 |
| 7.4 Implications of Temperature Profile Moments | 154 |
| 8. CONCLUSIONS | 155 |
| REFERENCES | 158 |
| APPENDIX A: Derivation of Kinetic Equations | 160 |
| APPENDIX B: Derivation of Sensitivity Equations | 169 |
| APPENDIX C: Computer Program | 177 |

## LIST OF TABLES


| Table | Description | Page |
|---|---|---|
| 2.1 | Model Features | 15 |
| 2.2 | Initiator Rate Constants | 22 |
| 2.3 | Rate Constants | 23 |
| 2.4 | Reactor Specifications | 27 |
| 2.5 | Thermodynamic Properties | 29 |
| 3.1 | Base Case Conditions | 32 |
| 3.2 | Effect of Jacket Temperature | 38 |
| 3.3 | Comparison of Multi-Zone and Base Case Reactors | 44 |
| 3.4 | Effect of Inlet Initiator Concentration | 46 |
| 3.5 | Effect of Initial Temperature | 51 |
| 3.6 | Comparison of Base Case and Isothermal Reaction Zone Reactors | 56 |
| 3.7 | Effect of Isothermal Temperature | 60 |
| 3.8 | Effect of Initiator Concentration in Isothermal Reactor | 63 |
| 3.9 | Effect of Initial Temperature in Isothermal Reactor | 66 |
| 4.1 | Jacket Temperature Sensitivities | 83 |
| 4.2 | Inlet Initiator Concentration Sensitivities | 85 |
| 4.3 | Rate Constant Sensitivities | 89 |
| 5.1 | Optimization Results - Jacket Temperature as Control Variable | 95 |

List of Tables (cont)


| Table | Description | Page |
|---|---|---|
| 5.2 | Optimization Results - Inlet Initiator Concentration as Control Variable | 99 |
| 5.3 | Optimization Results - Jacket Temperature and Inlet Initiator Concentration as Control Variables | 103 |
| 5.4 | Optimization Results - Jacket Zone Temperatures as Control Variables | 105 |
| 5.5 | Optimization Results - Jacket Zone Lengths as Control Variables | 108 |
| 5.6 | Optimization Results - Multiple Initiator Injection Concentrations as Control Variables | 111 |
| 5.7 | Comparison of Constant Jacket Temperature Reactors with One and Two Injection Points | 112 |
| 5.8 | Optimization Results - Location of Initiator Injection Point as Control Variable | 115 |
| 5.9 | Optimization Results - Multiple Initiator Type Concentrations as Control Variables | 120 |
| 5.10 | Comparison of Constant Jacket Temperature Reactor Outputs with Single and Multiple Initiators | 122 |
| 6.1 | Features of the Preliminary Conversion Improvement Schemes | 128 |
| 6.2 | Comparison of the Preliminary Conversion Improvement Schemes | 130 |
| 6.3 | Comparison of Conversion Improvement and Base Type Reactors | 133 |
| 6.4 | Effect of Initiator Injection Concentration on Conversion Improvement | 136 |
| 6.5 | Effect of Injection Spacing on Conversion Improvement | 137 |

List of Tables (cont)


| Table | Description | Page |
|---|---|---|
| 6.6 | Effect of Jacket Temperature on Conversion Improvement | 138 |
| 6.7 | Effect of Multiple Heating and Cooling Zones | 140 |
| 7.1 | Effect of Jacket Temperature on Moments | 149 |
| 7.2 | Effect of Inlet Initiator Concentration on Moments | 152 |

## LIST OF FIGURES


| Figure | Description | Page |
|---|---|---|
| 1.1 | Tubular High Pressure Polyethylene Reactor | 2 |
| 2.1 | Rate Constants | 24 |
| 3.1 | Reactor Profiles | 33 |
| 3.2 | Division of Reactor into Zones | 34 |
| 3.3 | Molecular Weight Profiles | 35 |
| 3.4 | Effect of Jacket Temperature | 39 |
| 3.5 | Temperature Profiles for Different Jacket Temperatures | 41 |
| 3.6 | Reactor Profiles for Multi-Zone and Base Case | 43 |
| 3.7 | Effect of Inlet Initiator Concentration | 47 |
| 3.8 | Temperature Profiles for Different Initiator Concentrations | 49 |
| 3.9 | Effect of Inlet Temperature | 52 |
| 3.10 | Temperature Profiles for Different Inlet Temperatures | 54 |
| 3.11 | Isothermal Reaction Zone Profiles | 57 |
| 3.12 | Effect of Isothermal Temperature | 61 |
| 3.13 | Effect of Inlet Initiator Concentration in Isothermal Reaction Zone Reactor | 64 |
| 3.14 | Effect of Initial Temperature in Isothermal Reactor | 67 |
| 4.1 | Conversion and Temperature Sensitivities with respect to Jacket Temperatures | 73 |
| 4.2 | Molecular Weight Sensitivities with respect to Jacket Temperature | 74 |

List of Figures (cont)


| Figure | Description | Page |
|---|---|---|
| 4.3 | Moment Sensitivities with respect to Jacket Temperature | 75 |
| 4.4 | Conversion and Temperature Sensitivities with respect to Inlet Initiator Concentration | 77 |
| 4.5 | Molecular Weight Sensitivities with respect to Inlet Initiator Concentration | 78 |
| 4.6 | Moment Sensitivities with respect to Inlet Initiator Concentration | 79 |
| 5.1 | Comparison of Reactor Profiles with One and Two Initiator Injection Points | 113 |
| 5.2 | Initiator Decomposition Rates | 118 |
| 5.3 | Comparison of Reactor Profiles with Single and Mixed Initiators | 121 |
| 6.1 | Molecular Weight and Conversion Profiles for Constant Initiator Injection | 126 |
| 6.2 | Overall Conversion Improvement Scheme | 132 |
| 6.3 | Conversion Improvement and Base Type Reactor Comparison | 134 |
| 7.1 | Definition of Temperature Moments for Base Case Reactor | 146 |
| 7.2 | Relationship Between Temperature and Molecular Weight Profiles | 147 |
| 7.3 | Effect of Jacket Temperature on Moments | 150 |
| 7.4 | Effect of Inlet Initiator Concentration Moments | 153 |

## NOMENCLATURE

| | | |
|---|---|---|
| $a_i$ | : | weighting factors in objective function |
| $C_I$ | : | initiator concentration per injection (mol/l) |
| $C_{IO}$ | : | initiator concentration at t=0 (mol/l) |
| $C_{I1}, C_{I2}$ | : | additional initiator concentration (mol/l) |
| $C_p$ | : | fluid heat capacity [cal/(g°C)] |
| D | : | reactor diameter (m) |
| E | : | activation energy (cal/mol) |
| f | : | initiator efficiency factor |
| $g_i$ | : | lower limit on constrained variable in Box's transformation |
| G(l,t) | : | zeroth moment of live radical distribution (mol/l) |
| G'(l,t) | : | first moment of live radical distribution (mol/l) |
| G"(l,t) | : | second moment of live radical distribution (mol/l) |
| $h_i$ | : | upper limit on constrained variable in Box's transformation |
| H(l,t) | : | zeroth moment of live and dead polymer distribution (mol/l) |
| H'(l,t) | : | first moment of live and dead polymer distribution (mol/l) |
| H"(l,t) | : | second moment of live and dead polymer distribution (mol/l) |
| $\Delta H_r$ | : | heat of propagation (cal/mol) |
| [I] | : | initiator concentration (mol/l) |
| J | : | objective function |
| $k_d$ | : | initiator decomposition rate constant ($s^{-1}$) |
| $k_{fp}$ | : | transfer to polymer rate constant [l/(mol.s)] |

Nomenclature (continued)

| | | |
|---|---|---|
| $k_j$ | : | general rate constant for reaction j [1/(mol.s)] |
| $k_p$ | : | propagation rate constant [1/(mol.s)] |
| $k_t$ | : | termination rate constant [1/(mol.s)] |
| | | $k_t = k_{tc} + k_{td}$ |
| $k_{tc}$ | : | termination by combination rate constant (1/(mol.s)) |
| $k_{td}$ | : | termination by disproportionation rate constant (1/(mol.s)) |
| [M] | : | monomer concentration (mol/l) |
| $M_{C_2H_4}$ | : | molecular weight of ethylene (g/mol) |
| $M_N$ | : | number average molecular weight |
| $M_{Nd}$ | : | desired number average molecular weight |
| $M_W$ | : | weight average molecular weight |
| $M_{Wd}$ | : | desired weight average molecular weight |
| $n_i$ | : | beginning point of reaction zone |
| $n_f$ | : | endpoint of reaction zone |
| N | : | number of points in reaction zone or number of constrained variables in Box's transformation |
| p | : | vector of sensitivity coefficient parameters $p = (T_J, C_{IO})$ |
| P | : | reactor pressure (atm) |
| PD: | : | polydispersity $PD = M_W/M_N$ |
| $[P_x]$ | : | concentration of dead polymer chains of length x (mol/l) |
| R | : | universal gas constant |
| $[R_o]$ | : | initiator radical concentration (mol/l) |
| $[R_o^*]$ | : | activated initiator radical concentration (mol/l) |

Nomenclature (continued)

| | | |
|---|---|---|
| $R_p$ | : | rate of propagation (mol/(l.s)) |
| $[R_x^*]$ | : | concentration of live radicals of chain lenght x (mol/l) |
| $t$ | : | reactor coordinate (s) |
| $t_f$ | : | reactor coordinate at end of reaction zone |
| $t_k$ | : | reactor coordinate at point k (s) |
| $T$ | : | reactor temperature (K) |
| $T_{AV}$ | : | average of reactor temperature profile (K) |
| $T_{ISO}$ | : | isothermal reaction zone temperature (K) |
| $T_J$ | : | jacket temperature (K) |
| $T_{J1}$, $T_{J2}$, $T_{J3}$ | : | jacket temperature in zone 1, 2, 3 (K) |
| $T_k$ | : | reactor temperature at point k (K) |
| $T_{MAX}$ | : | maximum reactor temperature (K) |
| $T_o$ | : | initial reactor temperature (K) |
| $T_{SD}$ | : | standard deviation of reactor temperature profile (K) |
| $U$ | : | overall heat transfer coefficient (cal/($m^2$ s°C)) |
| $\underset{\sim}{u}$ | : | vector of control variables |
| $x_i$ | : | control variable in Box's transformation |
| $X_I$ | : | initiator conversion |
| $X_M$ | : | monomer conversion |
| $X_{Md}$ | : | desired monomer conversion |
| $y_i$ | : | transformed control variable in Box's transformation |

Nomenclature (continued)

$\underset{\sim}{y}$ : vector of state variables
$\underset{\sim}{y} = (X_M, X_I, G, G', H, H'', T/T_o)^T$

Greek Symbols

$\rho$ : fluid density (g/l)

$\Phi_{ij}$ : sensitivity coefficient for parameter $p_j$ and output $y_i$

$\tau$ : reactor residence time (s)

$\lambda_k$ : $k^{th}$ moment of live radical distribution (mol/l)

$\mu_k$ : $k^{th}$ moment of dead polymer distribution (mol/l)

# 1. INTRODUCTION

## 1.1 Background on Polyethylene

Polyethylene was first synthesized in 1933 by E.W.M. Fawcett and R.O. Gibson of Imperial Chemical Industries, Ltd. In the 50 years since its discovery it has become a widely used polymer. Currently its main uses are for plastic films, wire coatings, plastic containers and pipes.

Polyethylenes are divided into two classes: low density and high density. Low density polyethylene (LDPE) is produced at moderate to high pressures, greater than 500 atm, in autoclave or tubular reactors. This type of polyethylene is more highly branched, less crystalline, less dense and weaker than high density polyethylene. High density polyethylene is usually synthesized at low pressures using Ziegler-Natta catalysts in batch or continuous reactors.

A typical high pressure, tubular polyethylene reactor is shown in Figure 1.1.

Figure 1.1 has been omitted because copyright permission was not available at the time of submission. The Figure showed the main process flows for a typical polyethylene reactor. The original drawing was taken from Hwu, M.C. and Foster, R.D., Chem. Eng. Prog., 78, pp. 62-68 (1982).

## 1.2 Objectives

Although polyethylene has been in production for 50 years very few simulation and control studies have been reported for polyethylene reactors, especially high pressure tubular reactors. More research is needed in this area to improve reactor design and determine optimum operating conditions.

The primary objective of this work is to perform a series of runs on a simulated tubular polyethylene reactor to test the validity of this kinetic model. A secondary objective is to investigate ways to improve reactor performance based on optimal operating policies. Also, implementation of a practical control scheme will be investigated.

This thesis is divided into eight chapters. In the first chapter, an introduction to polyethylene production is provided and the objectives of the study are stated.

The development of a kinetic model for a high pressure polyethylene reactor is presented in the second chapter. It includes background information on polyethylene reactor models and optimal control of polymer

reactors. The derivation of a polyethylene reactor model, including identification of all variables and parameters, is included in this chapter and in Appendix A.

In Chapter Three simulation studies for a base case reactor, constant jacket temperature reactor and an isothermal reactor are presented. The base case reactor is similar to those presented in the literataure (Agrawal and Han (1975), Chen et.al. (1976), Lee and Marano (1979)). The isothermal reactor simplifies the interpretation of the model. From studies on these two reactors the effects of input variables on the polymer product are determined.

The sensitivities of the model outputs to changes in model parameters and to uncertainty in the kinetic parameters are presented in Chapter Four.

In Chapter Five simulations are analyzed to determine the optimal operating conditions for producing a desired polymer. This analysis is based on static optimization theory. Several reactor configurations, including single and multiple initiator injections and single and multiple jacket temperature zones are investigated.

In Chapter Six, three reactor configurations, designed to improve conversion, are presented and compared. From these an overall reactor control scheme to improve conversion is proposed. The objective of this reactor configuration is to produce a polymer of desired molecular weights at maximum monomer conversion.

In Chapter Seven the quantitative relationship between temperature profiles and molecular weights is investigated. Using these relationships molecular weight trends can be inferred from temperature profile trends.

In Chapter Eight the results of this work are summarized. Suggestions for additional studies in this area are provided.

## 2. POLYETHYLENE REACTOR MODEL DEVELOPMENT

### 2.1 Literature Survey

Since the first synthesis of polyethylene in 1933 numerous investigations have been performed concerning the effects of reactor conditions on molecular weights and their distributions. Recently, simulations of tubular polyethylene reactors have been reported.

Hoftyzer and Zweiterung (1961) developed a nonlinear mathematical model of a continuous polyethylene reactor. The model consisted of differential equations representing heat and material balances. For stability studies they linearized the model about the steady state solutions. They suggested that proportional control of the initiator concentration be implemented to maintain reactor stability.

In 1963 the first simple simulation of a tubular polyethylene reactor was published by Volter. He investigated the stability of a kinetic model of an industrial, experimental, tubular polyethylene reactor. He concluded that the reactor stability is related to the observed oscillations in temperature, conversion and product quality.

Cintron-Cordero et.al. (1968) simulated a tubular polymerization reactor. It was observed that polymers with lower number average molecular weight ($M_N$) and higher polydispersity were formed under severe conditions of high inlet and wall temperatures. Under such conditions temperature ignition occurs in the reactor. The mechanism and effect of long chain branching has been studied by several authors. Mulliken and Mortimer (1970, 1972) applied probability theory to long chain branching. They assumed that the probability of branching was directly related to the exposure time of the branch site. Molecular weights, calculated using their model, agreed well with the published experimental results of Billmeyer (1953).

The first rigorous tubular polyethylene reactor simulation was reported by Agrawal and Han (1975). Their kinetic model included a branching reaction. It was shown that branching broadens the molecular weight distribution and increases the polydispersity. They investigated the effects of axial dispersion on molecular weights. It was found that increases in axial mixing increase the overall conversion and polymer molecular weights. The axial dispersion model of Agrawal and Han was not used in this study because, under normal operating conditions, the degree of axial dispersion in a tubular polyethylene

reactor is low. Agrawal and Han also reported that initiator concentration, heat transfer parameters and inlet temperature also have significant effects on conversion and reactor temperature profiles.

Chen et.al. (1976) reported another model for tubular high pressure polyethylene reactors. This model omitted axial dispersion by claiming that the pressure pulses generated by the outlet valve on the reactor do not induce significant axial mixing. The main features of Chen's model include variable fluid density, unsteady state radical concentration and long chain branching. The model calculates radical and polymer size distribution and long chain branching moments at any point in the reactor. Chen's simulations showed that conversion and polymer properties are directly related to the size and location of the polymerization zone of the reactor.

Thies (1979) reported a kinetic model of a tubular polyethylene reactor. The objective of Thies' study was to use modelling to overcome the difficulties of scaling-up pilot plants. A simple batch model and a continuous stirred tank model were presented, and conversion and temperature profiles were calculated for both of these models. A mathematical model was developed for the tubular reactor from the batch and stirred tank

models, however, no kinetic data was supplied. The polymer qualities predicted by the model agreed well with industrial test data. Goto et. al. (1981) presented a computer model of a tubular polyethylene reactor. Their study included determination of rate constants, development of reaction mechanisms and calculation of molecular structure. They developed simulations for both CSTR and plug flow reactors. The predictions of the tubular reactor model agreed well with conversions and molecular weights obtained from a commercial reactor.

Donati et.al. (1982) published a mathematical model describing temperature and conversion profiles in a tubular polyethylene reactor, represented as a series of stirred tanks with non-uniform jacket temperature. This treatment of the cooling jacket is more realistic than that of previous models. A more tedious mathematical technique was required to solve Donati's simultaneous heat and material balances. No attempt was made by the authors to solve the polymer moment balance equations.

Hwu and Foster (1982) reported a practical model for a tubular polyethylene reactor which can be used to predict fouling. Fouling in reactors is undesirable because it reduces the heat transfer rate between the reactants and the surrounding jacket, giving less control

over the reactor temperature profile and, hence, molecular weights. Time series analysis was used by Hwu and Foster to predict polymer properties and compare these propeties with the actual values. Using this method fouling can be detected before it affects the reactor performance significantly.

The model of Lee and Marano (1979) was used as the basis for simulation in this work. The features of this model are plug flow conditions, constant jacket temperature, unsteady state radical concentrations and long chain branching. Lee and Marano reported the effects of initiator type and concentration, jacket temperature, solvent concentration and heat transfer coefficient on polymer molecular weights and conversion. By constructing operating lines for desired properties versus reactor parameters the authors reached several conclusions. Conversion depends on both the initial initiator concentration and the jacket temperature. The polymer molecular weights depend on the temperature profile and conversion. For a given constant jacket temperature reactor with initiator injection at the inlet, there exists an optimum initiator type, as defined by its rate constant, and concentration for producing a polymer of desired properties.

The kinetic model developed in Chapter 2 of this study is used to investigate some of the characteristics of a tubular polyethylene reactor, described previously by other authors. The effects of inlet and jacket temperatures on the product quality, described by Cintron-Cordero et.al., will be addressed in Chapter 3. The effects of inlet initiator concentration on conversion and temperature profiles, as described by Agrawal and Han, will be studied in the simulation, optimization and control studies. The study of the moments of the temperature profile, in Chapter 7, arise from the observations of Chen et. al. and Lee and Marano, relating conversion and molecular weights to the size of the reaction zone and the shape of the temperature profile and from the simulation studies in Chapter 3.

## 2.2 Description of the Reaction Mechanism

High pressure polymerization of ethylene is a free-radical type addition polymerization. The general polymerization reaction is:

$$n\ CH_2 = CH_2 \longrightarrow H - (CH_2 - CH_2-)_n\ H$$

where n is the number of ethylene units

In the following reactions describing the polymerization steps:

| | | |
|---|---|---|
| $I$ | : | represents the initiator molecules |
| $R_o$ | : | the initiator radicals |
| $R_o^*$ | : | the activated initiator radicals |
| $M$ | : | monomer units |
| $f$ | : | initiator efficiency factor |
| $R_x^*$ | : | live radical with x monomer units |
| $P_x$ | : | dead polymer chain with x monomer units |
| $k_d$ | : | initiator decomposition rate constant (1/s) |
| $k_I$ | : | chain initiation rate constant (1/(mol.s)) |
| $k_p$ | : | propagation rate constant (1/(mol.s)) |
| $k_{fp}$ | : | transfer to polymer rate constant (1/(mol.s)) |
| $k_{tc}$ | : | termination by combination rate constant (1/(mol.s)) |
| $k_{td}$ | : | termination by disproportionation rate constant (1/(mol.s)) |

Polymerization proceeds through the following basic reactions:

(i) Initiation

Initiation is composed of two reaction steps:

(a) initiator decomposition:

$$I \xrightarrow{k_d} 2\ R_o \longrightarrow 2\ f\ R_o^*$$

(b) chain initiation:

$$R_0^* + M \xrightarrow{k_I} R_1^*$$

(ii) Propagation

During propagation live radical chains grow by adding monomer units:

$$R_x^* + M \xrightarrow{k_p} R_x^* + 1 \qquad x \in [1, \infty)$$

(iii) Transfer Reactions

Transfer reactions may occur between live radical chains and monomer, solvent or dead polymer chains. In this model only transfer to polymer is considered:

$$R_0^* + P_y \xrightarrow{k_{fp}} P_x + R_y^* \qquad x \in [1, \infty), \; y \in [1, \infty)$$

(iv) Termination

Termination of two live radical chains may occur by either combination or disproportionation.

(a) termination by combination:

$$R^*_x + R^*_y \xrightarrow{k_{tc}} P_{x+y} \quad x,y \in [1, \infty)$$

(b) termination by disproportionation:

$$R^*_x + R^*_y \xrightarrow{k_{td}} P_x + P_y \quad x,y \in [1, \infty)$$

In the derivation of the kinetic model it is assumed that:

(i) all reactions are irreversible and elementary

(ii) reaction rate constants are independent of chain length.

## 2.3 Derivation of Kinetic Equations

The high pressure tubular reactor is assumed to be a plug flow reactor with a constant temperature cooling jacket. Using the above reaction mechanism and the characteristics of plug flow reactors, material and energy balances can be made for a volume element of the reactor and integrated, with time, over the length of the reactor. Time is selected as the reactor coordinate, and defined as the ratio of the reactor volume to the volumetric flow rate of the reactants and products. The features of this model are summarized in Table 2.1.

The initiator decomposition reaction follows first order kinetics. The rate of initiator disappearance is given by the following differential equation:

$$\frac{d[I]}{dt} = -2\, k_d[I] \qquad (2.1)$$

where [I] is the initiator concentration (mol/l)

t is the reactor coordinate(s)

Table 2.1 Model Features

| | |
|---|---|
| 1. | Plug flow reactor with no axial or backmixing. |
| 2. | Steady state reactor operation. |
| 3. | Constant reactor pressure. |
| 4. | Constant overall heat transfer coefficient. |
| 5. | Constant reactant fluid heat capacity and density. |
| 6. | Radical concentration not at steady state. |
| 7. | Long chain branching of polymer molecules. |
| 8. | No volume changes due to reaction |

Material balances for other species in the reactor require the use of radical and polymer moments. The $k^{th}$ moment of a live radical distribution is defined as:

$$\lambda_k = \sum_{x=1}^{\infty} x^k [R_x^*] \qquad (2.2)$$

where $[R_x^*]$ is the concentration of live radicals of chain length x (mol/l)

The relationships between the live radical moments in Equation 2.2 and those of the model are:

$$G(1,t) = \lambda_0 \qquad (2.3)$$

$$G'(1,t) = \lambda_1 \qquad (2.4)$$

$$G''(1,t) = \lambda_2 - \lambda_1 \qquad (2.5)$$

Similarly, the $k^{th}$ moment of the polymer concentration is defined as:

$$\mu_k = \sum_{x=1}^{\infty} x^k [P_x] \qquad (2.6)$$

where $[P_x]$ is the concentration of dead polymer molecules of chain length x (mol/l).

In this model the dead polymer moments are redefined as:

$$H(1,t) = \mu_0 + \lambda_0 \tag{2.7}$$

$$H'(1,t) = \mu_1 + \lambda_1 \tag{2.8}$$

$$H''(1,t) = \mu_2 + \lambda_2 - (\mu_1 + \lambda_1) \tag{2.9}$$

A detailed derivation of the material balances for monomer, radicals and polymer molecules is given in Appendix A. The results of those derivations are presented here.

The rate of disappearance of monomer is described as:

$$\frac{-d[M]}{dt} = k_p[M]G(1,t) \tag{2.10}$$

where [M] is the monomer concentration (mol/l)

The rate of change of the zeroth and first live radical moments are expressed as:

$$\frac{dG(1,t)}{dt} = 2fk_d[I] - k_t G^2(1,t) \tag{2.11}$$

$$\frac{dG'(1,t)}{dt} = 2fk_d[I] + k_p[M]G(1,t) - k_t G(1,t)G'(1,t) - k_{fp}[(H'(1,t)(G'(1,t)-G'(1,t)) - H''(1,t)G(1,t)] \tag{2.12}$$

where $f$ is the initiator efficiency factor, and

$k_t$ is the sum of the termination rate constants, $k_{tc} + k_{td}$, (l/(mol.s))

The rate of change of zeroth, first and second moments of dead polymer concentration are:

$$\frac{dH(l,t)}{dt} = 2fk_d[I] - 1/2\ k_{tc}G^2(l,t) \qquad (2.13)$$

$$\frac{dH'(l,t)}{dt} = 2fk_d[I] + k_p[M]G(l,t) \qquad (2.14)$$

$$\frac{dH''(l,t)}{dt} = 2k_p[M]G'(l,t) + k_{tc}(G'(l,t))^2 \qquad (2.15)$$

The propagation reaction is highly exothermic and all other reactions have negligible heats of reaction. Therefore, only propagation is considered in the overall energy balance. The rate of propagation, $R_p$, is equivalent to the monomer consumption rate:

$$R_p = \frac{-d[M]}{dt} = k_p[M]G(l,t) \qquad (2.16)$$

The overall energy balance is described as:

$$\frac{dT}{dt} = \frac{-\Delta HR_p}{c_p \rho} - \frac{4U}{D\rho c_p}(T - T_J) \qquad (2.17)$$

where $T$ is the reactor temperature (K),

$\Delta H$ is the heat of propagation (cal/mol),

$\rho$ is the reactor fluid density (g/l),

$c_p$ is the fluid heat capacity (cal/g°C),

$D$ is the reactor diameter (m),

$U$ is the overall heat transfer coefficient ($cal/m^2 s\ °C$), and

$T_J$ is the jacket temperature (K)

The second term in the energy balance accounts for the heating and cooling provided by the constant temperature jacket.

The molecular weights and polydispersity of the polymer are calculated as follows:

$$M_N = M_{C_2H_4} \frac{H'(1,t)}{H(1,t)} \qquad (2.18)$$

$$M_W = M_{C_2H_4} \left( \frac{H''(1,t)}{H'(1,t)} + 1 \right) \qquad (2.19)$$

$$PD = \frac{M_W}{M_N} \qquad (2.20)$$

where: $M_{C_2H_4}$ is the molecular weight of ethylene

$M_N$ is the number average molecular weight

$M_W$ is the weight average molecular weight

PD is the polydispersity

## 2.4 Parameter Estimates

In the kinetic model presented in the previous section the rate constants, and thermodynamic and system operating parameters must be specified.

For initiator decomposition both the rate constant, $k_d$, and efficiency factor, f, must be specified. The initiator efficiency factor is an empirical factor with values ranging from 0 to 1. For commercial initiators this factor is usually between 0.5 and 1.0 (Hamielec and Friis, 1975). In this model the value of f is assumed to be 0.5.

Rate constants are expressed in the Arrhenius form:

$$k_j = k_{jo} \exp\left(\frac{-E_j}{R\ T}\right) \qquad (2.21)$$

where

$k_j$ is the rate constant (l/(mol.s))

$k_{jo}$ is the frequency factor (l/(mol.s))

$E_j$ is the activation energy (cal/mol)

R is the universal gas constant and

T is absolute temperature (K)

Many commercial initiators are available for use in polymer reactors, with peroxides and azo-compounds being the most common initiator types. The choice of initiator depends on its reactivity, $k_d$, at the polymerization temperature. Rate constants for several different initiators are listed in Table 2.2. For this study, benzoyl peroxide was chosen as the initiator. It has an activation energy of 29,700 cal/mol and a frequency factor of $6.38 \times 10^{13}$ $s^{-1}$ (Hamielec and Friis, 1975). This initiator decomposes at a moderate rate in the range of temperatures encountered in this reactor, 370 to 500 K. For example, at 410 K, a typical initial temperature in the polyethylene reactor, the initiator decomposition rate is 0.9 $s^{-1}$.

All other rate constants used in the model are those reported by Chen et.al. (1976). The rate constants are listed in Table 2.3 and shown in Figure 2.1. Rate constants from other literature sources are also listed in

Table 2.2 Initiator Rate Constants

| Initiator | Source | Frequency Factor $s^{-1}$ | Activation Energy cal/mol |
|---|---|---|---|
| acetyl peroxide | Hamielec and Friis | $1.16 \times 10^{16}$ | 32500 |
| AIBN | Hamielec and Friis | $1.96 \times 10^{14}$ | 29500 |
| benzoyl peroxide | Hamielec and Friis | $6.38 \times 10^{13}$ * | 29700* |
| t-butyl peroxide | Hamielec and Friis | $3.26 \times 10^{14}$ | 35100 |
| t-butyl hydro-peroxide | Agrawal & Han | $8.20 \times 10^{11}$ | 25000+0.17P |
| di-t-butyl peroxide | Chen et.al. | $1.60 \times 10^{16}$ | 38400 |
| peroxide | Donati et.al. | $1.608 \times 10^{11}$ l/mol/s | 30670-0.6(P-1) |

* used in simulation

P: pressure (atm)

Table 2.3 Rate Constants

| Initiator | Source | Frequency Factor $s^{-1}$ | Activation Energy cal/mol |
|---|---|---|---|
| $k_p$ | Chen et.al. | $2.95 \times 10^7$* | 8200-.555P |
| | Donati et.al. | $3.1 \times 10^4$ | 6164-0.6(P-1) |
| | Lee & Marano | $5.88 \times 10^7$ | 7100-.556P |
| | Agrawal & Han | $1.25 \times 10^8$ | 7800+0.5P |
| $k_{tc}$ | Chen et.al. | $1.6 \times 10^9$* | 2400* |
| | Donati et.al. | $4.0 \times 10^4$ | 750 |
| | Lee & Marano | $1.08 \times 10^9$ | 300-.34P |
| | Agrawal & Han | $2.2 \times 10^{10}$ | 1000+.244P |
| $k_{td}$ | Chen et.al. | $2.72 \times 10^{11}$* | 20000* |
| | Lee & Marano | $3.25 \times 10^8$ | -0.12P |
| $k_{fp}$ | Chen et.al. | $9.0 \times 10^5$* | 9000* |
| | Lee & Marano | $4.1 \times 10^5$ | 7160-.48P |
| | Agrawal & Han | - | 12000 |

* used in simulation

P: pressure (atm)

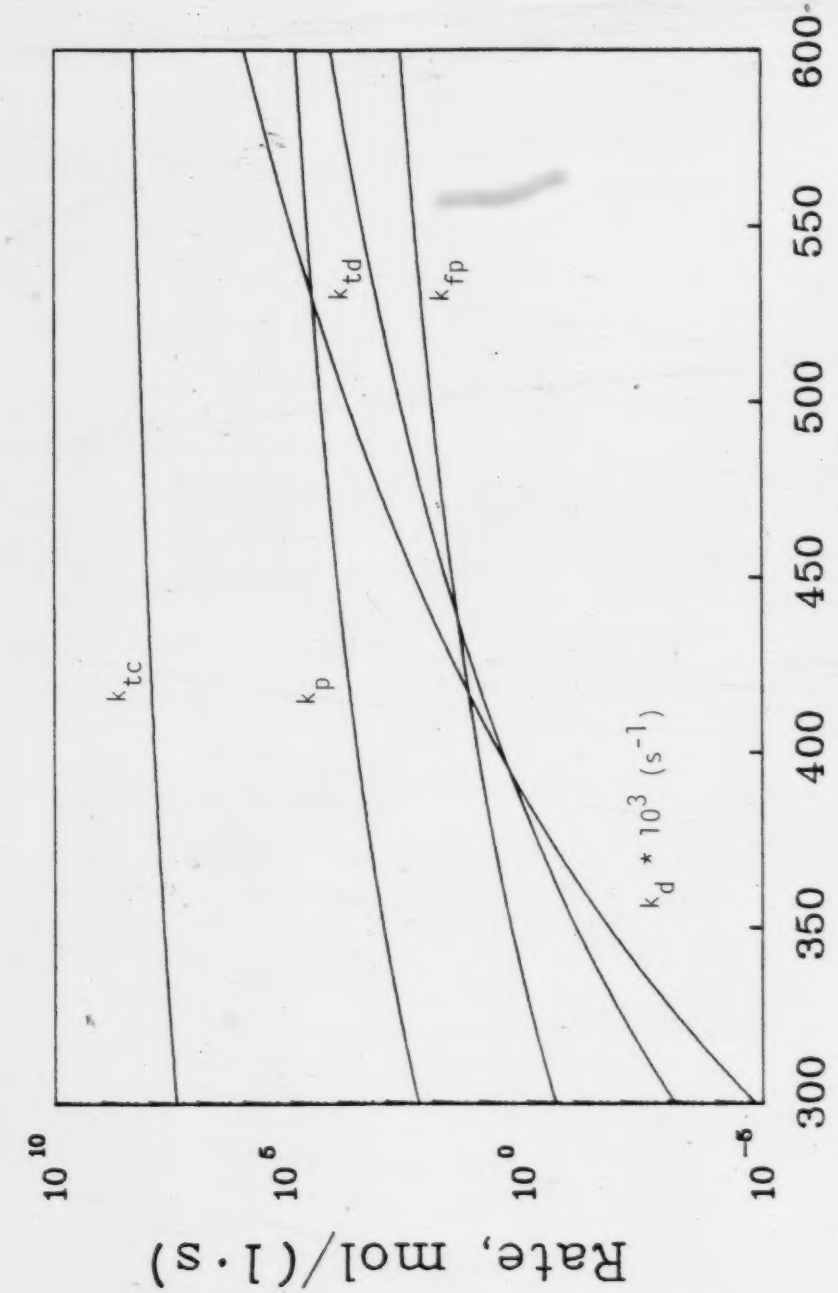


Figure 2.1 Rate Constants

Table 2.3. Numerical values for the rate constants in ethylene polymerization are not well known, as can be seen from the wide variation of values listed in Table 2.3. If a detailed kinetic study were to be undertaken for this system, experimental work to determine acceptable rate constants would be required.

The value of the ratio of propagation and termination rates has been studied. Ehrlich and Mortimer (1970) correlated results from several authors on the value of $k_p/k_{tc}^{1/2}$. At 2500 atm and 129°C this factor is 0.73. Using the rate constants in Table 2.3, $k_p/k_{tc}^{1/2}$ is 0.65, which agrees well with Ehrlich and Mortimer's value.

Ehrlich and Mortimer also suggest that the value of $k_{td}$ is significantly less than other rate constants at temperatures less than 200°C. This is true for Chen et.al.'s value of $k_{td}$ given in Table 2.3.

Lee and Marano (1979) report a value of $k_{fp}$ which is approximately ten times that of Chen et.al. over the range of reactor temperatures. Since $k_{fp}$ is only known qualitatively the value reported in Table 2.3 is acceptable.

The system parameters which must be specified in reactor design are reactor length, reactor diameter, residence time and operating pressure. Ranges of values for these reactor specifications reported in the literature are listed in Table 2.4. Common practice in industry dictates reactor length, diameter and residence time. Sittig (1976) reports that reaction times in tubular reactors range from 20 to 60s. Reactor length/diameter ratios range from 300 to 40,000 and tube internal diameters from 1.5 to 9 cm. Using a length of 600 m, diameter of 2 cm and residence time of 30 s all of the above criteria are satisfied.

High pressure ethylene polymerization is usually carried out at pressures between 1000 and 3000 atm (Sittig, 1976). The reactor pressure chosen for this model is 2000 atm, which is within this range and close to the other literature values.

For the base case simulation of this model only one initiator injection point, at the reactor inlet, and one cooling jacket zone are considered. In the optimal control and conversion improvement studies multiple injection points and jacket temperature zones will be considered.

Table 2.4 Reactor Specifications

| Parameter | Source | Value |
|---|---|---|
| reactor length, L | simulation | 600 m |
| | Romanini | 800 m |
| | Donati et.al. | > 500-1000 m |
| | Agrawal & Han | 450-1500 m |
| | Chen et.al. | 1200 m |
| reactor diameter, D | simulation | 2 cm |
| | Romanini | < 7-8 cm |
| | Donati et.al. | 2.5-5 cm |
| | Agrawal & Han | 2.54 cm |
| | Chen et.al. | 5 |
| | Sittig | 1.5-9 cm |
| L/D ratio | simulation | 30,000 |
| | Donati et.al. | 1000-15,000 |
| | Agrawal & Han | 250-12,000 |
| | Sittig | 300-40,000 |
| reaction time | simulation | 30 s (residence time) |
| | Sittig | 20-60 s |
| pressure | simulation | 2000 atm |
| | Agrawal & Han | 2500 atm |
| | Chen et.al. | 2000 atm |
| | Lee & Marano | 2245 atm |
| | Sittig | 1000-3000 atm |

Thermodynamic properties of the ethylene/ polyethylene system required for this model are heat capacity, $c_p$, heat of polymerization, $\Delta H$, and overall heat transfer coefficient, U. The literature values of these constants are listed in Table 2.5. The values of $c_p$ reported in the literature range from 0.48 to 0.61 over the range of reactor temperatures. A constant value of $c_p$ was used in this model, 0.58 cal/(g°C), which is within the reported range. Literature values for the heat of ethylene polymerization range from -21000 to -24200 cal/mol. For this model $\Delta H$ is assumed to be -21400, which is consistent with literature values. From the reported literature values for a reactor with little fouling the average overall heat transfer coefficient, U, is assumed to be 250 cal/($m^2$s °C).

The input variables for the polyethylene reactor are monomer concentration, initiator concentration, inlet temperature and jacket temperature. The inlet feed stream is essentially pure monomer. Chen et. al. report that the density of ethylene at 2000 atm and 373 K is 540 g/l, its concentration is 19.4 mol/l. The initiator concentration may range from 1 ppm to 10 weight %, depending upon the initiator type and the desired properties of the product polymer. The inlet temperature may vary from 323 to 373 K, depending upon the amount of preheat available for

Table 2.5 Thermodynamic Properties

| Parameter | Source | Value |
|---|---|---|
| heat capacity, $c_p$ | Brandup & Immergut | 0.4755 cal/(g°C) at 0°C |
| | Hellwege | 0.248+0.00154T cal/g°C |
| | Lee & Marano | 0.58 cal/g°C* |
| | Agrawal & Han | 0.85 cal/g°C |
| heat of polymerization, $\Delta H$ | Hamielec & Friis | -21000 cal/mol |
| | Brandup & Immergut | -24200 cal/mol |
| | Chen et.al. | -21400 cal/mol* |
| | Lee & Marano | -22300 cal/mol |
| | Hwu & Foster | -23500 cal/mol |
| overall heat transfer coefficient, U | Chen et.al. | 235 cal/$m^2$s°C |
| | Lee & Marano | 40-150 cal/$m^2$s°C |
| | Agrawal & Han | 270-550 cal/$m^2$s°C |
| | simulation | 250 cal/$m^2$s°C* |

* used in simulation

the feed stream. The jacket temperature may range from 373 to 533 K, depending on the desired reactor temperature.

The values of the rate constants, reactor parameters and thermodynamic properties defined in Tables 2.2, 2.3 and 2.4 are used in the reactor model to provide typical conditions for a polyethylene reactor simulation.

# 3. MODEL EVALUATION

## 3.1 Base Case Simulation

The polyethylene reactor described in Chapter 2 can be operated at many different values of the input variables. For the simulation studies a reference set of conditions known as the base case conditions, were chosen. These inputs are listed in Table 3.1 The differential equations describing the model were integrated using a Runge-Kutta method, IMSL subroutine DVERK, to calculate reactor temperature, conversion, moment and molecular weight profiles.

The reactor temperature and conversion profiles for the base case simulation are shown in Figure 3.1. The heating, reaction and cooling zones are shown in Figure 3.2, and molecular weight profiles in Figure 3.3. The product polymer has a $M_N$ of 138300 and a $M_W$ of 625400. The final initiator conversion is 100% and monomer conversion is 6.2%.

Near the entrance the reactants are heated up by the surrounding jacket. This region is known as the heating zone. The derivative of the reactor temperature with respect to the reactor coordinate, time, is positive

Table 3.1 Base Case Conditions

| INPUT VARIABLES | | | | | MEASURED OUPPUTS | | | | |
|---|---|---|---|---|---|---|---|---|---|
| Pressure atm | Jacket Temperature K | Inlet Temperature K | Initiator Concentration mol/l | Monomer Concentration mol/l | $M_N$ | $M_W$ | PD | $X_M$ % | $X_I$ % |
| 2000 | 433 | 372 | $9.7 \times 10^{-4}$ | 19.4 | 138290 | 625420 | 4.52 | 6.17 | 100 |

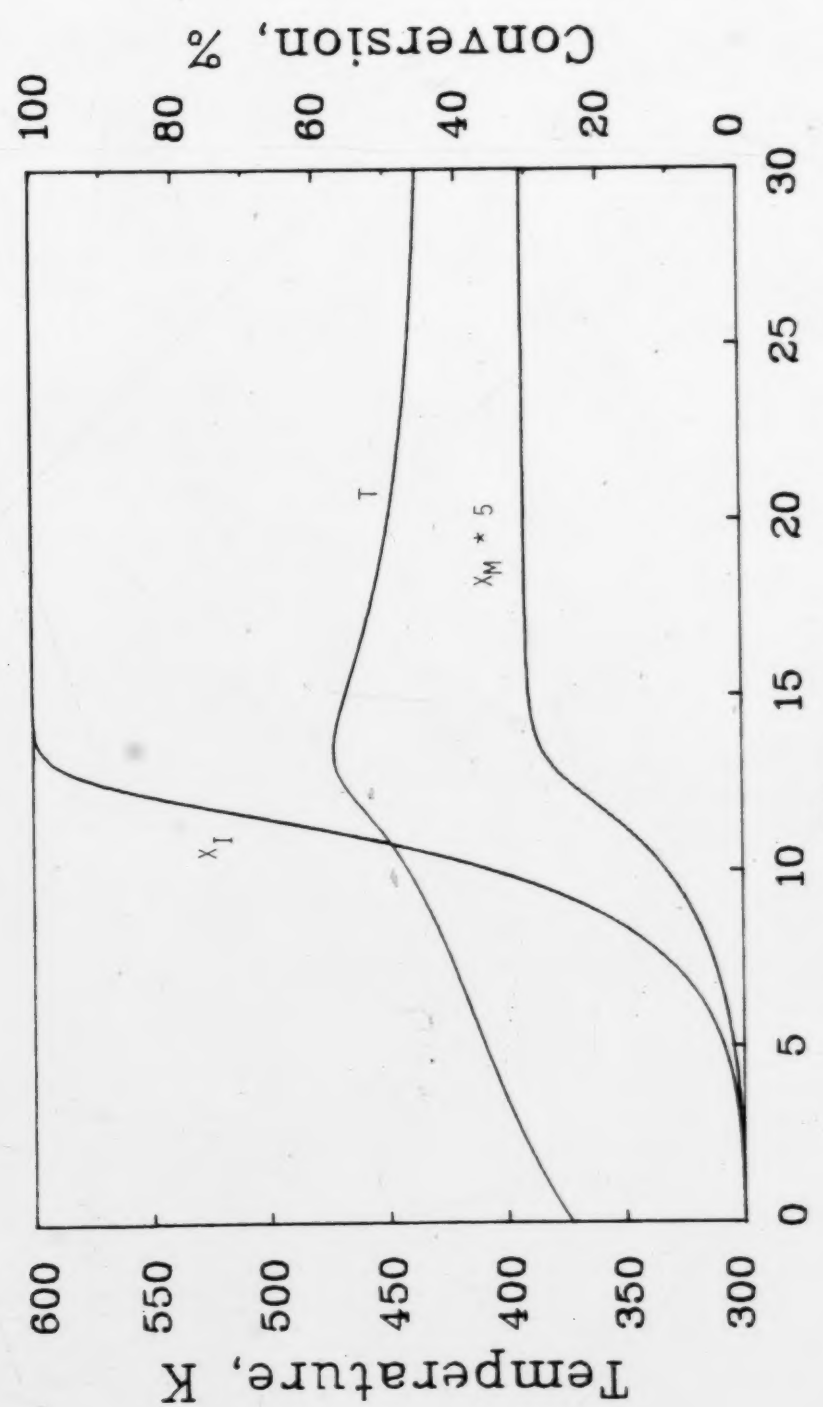


Figure 3.1 Reactor Profiles

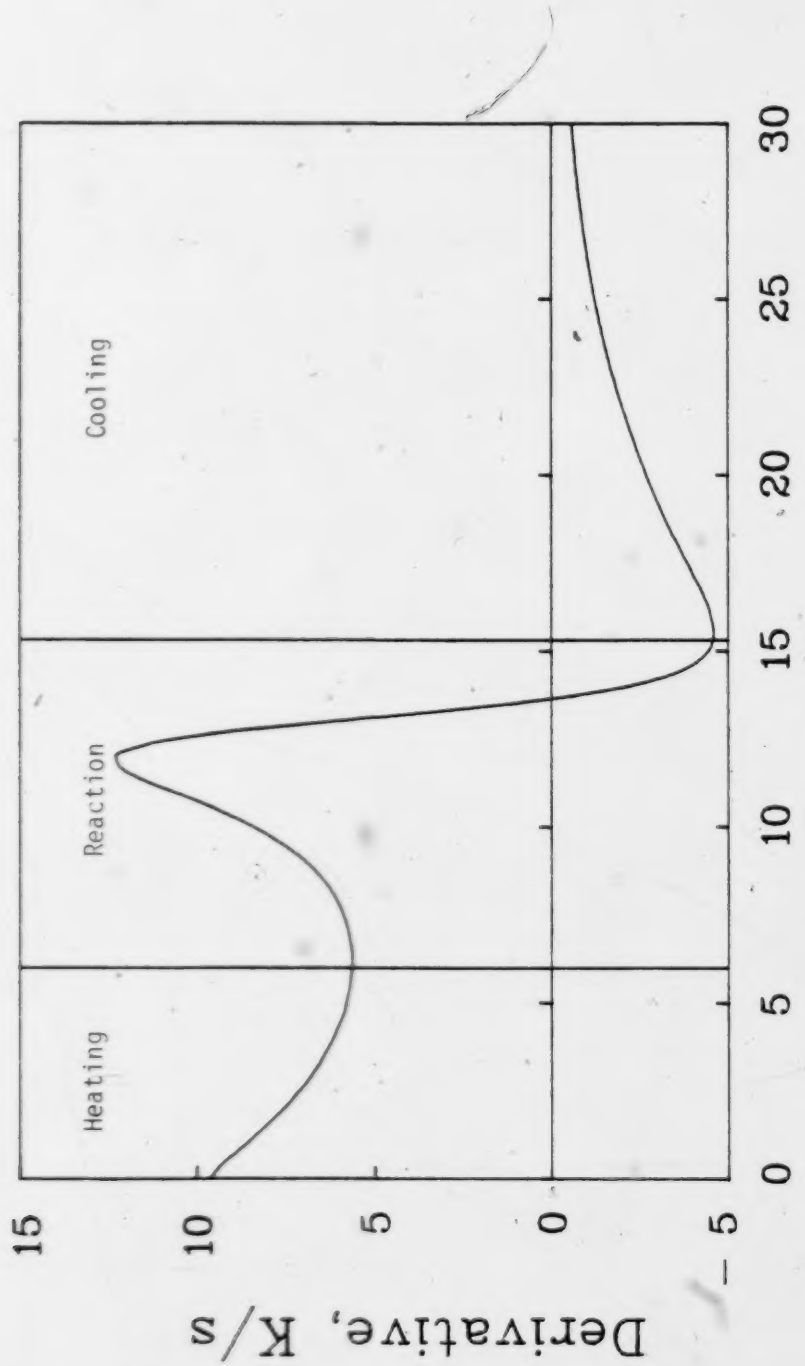


Figure 3.2 Division of Reactor into Zones

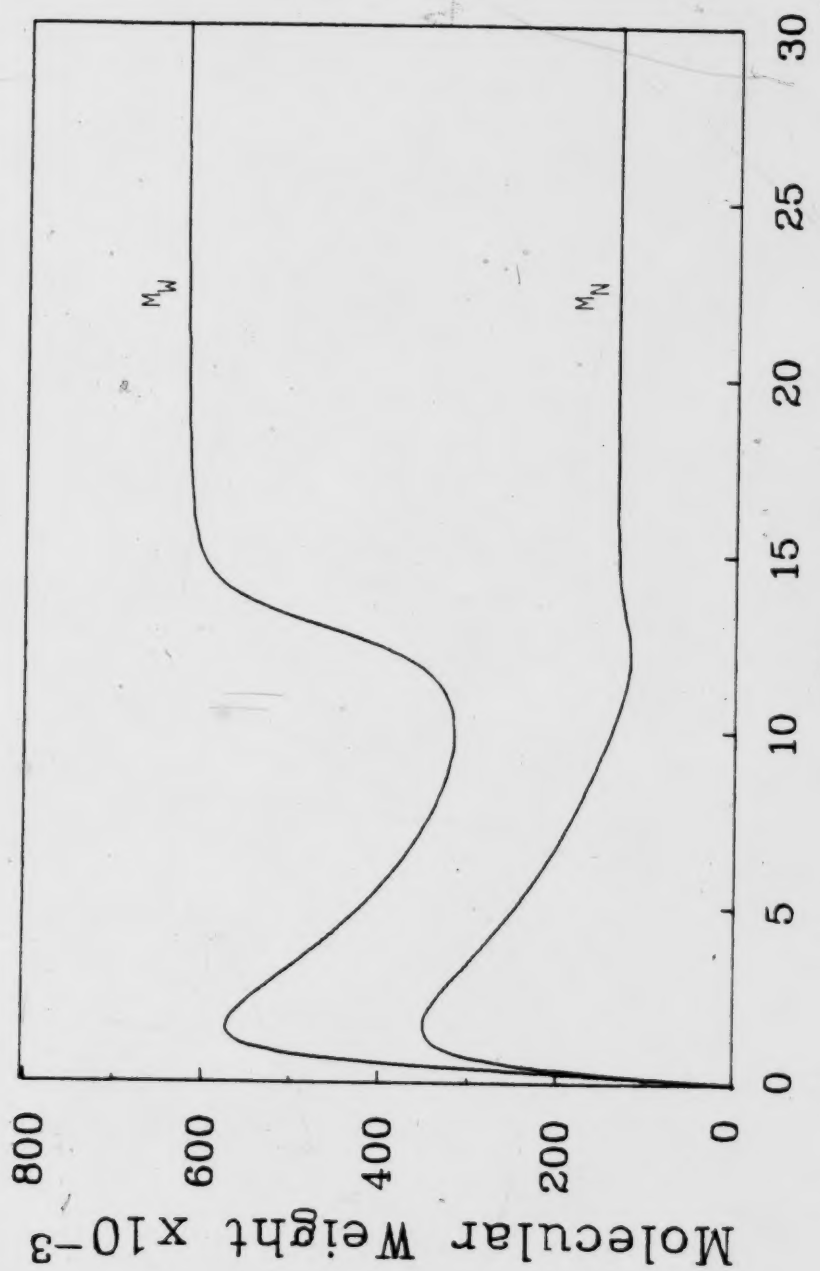


Figure 3.3 Molecular Weight Profiles

and decreasing in this zone. In the reaction zone the temperature increases rapidly, due to the exothermic polymerization reactions. The temperature peak in the reaction zone corresponds to the point where the initiator conversion is at its maximum, 100%. After this point no new initiated radicals are available and the propagation rate decreases. In the cooling zone the polymerization reactions do not occur at a significant rate, there is no change in monomer conversion and the reactor contents are cooled by the cooling jacket.

The molecular weights of the polymer are calculated continuously along the reactor coordinate. The molecular weight profiles for the base case are shown in Figure 3.3. The molecular weights are high near the reactor entrance, reach minima in the reaction zone, and increase to their final values near the beginning of the cooling zone. The significant increase in $M_W$ from its minimum of 319,000 to the final value of 625,400 is due to $k_{tc}$, $k_{td}$ and $k_{fp}$. Termination by combination dominates the termination reactions and long polymer molecules are formed. Also, transfer to polymer results in large amounts of long chain branching. Thus $M_W$ increases while $M_N$ remains constant.

## 3.2 Effect of Jacket Temperature

The reactor variable that can be most easily manipulated is the jacket temperature. Jacket temperatures ranging from 403 to 553 K were used in the reactor model. The model predictions for these cases are listed in Table 3.2.

The effects of jacket temperature on molecular weights, polydispersity and conversion are shown in Figure 3.4. Excluding the first data point, $T_J$ = 403 K, where the initiator decomposition is not complete, the molecular weights, polydispersity and conversion all decrease with increasing jacket temperature. At higher jacket temperatures the reactor temperature is correspondingly higher and all reactions proceed at higher rates. However, the overall rate of polymerization decreases due to the higher relative decrease in G(1,t).

For the very low jacket temperature, 403 K, initiator decomposition occurs at a low rate and never becomes large enough to cause significant propagation and reactor temperature increases. As a result, the monomer conversion is low. For high jacket temperatures the molecular weights, polydispersity, and conversion approach

Table 3.2 Effect of Jacket Temperature

| INPUT VARIABLES | | | MEASURED OUTPUTS | | | | |
|---|---|---|---|---|---|---|---|
| Jacket Temperature K | $T_o$ K | $C_{IO}$ mol/l | $M_N$ | $M_W$ | PD | $X_M$ % | $X_I$ % |
| 403 | 373 | $9.7 \times 10^{-4}$ | 213930 | 676450 | 3.20 | 3.42 | 36.3 |
| 423 | 373 | $9.7 \times 10^{-4}$ | 155760 | 956610 | 6.14 | 6.95 | 100 |
| 433 | 373 | $9.7 \times 10^{-4}$ | 138290 | 625420 | 4.52 | 6.17 | 100 |
| 443 | 373 | $9.7 \times 10^{-4}$ | 127550 | 495230 | 3.88 | 5.69 | 100 |
| 450 | 373 | $9.7 \times 10^{-4}$ | 122140 | 442370 | 3.62 | 5.45 | 100 |
| 453 | 373 | $9.7 \times 10^{-4}$ | 120170 | 424910 | 3.54 | 5.36 | 100 |
| 463 | 373 | $9.7 \times 10^{-4}$ | 114690 | 380590 | 3.32 | 5.12 | 100 |
| 473 | 373 | $9.7 \times 10^{-4}$ | 110470 | 350320 | 3.17 | 4.93 | 100 |
| 490 | 373 | $9.7 \times 10^{-4}$ | 105190 | 316880 | 3.01 | 4.70 | 100 |
| 553 | 373 | $9.7 \times 10^{-4}$ | 91616 | 248590 | 2.71 | 4.09 | 100 |

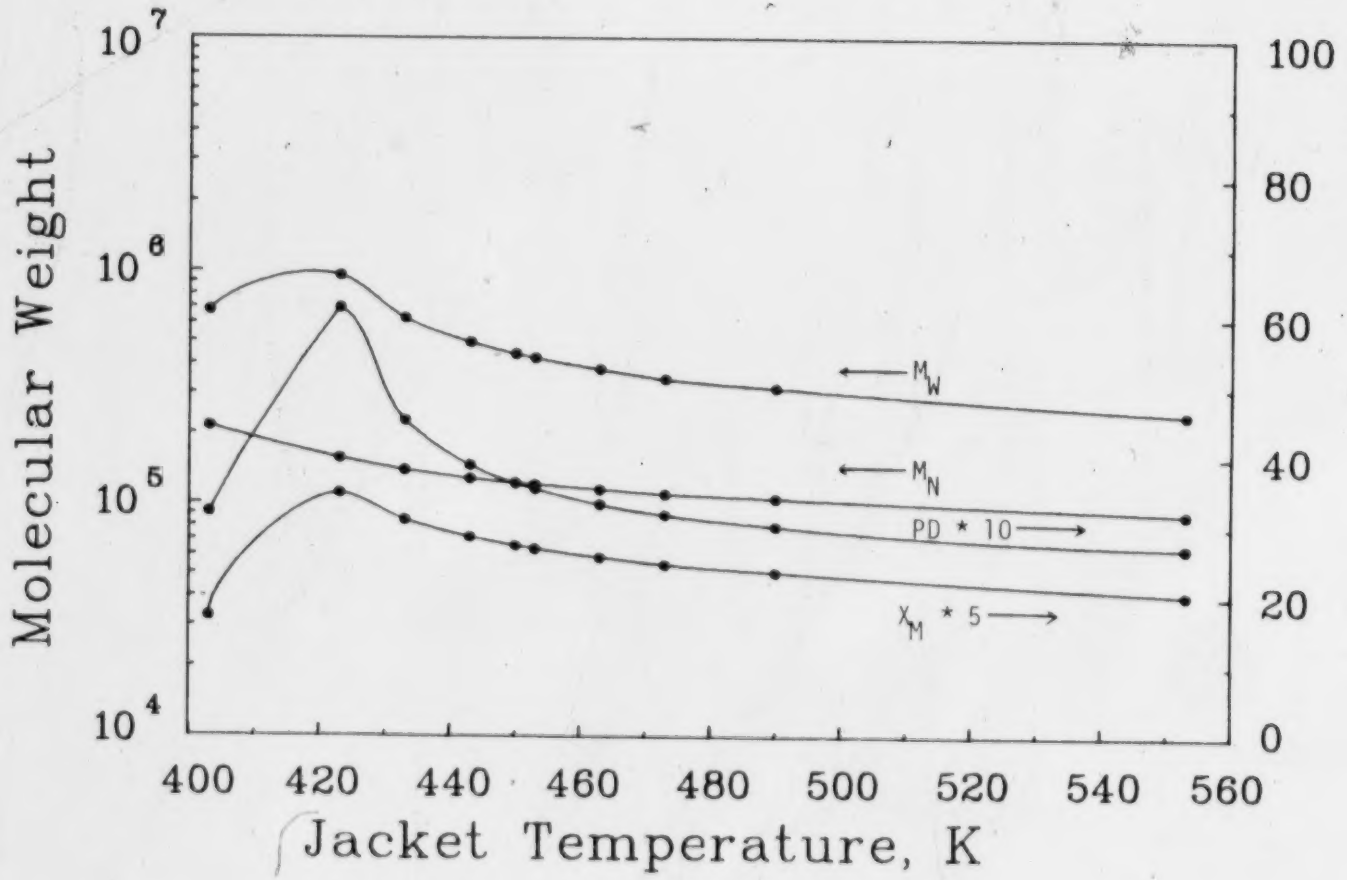


Figure 3.4 Effect of Jacket Temperature

minima. These minima are governed by more favourable termination versus propagation reactions. A practical constraint is placed on the maximum jacket temperature. Above reactor temperatures of 300°C (573 K) ethylene decomposition occurs, resulting in discoloration of the polymer product and explosions. To avoid these problems the jacket temperature is usually set at a temperature low enough to maintain the reactor temperature below 300°C.

The temperature profiles for three jacket temperature cases, 403, 433 and 473 K, are shown in Figure 3.5. For the low jacket temperature case the reactor temperature profile is monotonic. As the jacket temperature increases the magnitude of the reactor temperature peak increases and its location moves closer to the reactor inlet. Initiator decomposition occurs at a higher rate at higher temperatures, therefore the reactor temperature increases rapidly. The heat generation rate is greater than the jacket cooling rate when rapid initiation occurs, hence a higher maximum temperature is achieved.

Combining the effect of jacket temperature on the polymer product and the division of the cooling jacket into zones, control over the reaction zone can be implemented. The base type reactor model is modified with the cooling jacket zones having different temperatures.

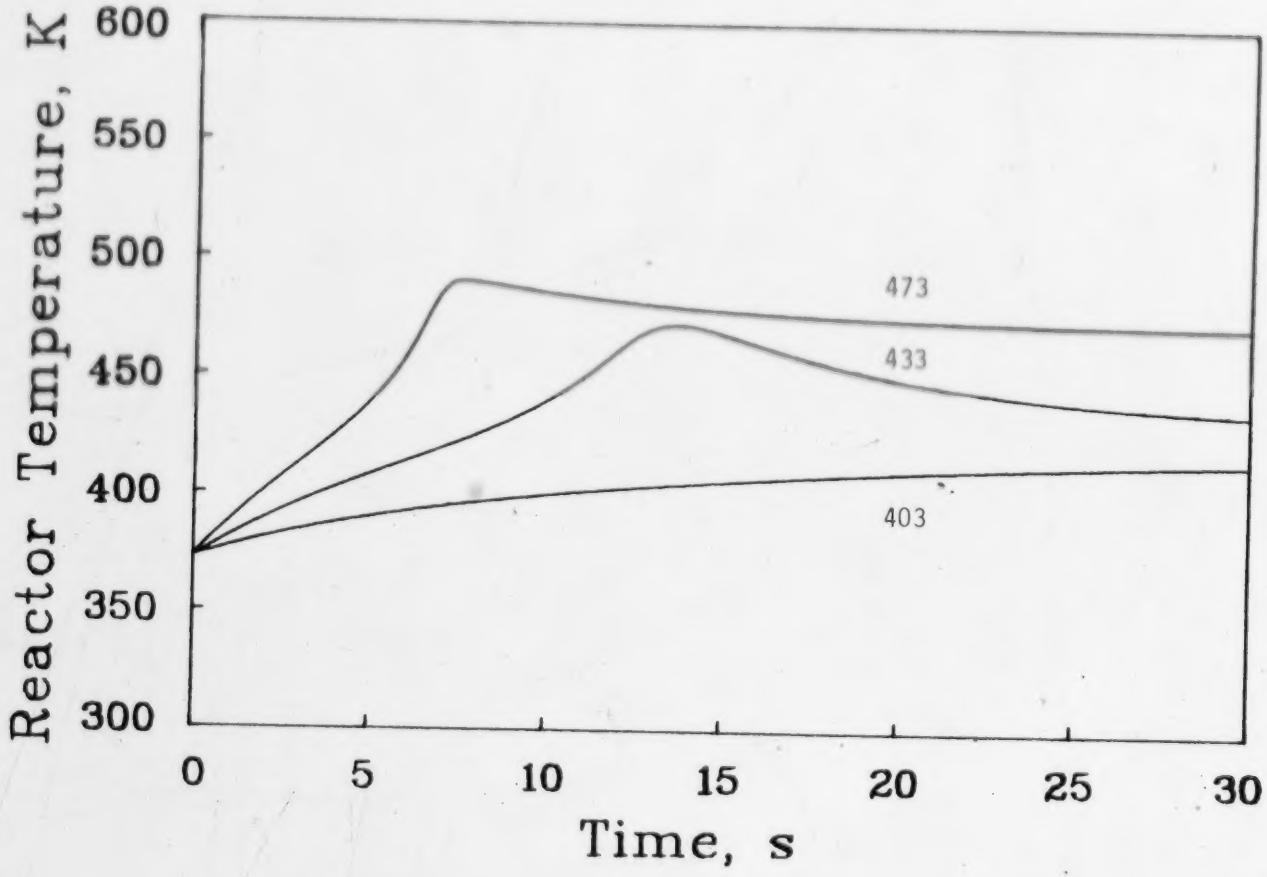


Figure 3.5 Temperature Profiles for Different Jacket Temperatures

This is referred to as a multi-zone reactor, named for the multiple cooling jacket zones.

The reactor temperature and monomer conversion profiles for this multi-zone reactor are compared with those of the base case in Figure 3.6. The molecular weights and conversions of both reactors are compared in Table 3.3. The multi-zone jacket temperatures are 453 K in the heating zone, 423 K in the reaction zone and 333 K in the cooling zone. The temperature rise in the heating zone of the multi-zone reactor is larger than that in the single jacket temperature zone reactor. This is due mainly to the higher jacket temperature of 453 K vs 433 K. The larger temperature rise induces faster initiator decomposition, monomer conversion and polymerization. The faster initiation rate in the heating zone of the multi-zone reactor causes the temperature peak to be located closer to the reactor entrance.

The slight decrease in overall monomer conversion in the multi-zone reactor is due mainly to the higher temperatures in the heating and reaction zones, which increase the rate of termination relative to the rate of propagation. The lower $M_w$ in the multi-zone reactor is also due to the higher heating and reaction zone temperatures in the reactor.

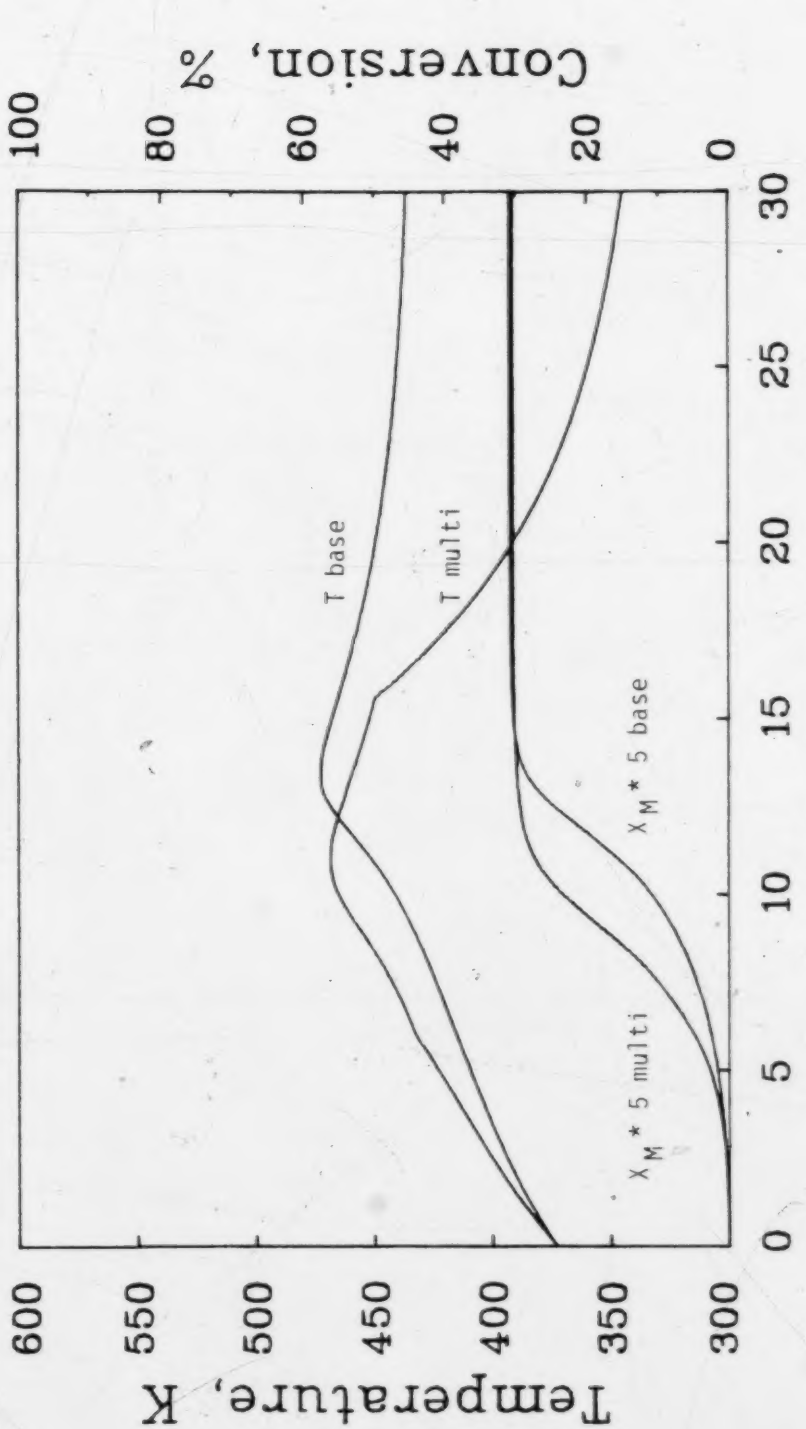


Figure 3.6 Reactor Profiles for Multi-Zone and Base Case

Table 3.3 Comparison of Multi-Zone and Base Case Reactors

| INPUT VARIABLES | | | | | MEASURED OUTPUTS | | | | |
|---|---|---|---|---|---|---|---|---|---|
| $T_J$ Zone 1 K | $T_J$ Zone 2 K | $T_J$ Zone 3 K | $T_o$ K | $C_{IO}$ mol/l | $M_N$ | $M_W$ | PD | $X_M$ % | $X_I$ % |
| 433 | 433 | 433 | 373 | $9.7 \times 10^{-4}$ | 138290 | 625420 | 4.52 | 6.17 | 100 |
| 453 | 423 | 333 | 373 | $9.7 \times 10^{-4}$ | 136350 | 550450 | 4.04 | 6.09 | 100 |

## 3.3 Effect of Initiator Concentration

Another important manipulated variable is the inlet initiator concentration. To study its effect on the base case model the concentration was varied from $1.0 \times 10^{-4}$ to $1.94 \times 10^{-2}$ mol/l. The results of the model for these cases are listed in Table 3.4.

The effects of initiator concentration on molecular weights, polydispersity and conversion are shown in Figure 3.7. The monomer conversion increases with increasing initial initiator concentration. The number of active radicals generated in the reactor is proportional to the initiator concentration. With more activated radicals the propagation rate, and hence the rate of monomer consumption, increases. As the rate of propagation increases the reactor temperature also increases. At higher temperatures the termination rate increases and the polymer chain lengths are shorter. Therefore, the molecular weights of the product polymer decrease with increasing inlet initiator concentration. The overall conversion increases with increasing inlet initiator concentration. For inlet initiator concentrations up to $2 \times 10^{-3}$ mol/l the polydispersity decreases with increasing inlet initiator concentration. After this concentration the polydispersity remains

Table 3.4 Effect of Inlet Initiator Concentration

| INPUT VARIABLES | | | MEASURED OUTPUTS | | | | |
|---|---|---|---|---|---|---|---|
| $T_J$ K | $T_O$ K | Initiator Concentration mol/l | $M_N$ | $M_W$ | PD | $X_M$ % | $X_I$ % |
| 433 | 373 | $1.0 \times 10^{-4}$ | 575175 | 5423800 | 9.43 | 2.61 | 98.3 |
| 433 | 373 | $2.425 \times 10^{-4}$ | 355470 | 2824900 | 7.96 | 3.96 | 99.8 |
| 433 | 373 | $4.85 \times 10^{-4}$ | 228760 | 1360900 | 5.95 | 5.11 | 100 |
| 433 | 373 | $9.7 \times 10^{-4}$ | 138290 | 625420 | 4.52 | 6.17 | 100 |
| 433 | 373 | $1.455 \times 10^{-3}$ | 101820 | 406160 | 3.99 | 6.82 | 100 |
| 433 | 373 | $1.94 \times 10^{-3}$ | 81772 | 303360 | 3.71 | 7.30 | 100 |
| 433 | 373 | $4.85 \times 10^{-3}$ | 40262 | 129470 | 3.22 | 8.99 | 100 |
| 433 | 373 | $9.7 \times 10^{-3}$ | 23259 | 72313 | 3.11 | 10.4 | 100 |
| 433 | 373 | $1.455 \times 10^{-2}$ | 16819 | 52701 | 3.13 | 11.3 | 100 |
| 433 | 373 | $1.94 \times 10^{-2}$ | 13340 | 42484 | 3.19 | 11.9 | 100 |

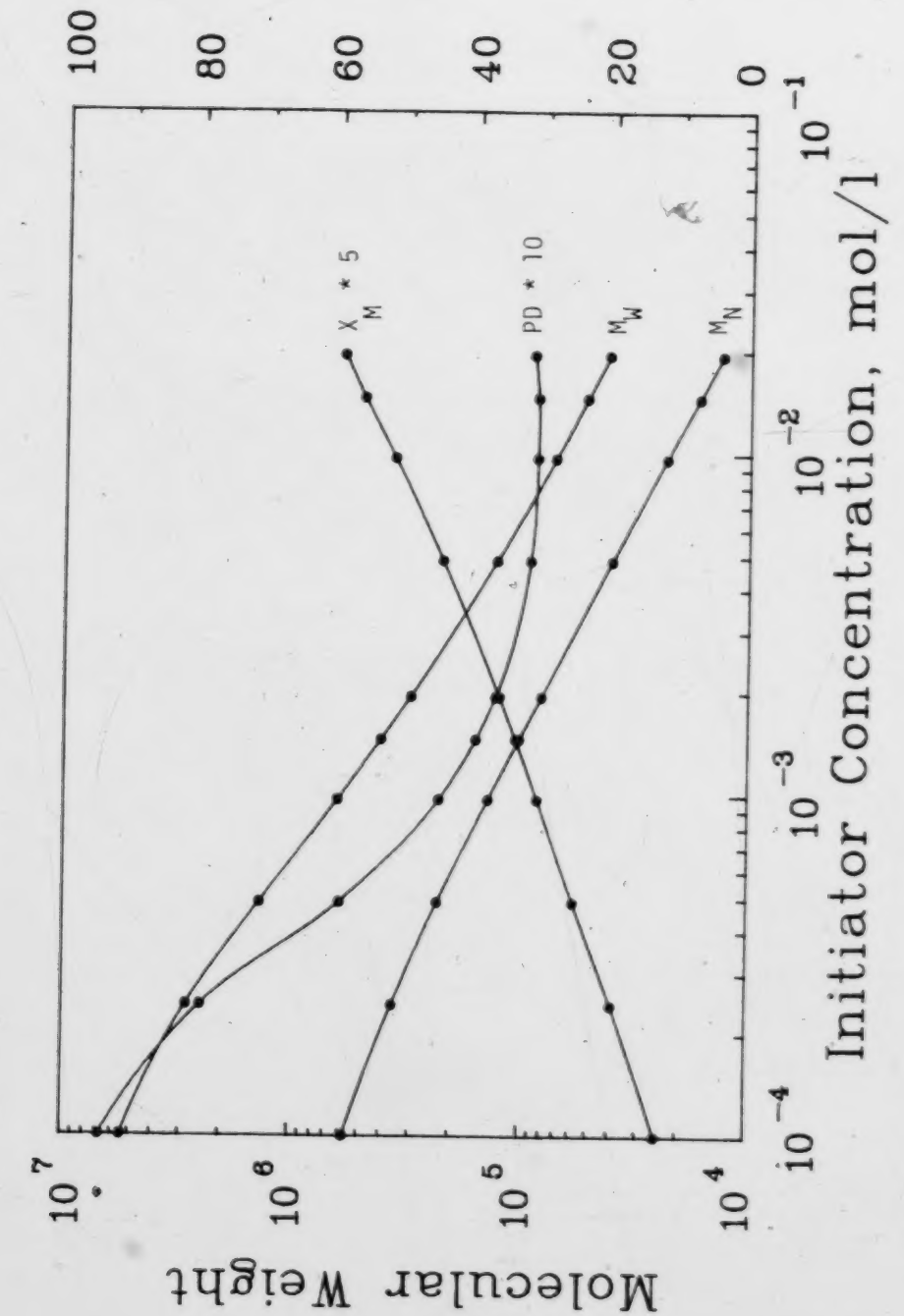


Figure 3.7 Effect of Inlet Initiator Concentration

constant at 3 because the molecular weights decrease at the same rate.

In Figure 3.8 the temperature profiles for three inlet initiator concentrations are plotted. For the low initiator concentration, $1.0 \times 10^{-4}$ mol/l, there is no temperature peak. In this system the rate of initiator decomposition is too slow to initiate significant propagation to give the temperature profile its characteristic peak. Also, the initiator conversion is 98.3% and that of the monomer, 2.6%. This long, slow reaction zone yields a product with high molecular weights.

As the inlet initiator concentration increases the temperature peak becomes more prominent and shifts towards the reactor entrance. In these cases the initiator decomposition has induced the propagation reaction, leading to a significant temperature rise. Accompanying the higher temperatures in the reaction zone are higher termination rates, hence the molecular weights of the product decrease.

## 3.4 Effect of Initial Temperature

The base case model assumes that there is a preheater before the reactor entrance which can heat the

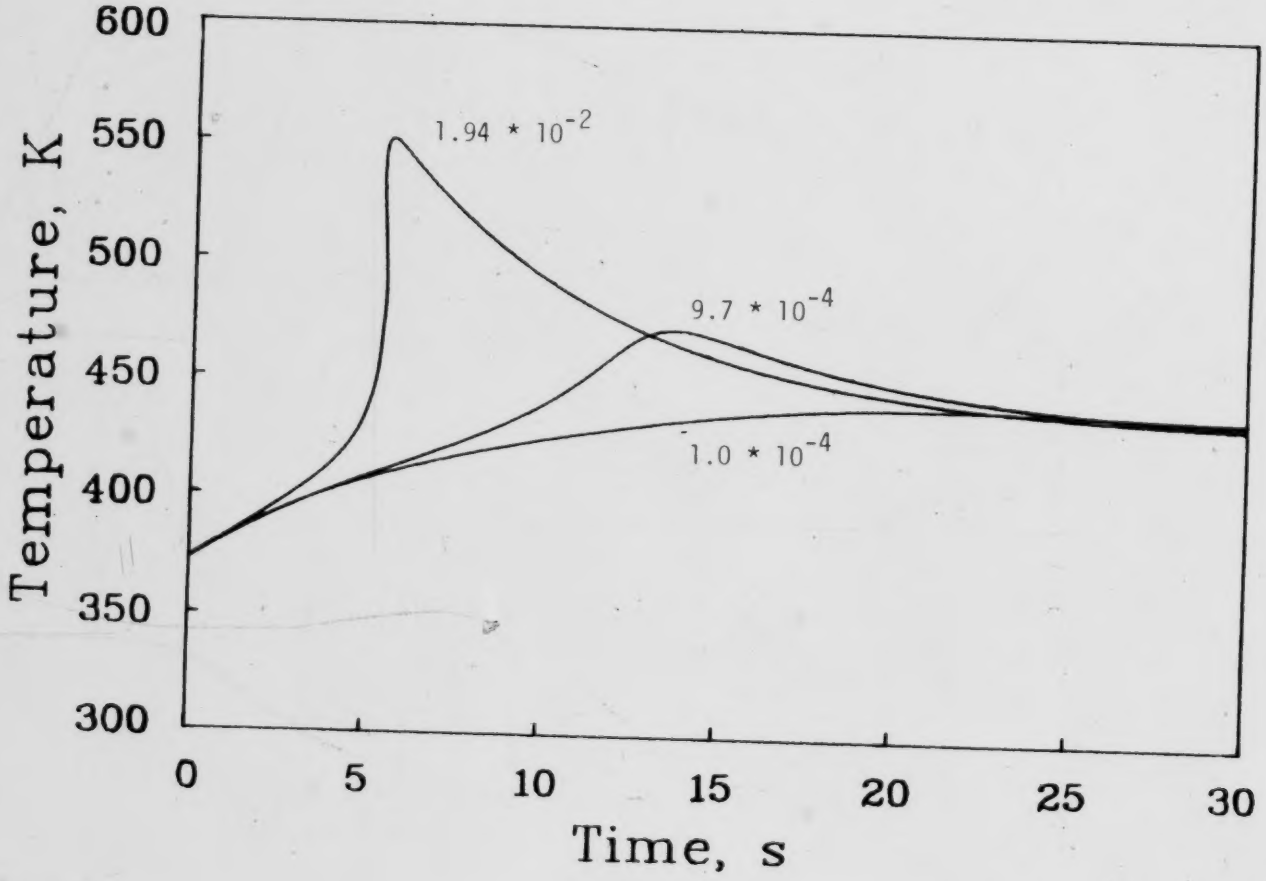


Figure 3.8 Temperature Profiles for Different Initiator Concentrations

monomer feed to any desired temperature, $T_o$. This inlet temperature affects the length of the reactor heating zone. With higher inlet temperatures shorter heating zones are needed to raise the reactants to the reaction temperatures.

The reactor inlet temperature or length of the heating zone is a design variable which affects the product quality. The results for inlet temperatures of 323 to 473 K are listed in Table 3.5 and shown in Figure 3.9. As the inlet temperature increases, and the length of the heating zone decreases, the molecular weights, polydispersity and conversion decrease. This effect is similar to that observed for increasing jacket temperatures.

At the very low inlet temperatures, less than 400 K, $M_N$ and conversion are almost constant. In this region the inlet temperatures are well below the temperature at which initiator decomposition occurs at a significant rate, 410 K. Therefore, increases in inlet temperature in this region do not change the reaction rates significantly and very little change in product quality is observed.

Table 3.5 Effect of Initial Temperature

| INPUT VARIABLES | | | | MEASURED OUTPUTS | | | | |
|---|---|---|---|---|---|---|---|---|
| $T_J$ K | Initial Temperature K | $C_{IO}$ mol/l | Heating Zone Length s | $M_N$ | $M_W$ | PD | $X_M$ % | $X_I$ % |
| 433 | 323 | $9.7 \times 10^{-4}$ | 9.9 | 138400 | 648200 | 4.68 | 6.18 | 100 |
| 433 | 343 | $9.7 \times 10^{-4}$ | 2.7 | 138450 | 647110 | 4.67 | 6.18 | 100 |
| 433 | 363 | $9.7 \times 10^{-4}$ | 6.9 | 138430 | 638000 | 4.61 | 6.18 | 100 |
| 433 | 373 | $9.7 \times 10^{-4}$ | 6.0 | 138290 | 625420 | 4.52 | 6.17 | 100 |
| 433 | 383 | $9.7 \times 10^{-4}$ | 4.8 | 137920 | 603510 | 4.38 | 6.16 | 100 |
| 433 | 403 | $9.7 \times 10^{-4}$ | 2.1 | 134840 | 516590 | 3.83 | 6.02 | 100 |
| 433 | 413 | $9.7 \times 10^{-4}$ | 0.9 | 130360 | 448830 | 3.45 | 5.83 | 100 |
| 433 | 423 | $9.7 \times 10^{-4}$ | 0.6 | 122600 | 374830 | 3.06 | 5.47 | 100 |
| 433 | 433 | $9.7 \times 10^{-4}$ | 0.6 | 111450 | 305730 | 2.74 | 4.98 | 100 |
| 433 | 443 | $9.7 \times 10^{-4}$ | 0.6 | 98696 | 251320 | 2.55 | 4.41 | 100 |
| 433 | 453 | $9.7 \times 10^{-4}$ | 0.6 | 86219 | 212260 | 2.46 | 3.85 | 100 |
| 433 | 473 | $9.7 \times 10^{-4}$ | 0.6 | 65659 | 171830 | 2.62 | 2.93 | 100 |

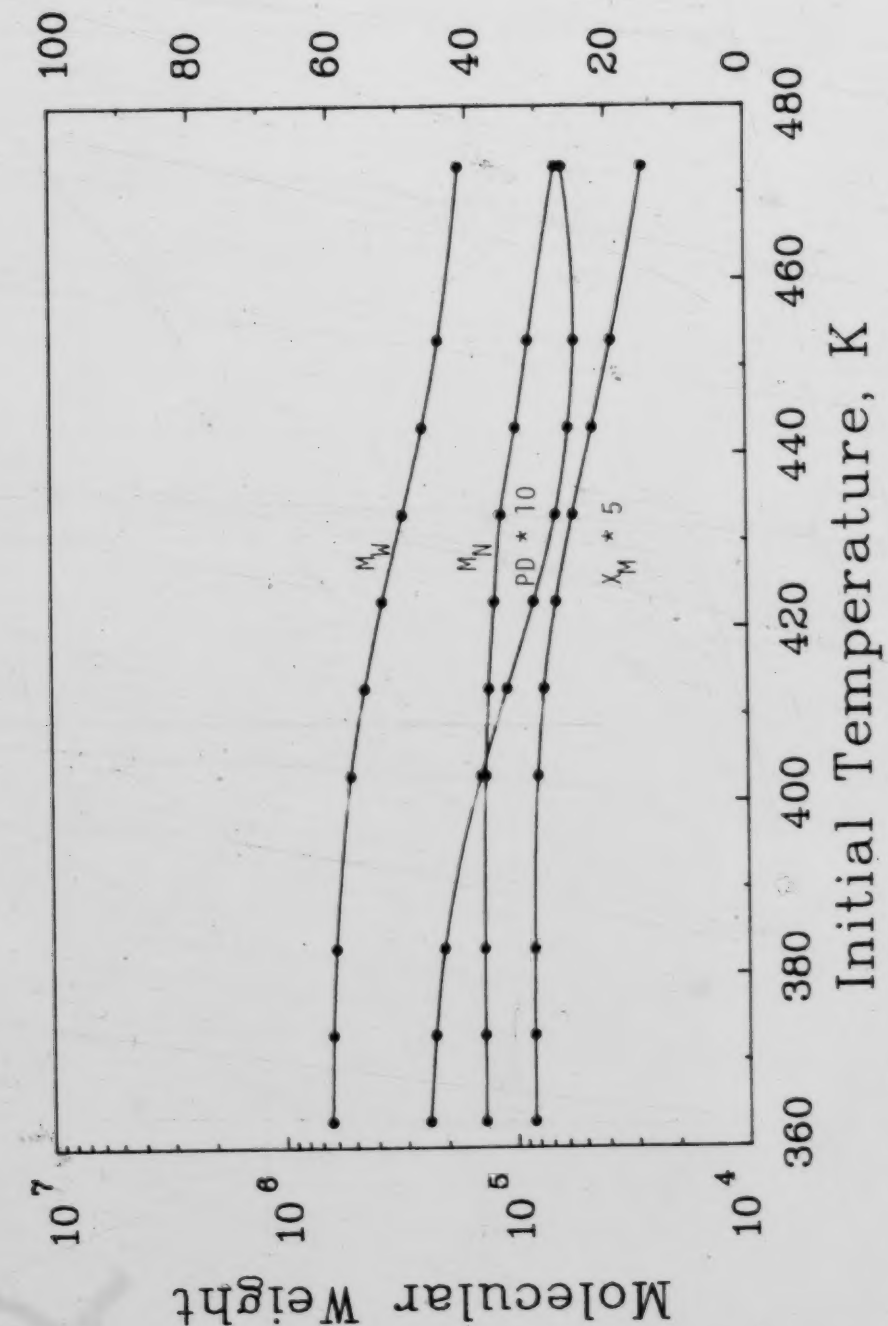


Figure 3.9 Effect of Inlet Temperature

Comparing the temperature profiles for inlet temperatures of 373, 413 and 443 K in Figure 3.10, the temperature peak is closer to the reactor inlet for higher inlet temperatures. Thus, the heating zone is shorter. For the higher inlet temperature the temperature peak is higher, 484 vs. 474 and 473 K, than at lower temperatures. Lower molecular weight products are produced in reactors with high temperature peaks located close to the reactor entrance.

A high pressure tubular polyethylene reactor does not usually have a feed preheater upstream of the reactor. Instead, initiator is injected into the reactor downstream of the entrance at the point at which the monomer feed has been heated to a desired temperature by the heating jacket. The design engineer must decide upon the approximate locations of the injection points during the reactor design stage. For him, knowledge of the effect of the heating zone length is important in determining the physical location of the injection points.

## 3.5 Isothermal Reaction Zone Reactor

An alternative to operating the tubular reactor at constant jacket temperature is to operate it isothermally in the reaction zone by manipulation of the

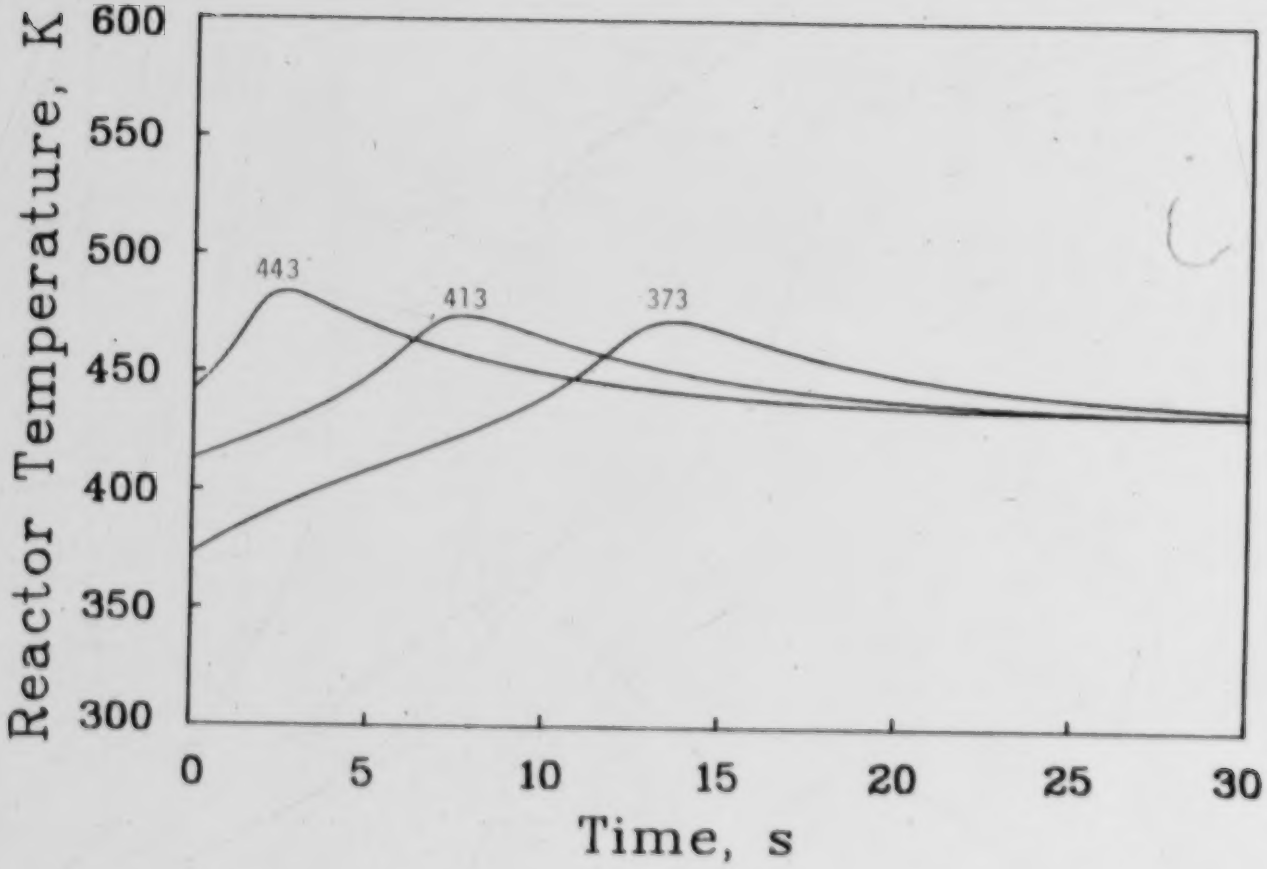


Figure 3.10 Temperature Profiles for Different Inlet Temperatures

jacket temperature. The main advantage of isothermal operation, in this study, is the ease of interpretation of results. By maintaining a constant reactor temperature in the reaction zone the temperature effects due to the exothermic propagation reaction are eliminated.

The base conditions for the isothermal and constant jacket temperature (base case) are compared in Table 3.6. The inlet conditions for both reactors are the same. Both reactors have a heating zone where the hot, constant temperature jacket fluid heats the reactants. The major difference in the reactor structures is at the beginning of the reaction zone. In the base case reactor the jacket temperatures over the entire length of the reactor is constant. In the isothermal reactor the jacket temperature is manipulated in the reaction and cooling zones to control the reactor temperature in these zones at 450 K. The temperature and conversion profiles for the isothermal reactor are shown in Figure 3.11.

In the constant temperature reaction zone the jacket temperature is manipulated to control the reactor temperature. From the energy balance in the reactor model the jacket temperature is:

Table 3.6 Comparison of Base Case and Isothermal Reaction Zone Reactors

| | INPUT VARIABLES | | | | MEASURED OUTPUTS | | | | |
|---|---|---|---|---|---|---|---|---|---|
| | $T_J$ K | $T_0$ K | $C_{I0}$ mol/l | Isothermal Temperature K | $M_N$ | $M_W$ | PD | $X_M$ % | $X_I$ % |
| Constant Jacket Temperature | 433 | 373 | $9.7 \times 10^{-4}$ | - | 138290 | 625420 | 4.52 | 6.17 | 100 |
| Isothermal | 433 (initial) | 373 | $9.7 \times 10^{-4}$ | 450 | 161590 | 929570 | 5.75 | 7.21 | 100 |

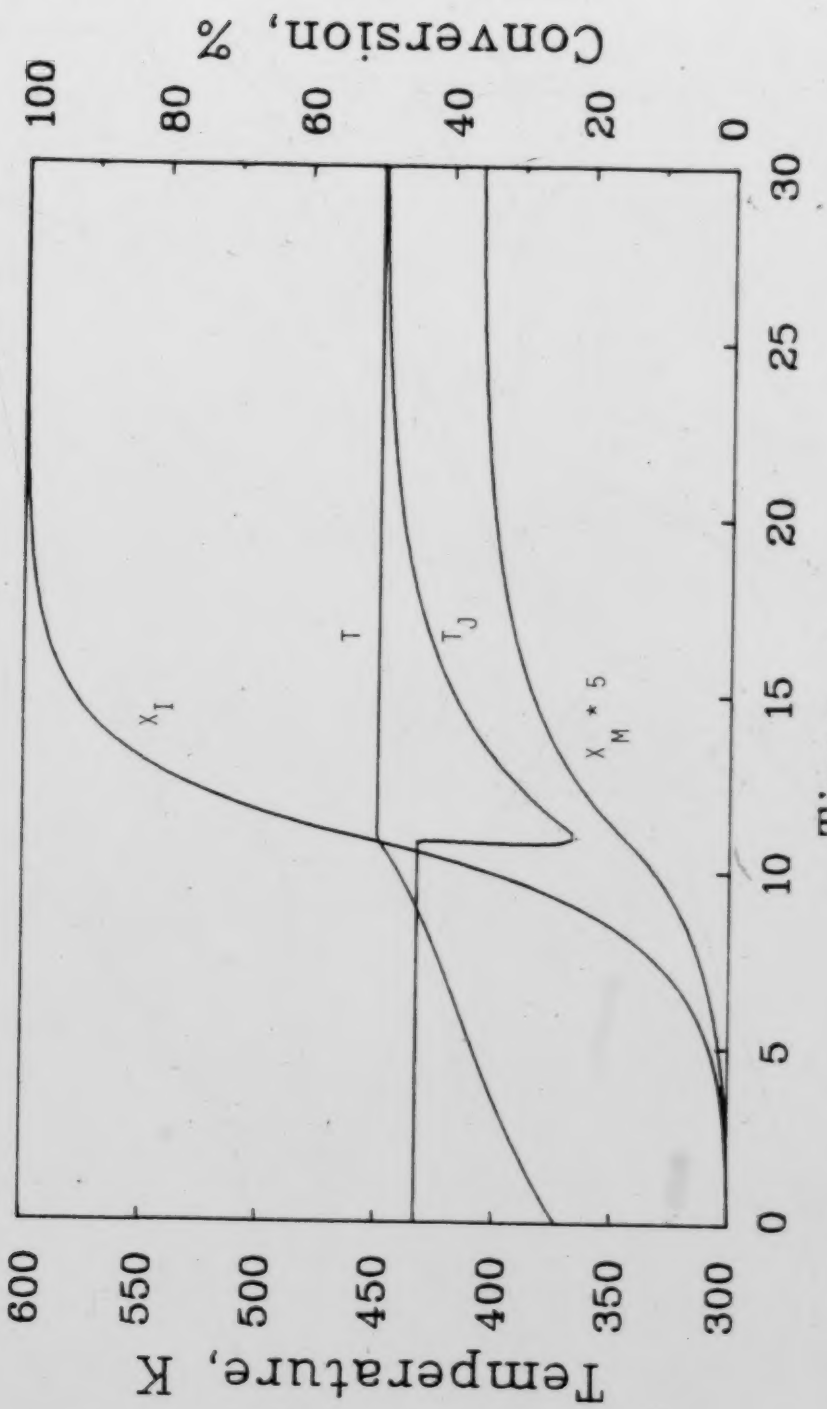


Figure 3.11 Isothermal Reaction Zone Profiles

$$T_J = T + \frac{\Delta H\, R_p\, D}{4\, U} \qquad (3.1)$$

Where

D is the reacor diameter, m

$\Delta H$ is the heat of polymerization, cal/mol

$R_p$ is the rate of propagation, mol/(l.s)

T is the reactor temperature, K

$T_J$ is the jacket temperature, K

U is the overall heat transfer coefficient, $(cal/m^2.s.^{\circ}C)$

At the beginning of the reaction zone the jacket temperature decreases from 433 to 368 K. Since the initiator is decomposing and propagation is occurring the jacket temperature must be less that the reactor fluid temperature in order to remove the exothermic heat of polymerization. In Figure 3.11 as time increases the jacket temperature approaches the isothermal temperature. The polymerization rate is high at the beginning of the reaction zone and slows down as the initiator is consumed. Hence, the jacket temperature approaches the reactor temperature because the rate of reaction decreases.

Comparing the isothermal and constant jacket temperature reactors, the reaction zone in the isothermal reactor is longer because the reactor temperature is controlled at 450 K. This results in an increase in molecular weights, polydispersity and conversion, due to the lower polymerization temperature and longer reaction time. This is similar to operating the constant jacket temperature reactor at lower jacket temperatures.

The main choices of control variables in the isothermal reactor are the constant reactor temperature in the reaction zone (isothermal temperature), inlet initiator concentration and initial reactor temperature. The effects of isothermal temperature on the polymer product are similar to those of the jacket temperature. The effects of initiator concentration and initial temperature are similar in both types of reactors. These three control variables will now be investigated for the isothermal reactor.

The effect of changes in the isothermal temperature on the polymer product are listed in Table 3.7 and shown in Figure 3.12. The isothermal temperature is varied from 430 to 500 K. In all these studies the effect of the heating zone was eliminated by injecting the monomer and initiator into the reactor at the desired

Table 3.7 Effect of Isothermal Temperature

| INPUT VARIABLES | | | | MEASURED OUTPUTS | | | | |
|---|---|---|---|---|---|---|---|---|
| Isothermal Temperature K | $T_{Jo}$ K | $T_o$ K | $C_{IO}$ mol/l | $M_N$ | $M_W$ | PD | $X_M$ % | $X_I$ % |
| 430 | 533 | 430 | $9.7 \times 10^{-4}$ | 182320 | 1104900 | 6.06 | 7.76 | 95.3 |
| 440 | 533 | 440 | $9.7 \times 10^{-4}$ | 169300 | 775800 | 4.59 | 7.55 | 99.9 |
| 450 | 533 | 450 | $9.7 \times 10^{-4}$ | 140690 | 487710 | 3.47 | 6.28 | 100 |
| 460 | 533 | 460 | $9.7 \times 10^{-4}$ | 114520 | 346290 | 3.02 | 5.11 | 100 |
| 470 | 533 | 470 | $9.7 \times 10^{-4}$ | 93943 | 269290 | 2.87 | 4.19 | 100 |
| 480 | 533 | 480 | $9.7 \times 10^{-4}$ | 77795 | 222730 | 2.86 | 3.47 | 100 |
| 490 | 533 | 490 | $9.7 \times 10^{-4}$ | 65070 | 194040 | 2.98 | 2.90 | 100 |
| 500 | 533 | 500 | $9.7 \times 10^{-4}$ | 54993 | 177460 | 3.23 | 2.45 | 100 |

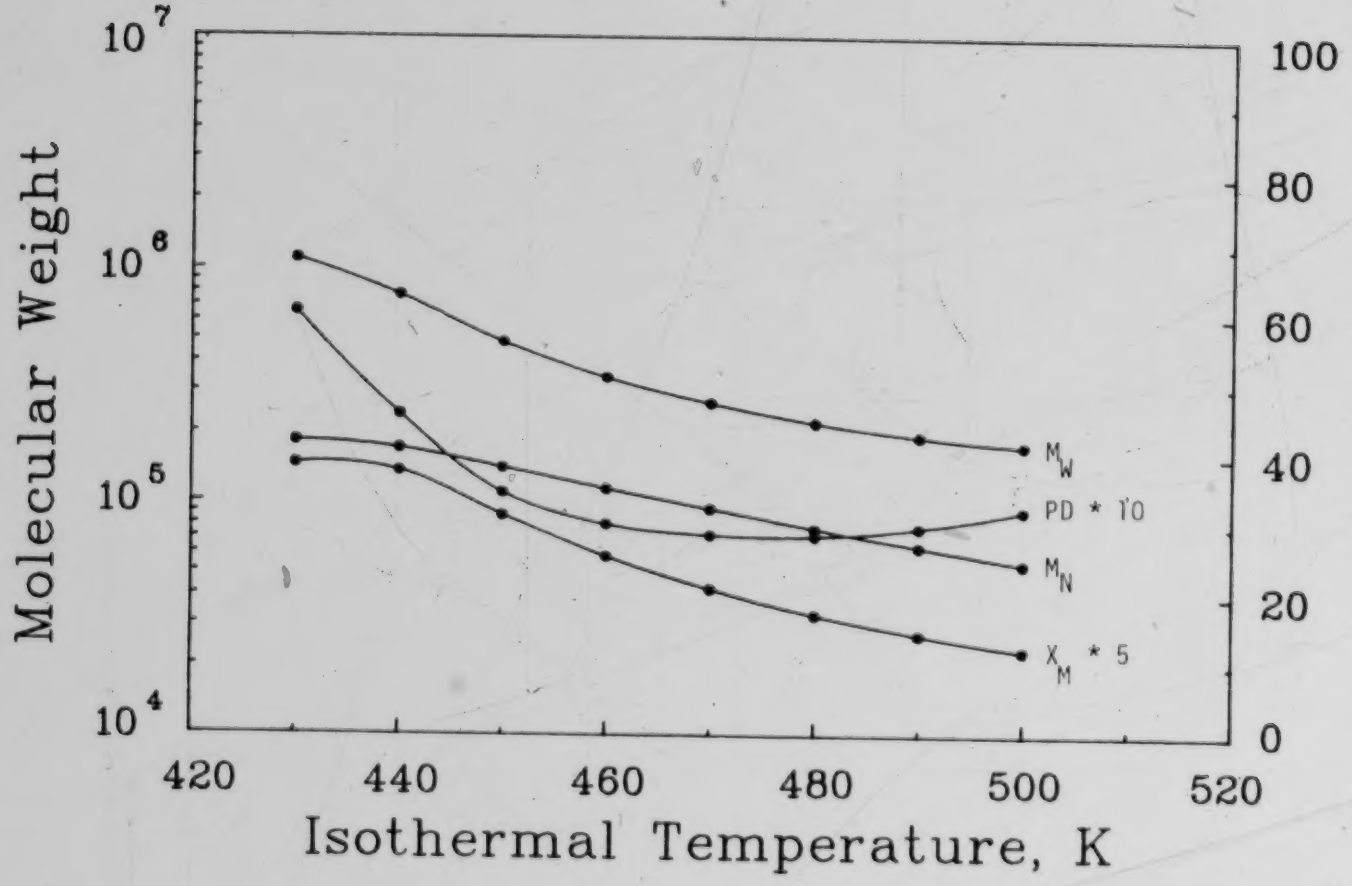


Figure 3.12 Effect of Isothermal Temperature

isothermal temperature. As the isothermal temperature increases the molecular weights and conversion all decrease. This is the same trend as was observed for increasing jacket temperature in the constant jacket temperature reactor. Two operating problems are encountered over this range of isothermal temperatures. With low isothermal temperatures, less than 440 K, the initiator does not completely decompose during the reactor residence time. Also, for isothermal operation above 470 K the jacket fluid must be less than 273 K to absorb large quantities of heat in the reaction zone.

The effects of variation of the inlet initiator concentration in the isothermal reactor are given in Table 3.8 and shown in Figure 3.13. As in the constant jacket temperature reactor, increases in the initiator concentration cause decreases in molecular weights and increases in conversion. Unlike the base type reactor, the polydispersity of the product polymer is constant for all inlet initiator concentrations. In the isothermal reactor the reactor temperature is constant at 450 K in the reaction zone. Therefore, the propagation, transfer and termination rate constants will all be constant. The amount of initiator that can be injected into the isothermal reactor is governed by the operating limits of the cooling jacket. At concentrations greater than 2.6 x

Table 3.8 Effect of Initiator Concentration in Isothermal Reactor

| INPUT VARIABLES | | | | MEASURED OUTPUTS | | | | |
|---|---|---|---|---|---|---|---|---|
| Isothermal Temperature K | $T_{Jo}$ K | $T_o$ K | $C_{IO}$ mol/l | $M_N$ | $M_W$ | PD | $X_M$ % | $X_I$ % |
| 450 | 473 | 410 | $4.85 \times 10^{-4}$ | 717170 | 2942600 | 4.10 | 1.60 | 100 |
| 450 | 473 | 410 | $9.7 \times 10^{-4}$ | 500750 | 2043400 | 4.08 | 2.23 | 100 |
| 450 | 473 | 410 | $1.455 \times 10^{-4}$ | 405420 | 1645300 | 4.06 | 2.71 | 100 |
| 450 | 473 | 410 | $1.94 \times 10^{-4}$ | 349170 | 1411600 | 4.04 | 3.12 | 100 |
| 450 | 473 | 410 | $4.85 \times 10^{-4}$ | 216260 | 858700 | 3.97 | 4.83 | 100 |
| 450 | 473 | 410 | $9.7 \times 10^{-4}$ | 149860 | 584430 | 3.90 | 6.69 | 100 |
| 450 | 473 | 410 | $1.164 \times 10^{-3}$ | 135870 | 525730 | 3.87 | 7.28 | 100 |
| 450 | 473 | 410 | $1.455 \times 10^{-3}$ | 120640 | 463860 | 3.84 | 8.08 | 100 |
| 450 | 473 | 410 | $1.94 \times 10^{-3}$ | 104450 | 402550 | 3.85 | 9.32 | 100 |
| 450 | 473 | 410 | $4.85 \times 10^{-3}$ | 63141 | 233360 | 3.70 | 14.1 | 100 |

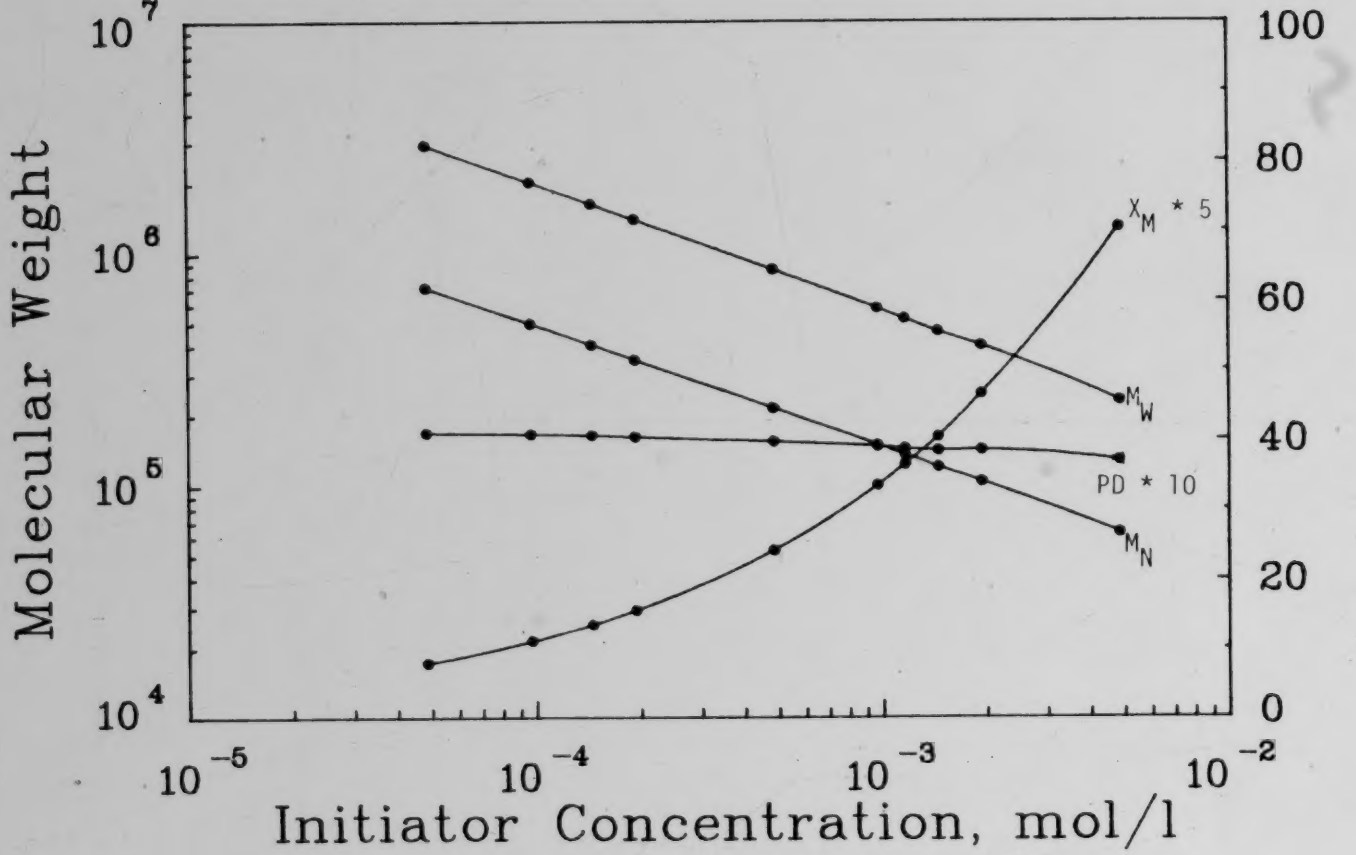


Figure 3.13 Effect of Inlet Initiator Concentration in Isothermal Reaction Zone Reactor

$10^{-3}$ mol/l the jacket temperature must be maintained below 273 K in order to control the isothermal reaction zone temperature at 450 K.

The effect of inlet reactor temperature is investigated by varying the temperature from 363 to 450 K, while keeping the reaction zone temperature constant at 450 K. These results are listed in Table 3.9 and shown in Figure 3.14. In these studies the heating zone length is defined as the fraction of the reactor length required to heat the reactants to the 450 K. As in the constant jacket temperature reactor, at initial temperatures less than 410 K, changes in temperature have very little effect on the polymer product. As the initial temperature is increased above 410 K the molecular weights, conversion and polydispersity decrease slightly with increasing inlet temperature and decreasing heating zone length. This effect was observed and explained for the constant jacket temperature reactor.

Overall, the isothermal reaction zone reactor behaves similarly to the constant jacket temperature reactor. In both reactors increases in the reactor

Table 3.9 Effect of Initial Temperature in Isothermal Reactor

| INPUT VARIABLES | | | | | MEASURED OUTPUTS | | | | |
|---|---|---|---|---|---|---|---|---|---|
| Isothermal Temperature K | $T_{Jo}$ K | $T_o$ K | $C_{IO}$ mol/l | Heating Zone Length s | $M_N$ | $M_W$ | PD | $X_M$ % | $X_I$ % |
| 450 | 473 | 363 | $9.7 \times 10^{-4}$ | 14.1 | 152000 | 671320 | 4.42 | 6.79 | 100 |
| 450 | 473 | 373 | $9.7 \times 10^{-4}$ | 14.1 | 152120 | 665710 | 4.38 | 6.79 | 100 |
| 450 | 473 | 383 | $9.7 \times 10^{-4}$ | 14.1 | 152250 | 656030 | 4.31 | 6.80 | 100 |
| 450 | 473 | 393 | $9.7 \times 10^{-4}$ | 14.1 | 152020 | 637800 | 4.20 | 6.79 | 100 |
| 450 | 473 | 400 | $9.7 \times 10^{-4}$ | 14.1 | 151500 | 619460 | 4.09 | 6.76 | 100 |
| 450 | 473 | 410 | $9.7 \times 10^{-4}$ | 14.1 | 149860 | 584430 | 3.90 | 6.69 | 100 |
| 450 | 473 | 420 | $9.7 \times 10^{-4}$ | 14.1 | 147670 | 548070 | 3.71 | 6.59 | 100 |
| 450 | 473 | 430 | $9.7 \times 10^{-4}$ | 14.1 | 145100 | 518090 | 3.57 | 6.48 | 100 |
| 450 | 473 | 440 | $9.7 \times 10^{-4}$ | 14.7 | 142400 | 497150 | 3.49 | 6.36 | 100 |
| 450 | 473 | 450 | $9.7 \times 10^{-4}$ | 14.7 | 140690 | 487710 | 3.47 | 6.28 | 100 |

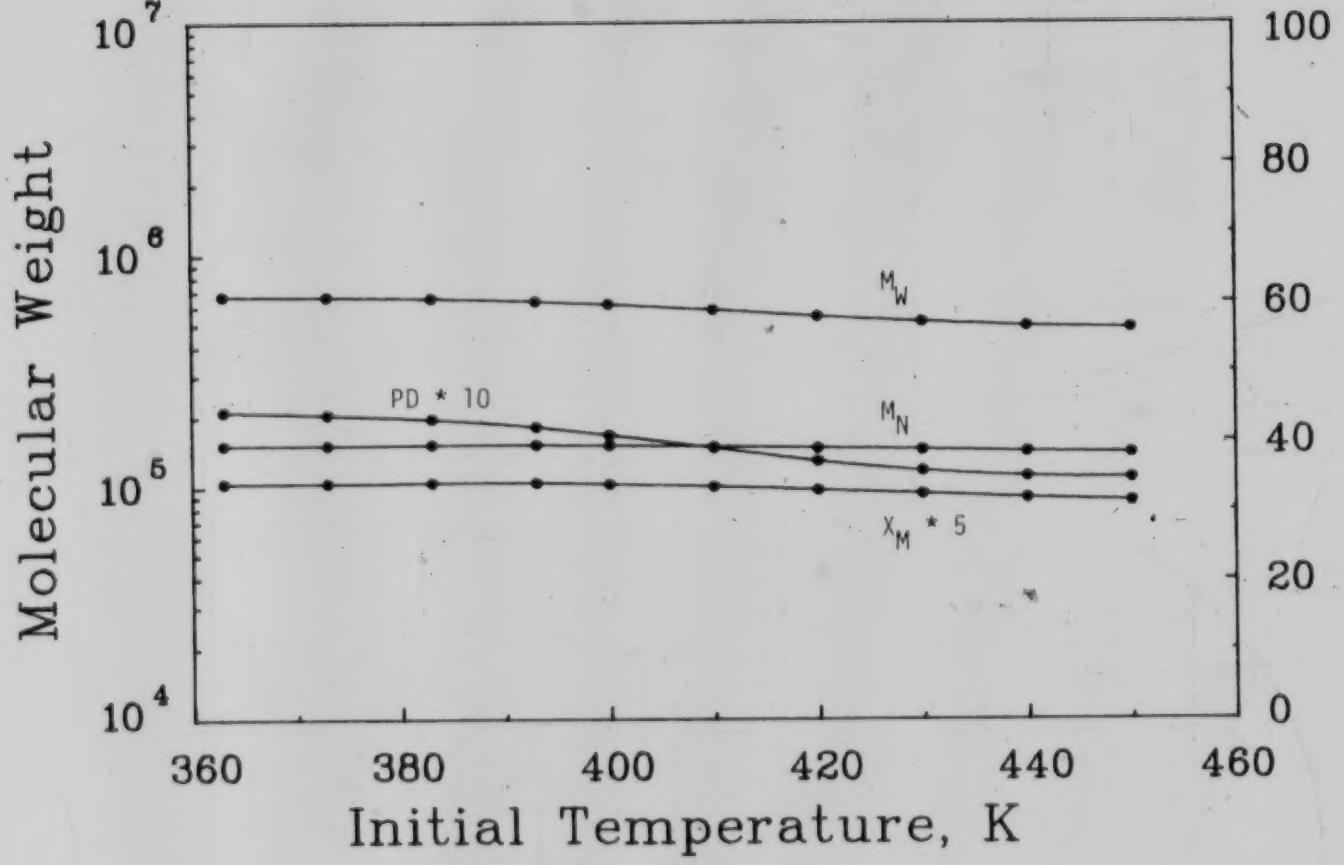


Figure 3.14 Effect of Initial Temperature in Isothermal Reactor

temperature, and manipulation of the jacket or inlet temperature all cause decreases in the product molecular weights and conversion. Increases in the inlet initiator concentration in both types of reactors cause decreases in the molecular weights and increases in the conversion. The advantage of an isothermal operation in the reaction zone is the increase in control over the product polymer properties. The disadvantage of this type of operation is the operational limitation in jacket temperature manipulations. To control the reaction zone temerature by jacket temperature manipulation many streams of coolant at different temperatures would have to be circulated around the reactor and each coolant zone must be carefully controlled. Thus, temperature control of an isothermal reactor is more difficult to implement. Also, the isothermal reaction zone design is not a practical design for an industrial reactor.

## 3.6 Model Features Observed in the Simulations

In the base case model simulations, it was assumed that the overall heat transfer coefficient is constant, the radical steady state hypothesis is invalid, and branching is an important reaction in the mechanism.

The effects of these features were observed in the simulations.

In the constant jacket temperature reactor higher reactor temperatures, either by higher jacket temperatures or higher inlet monomer temperatures, decreased the molecular weights and conversion. This effect was also observed in the isothermal reactor. From this it can be concluded that the reactor temperature is a primary variable which affects the polymer molecular weights.

In the derivation of the material balance equation for live radicals in the reactor, it was not assumed that the rate of change of radical concentration is zero or significantly less than the rates of change for other species. Thus the steady state hypothesis has not been made for the radical concentration. In the base case simulation the zeroth moment of the free radical concentration, G(1,t), changes from $5.9 \times 10^{-8}$ to $1.0 \times 10^{-4}$ in the heating and reaction zones. Using a modified model with the assumption that the steady state hypothesis is valid, the conversion and molecular weight profiles are the same as in the base case simulation. However, with high initiator concentrations the steady state hypothesis is no longer valid because the radical moments change rapidly in the reaction zone. With an

inlet initiator concentration of $1.94 \times 10^{-2}$ mol/l, the zeroth moment of the radical concentration changes from $1.3 \times 10^{-5}$ to $3.5 \times 10^{-8}$ in 0.3 s. Using the steady state hypothesis a numerical solution for this case cannot be obtained because the steady state assumption provides an incorrect value for the zeroth radical moment. Since this work is based on simulations it is important to be able to investigate wide ranges of control variable conditions. For this reason the steady state hypothesis was assumed not to be generally applicable.

The transfer to polymer, or branching, reaction is a feature of this model. Low density polyethylene produced in high pressure tubular reactors is characterized by its high degree of long chain branching. One indication of the degree of long chain branching is the polydispersity. Simulation examples with high polydispersity, greater than 5, include: the base-type simulation with a jacket temperature of 423 K; the base-type simulation with initiator concentrations less than $4.85 \times 10^{-4}$ mol/l; and isothermal simulation with an isothermal reaction temperature of 430 K. Under these conditions this reactor model predicts polyethylene properties which are typical of high pressure tubular reactors.

# 4. SENSITIVITY ANALYSIS

## 4.1 Mathematical Sensitivity Coefficients

Using statistical sensitivity analysis the effect of changes in the model inputs on the model outputs can be calculated. For the base case reactor model the sensitivity of all reactor outputs with respect to jacket temperature and inlet initiator concentration are investigated.

The sensitivity coefficient for the parameter, $p_j$, and the output, $y_i$, is defined as the first partial derivative of $y_i$ with respect to $p_j$:

$$\psi_{ij} = \frac{\partial y_i}{\partial p_j} \tag{4.1}$$

The normalized sensitivity coefficient is defined as:

$$\psi_{ij} = \psi_{ij} * \frac{p_j}{y_i} \tag{4.2}$$

Since the tubular polyethylene reactor model consists of a set of nonlinear differential equations the sensitivity coefficients cannot be written explicity. The method of sensitivity analysis presented by Atherton et.al.(1975) and Beck and Arnold (1977) yields a system of differential equations, the sensitivity equations. The variation of

the sensitivity coefficients with respect to the reactor coordinate, time, is obtained by numerically integrating the sensitivity equations. The sensitivity equations for the base case model are presented in Appendix B. Beck and Arnold (1977) also recommend a finite difference method for obtaining numerical sensitivity equations. This method was used to check the sensitivity equation calculations, and good agreement was achieved in all cases.

### 4.1.1 Jacket Temperature Sensitivities

The effects of perturbations in the jacket temperature are shown in Figures 4.1 to 4.3. In Figure 4.1 the normalized sensitivities of monomer and initiator conversion and dimensionless temperature, $T/T_0$, are plotted. Initiator conversion and monomer conversion are very sensitive to perturbations in jacket temperature in the hot reaction zone. The reactor temperature is much less sensitive to perturbations in jacket temperature, due to the use of dimensionless temperature.

Figure 4.2 shows the sensitivities of the molecular weights to changes in jacket temperature. Increases in jacket temperature decrease the molecular weights overall. In the reaction zone positive perturbations in the jacket temperature increase the molecular weights.

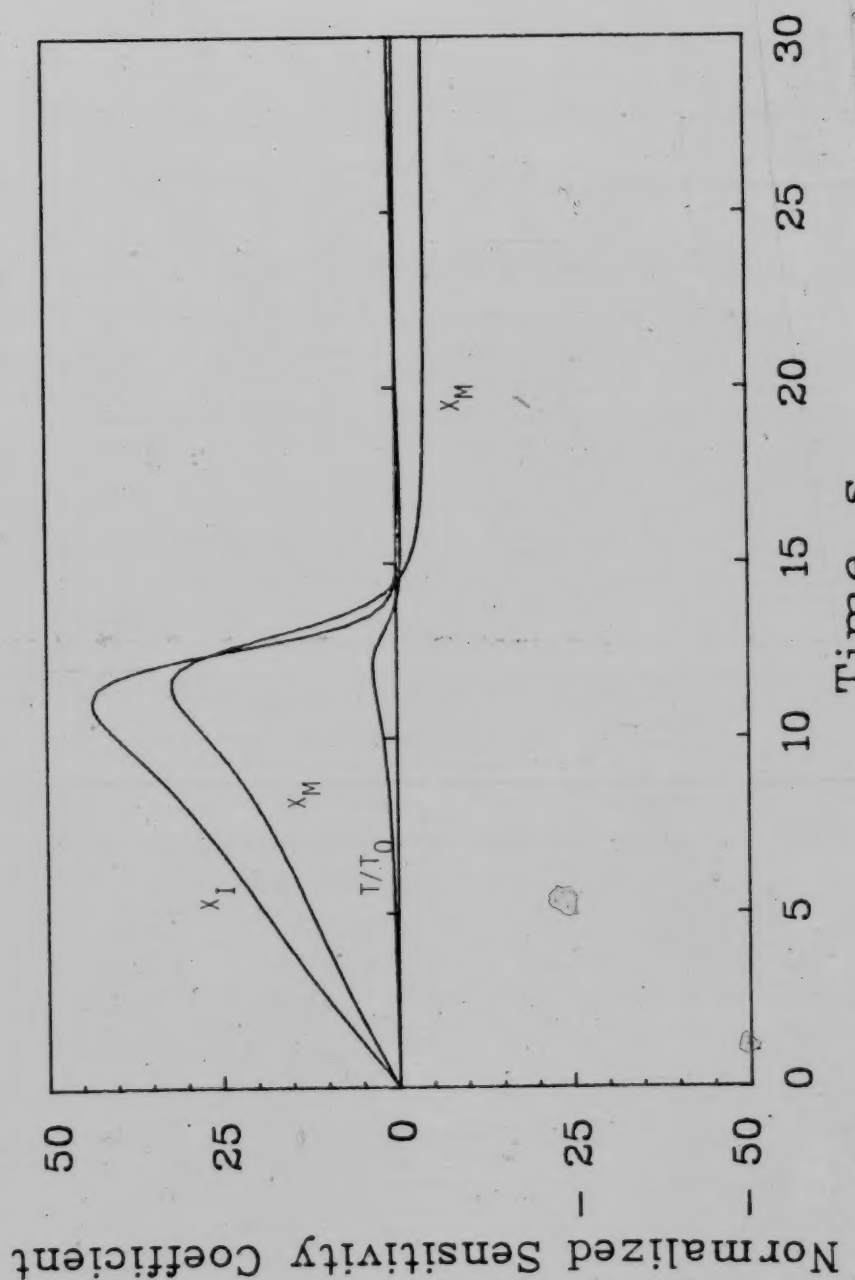


Figure 4.1 Conversion and Temperature Sensitivities with respect to Jacket Temperature

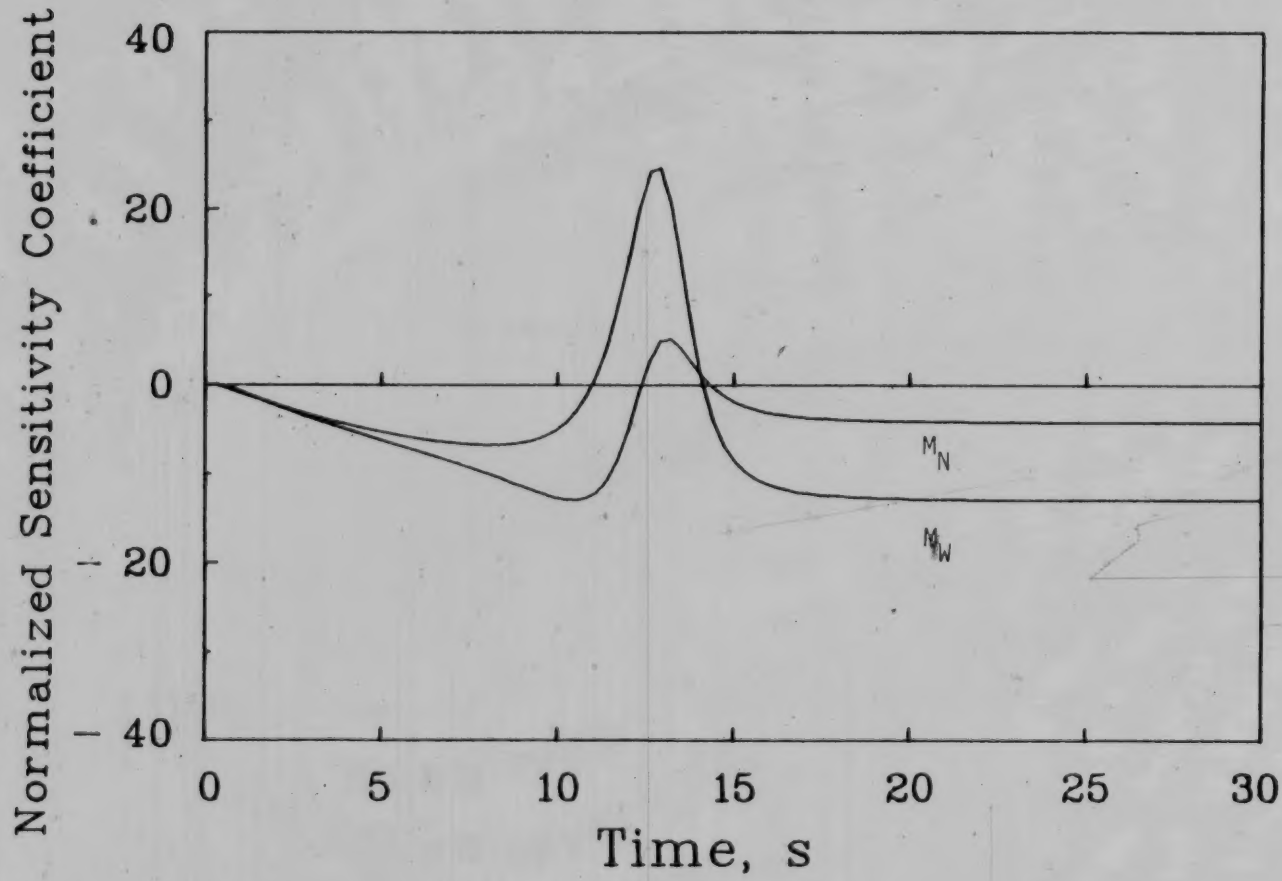


Figure 4.2 Molecular Weight Sensitivities with respect to Jacket Temperature

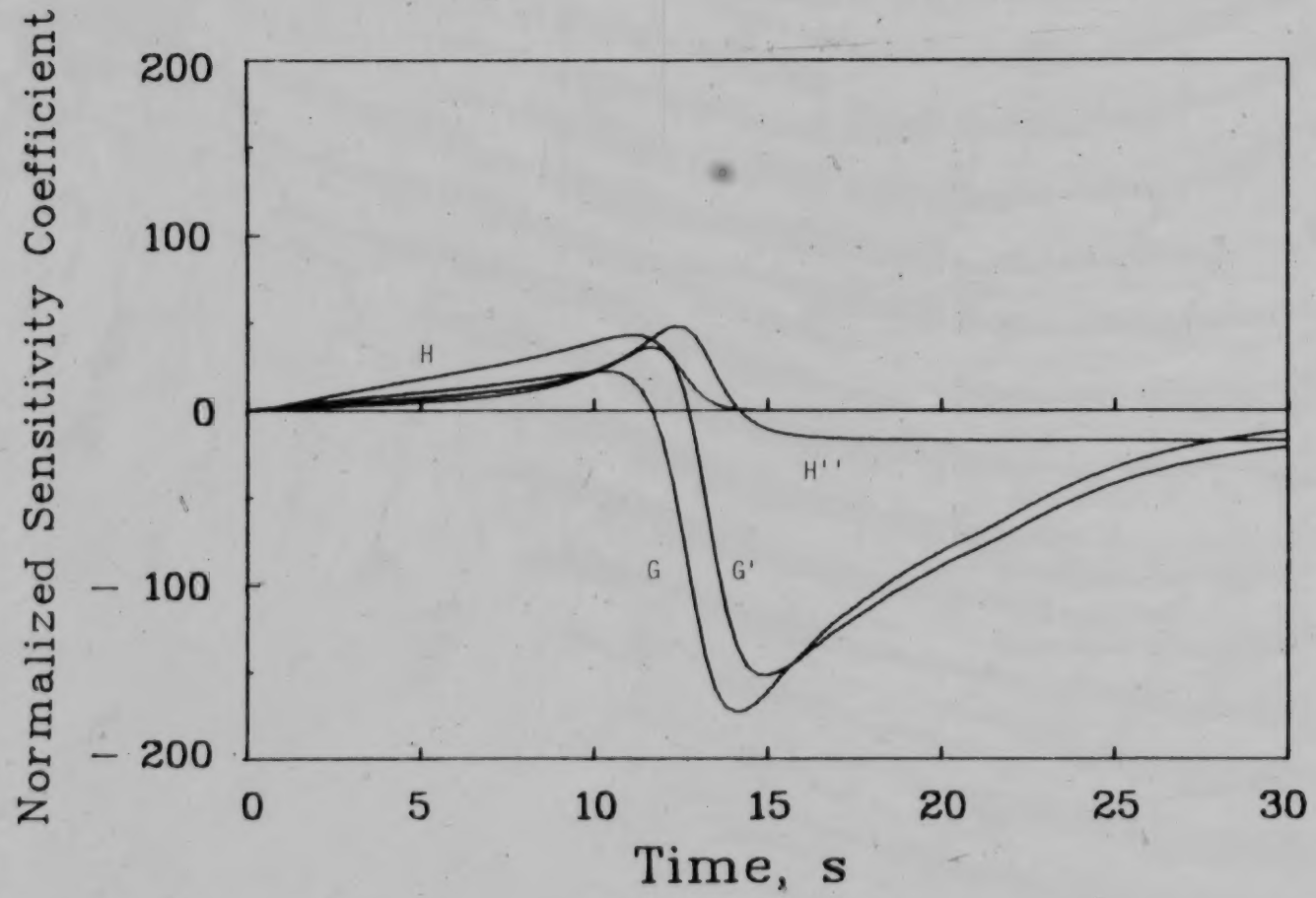


Figure 4.3 Moment Sensitivities with respect to Jacket Temperature

In Figure 4.3 the sensitivities of the radical and polymer moments are shown. Positive perturbations in jacket temperature decrease all of the radical moments and the second polymer moment overall and have little effect on the zeroth polymer moment. In the heating zone all of the moments have positive sensitivity coefficients. As in the conversion and molecular weight sensitivities, the signs of the sensitivities change in the reaction zone.

### 4.1.2 Inlet Initiator Concentration Sensitivities

The sensitivities of the model predictions with respect to the inlet initiator concentration are shown in Figures 4.4 to 4.6. In Figure 4.4 the conversion and temperature sensitivities are plotted. In the heating and reaction zones positive perturbations in the initiator concentration increase the initiator and monomer conversions. At the reactor outlet the initiator conversion sensitivity is zero, and that of the monomer conversion is 0.3. Throughout the entire reactor the temperature sensitivity is approximately zero.

The molecular weight sensitivities, shown in Figure 4.5, are generally small negative values. As in the jacket temperature case, the molecular weight sensitivities increase in the reaction zone and decrease

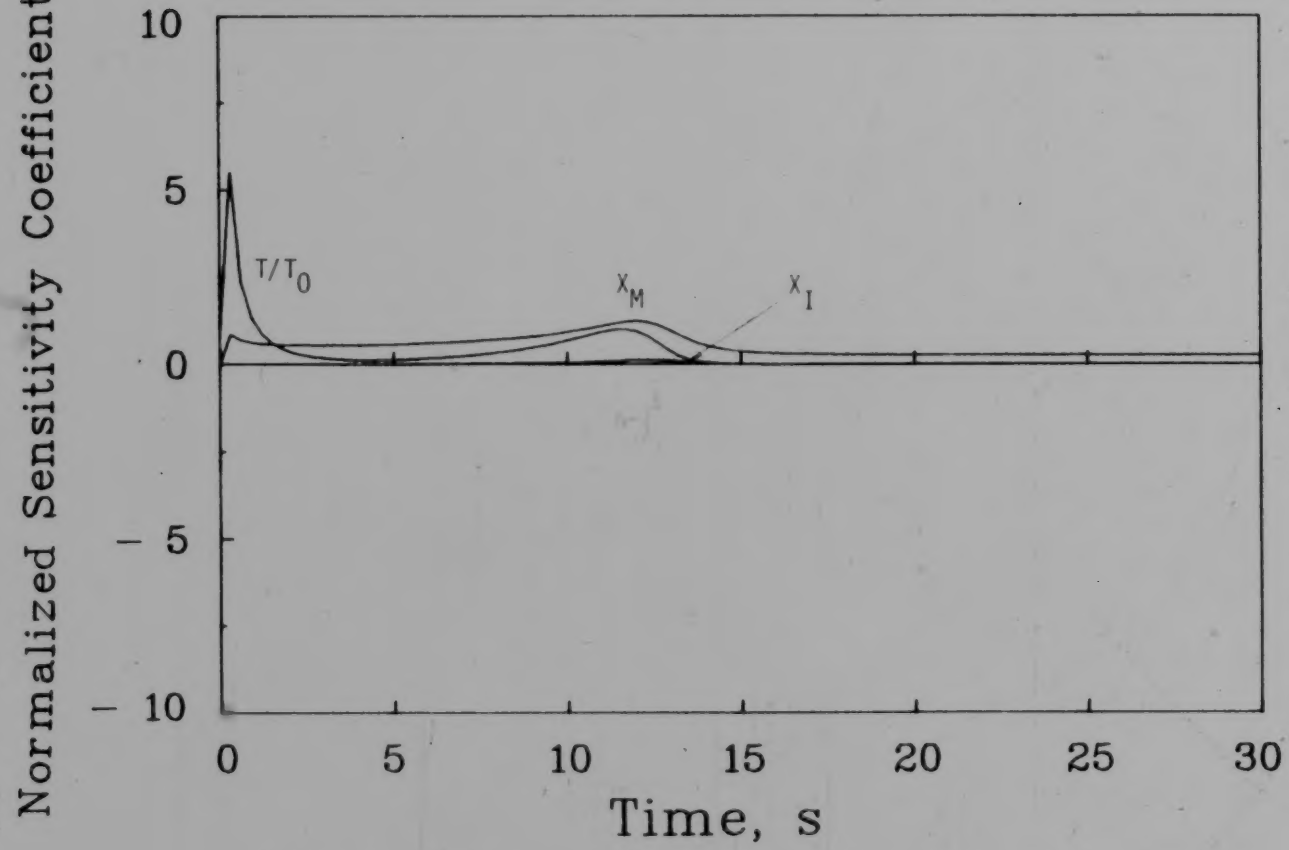


Figure 4.4 Conversion and Temperature Sensitivities with respect to Inlet Initiator Concentration

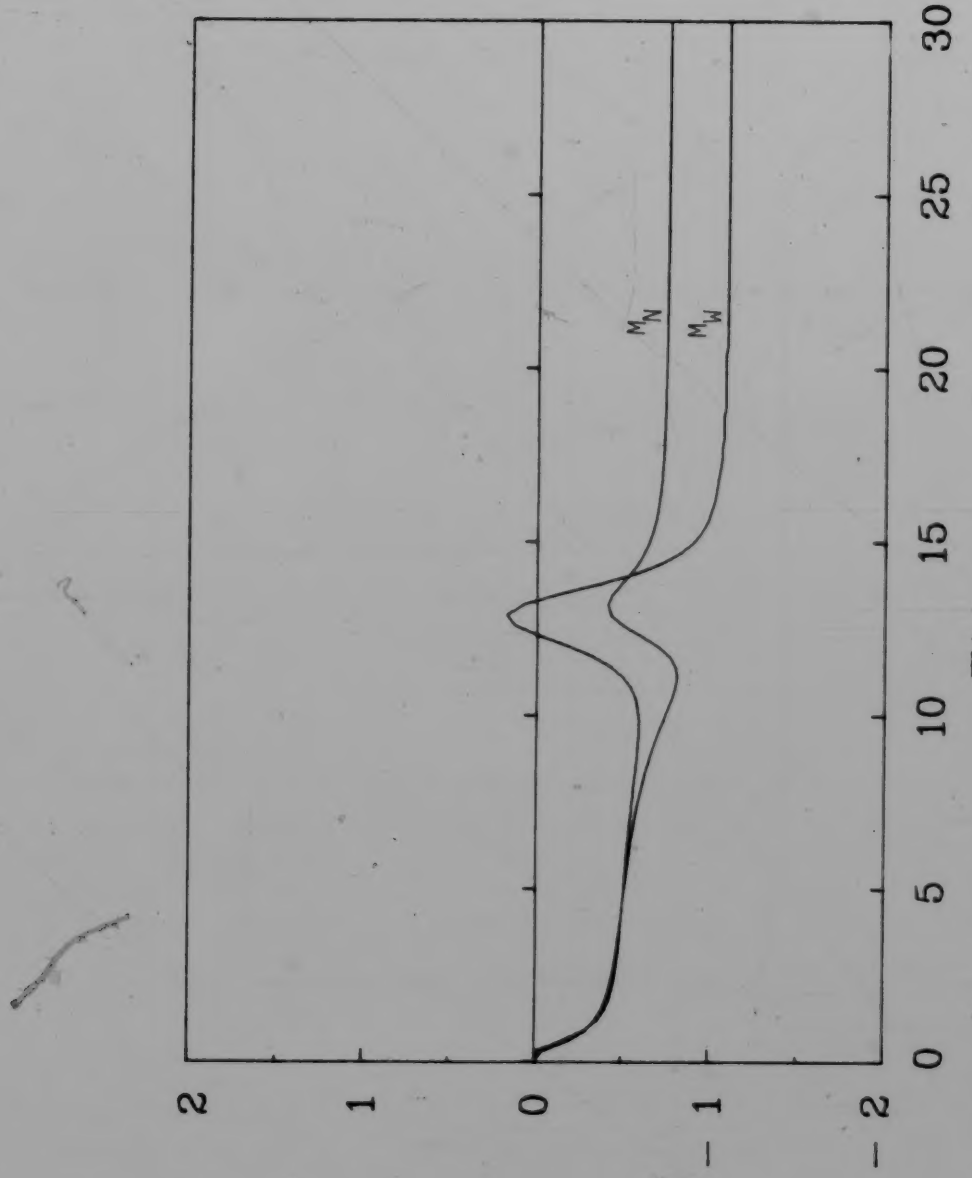


Figure 4.5 Molecular Weight Sensitivities with respect to Inlet Initiator Concentration

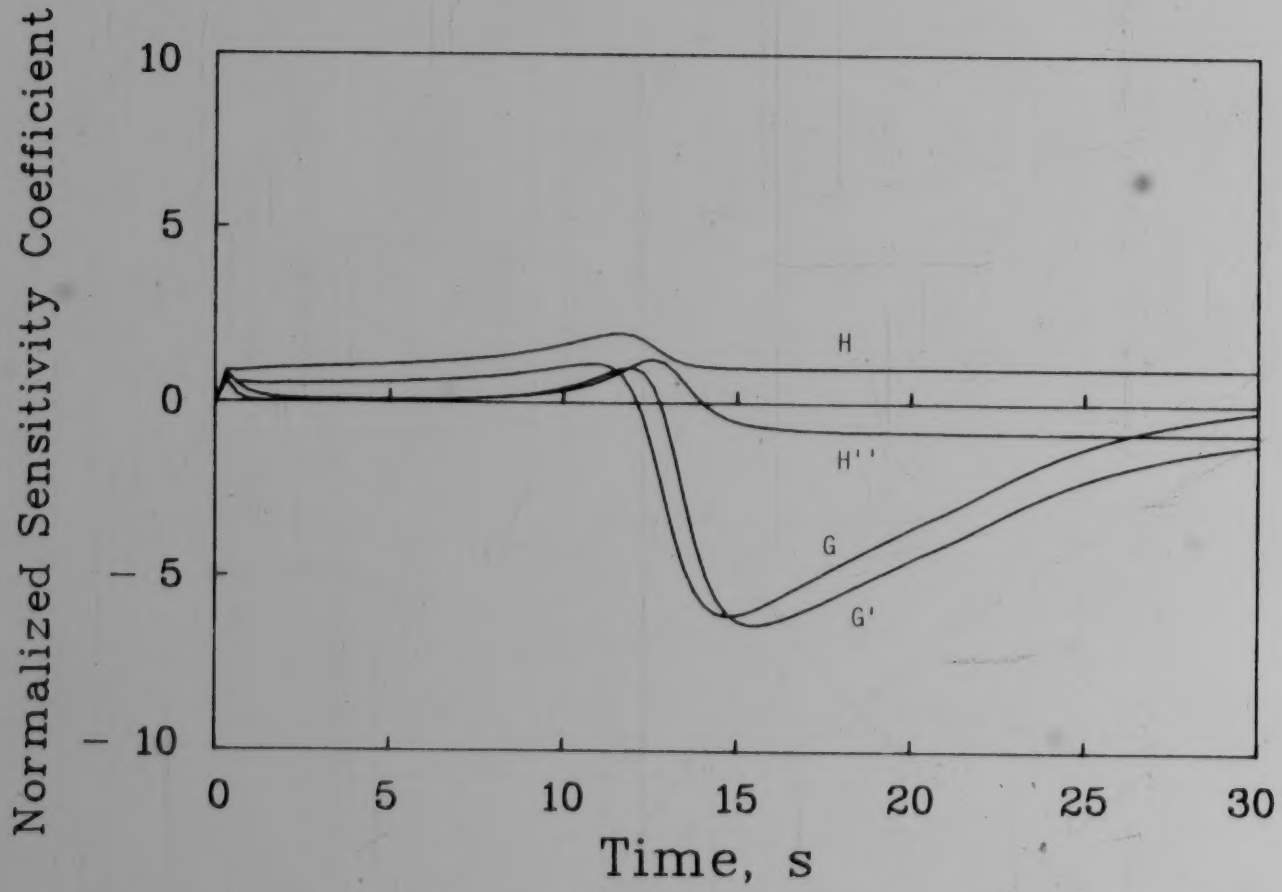


Figure 4.6 Moment Sensitivities with respect to Inlet Initiator Concentration

in the cooling zone. The molecular weight sensitivities with respect to inlet initiator concentration are much smaller in magnitude than those with respect to jacket temperature.

The sensitivities of the radical and polymer moments with respect to inlet initiator concentration, shown in Figure 4.6, are similar to the corresponding jacket temperature sensitivities. The final effects on the zeroth and first radical moments and the second polymer moment are slight decreases. In the concentration sensitivities, however, the overall effect on the zeroth polymer moment is a slight increase.

In all cases the sensitivities with respect to inlet initiator concentration are much smaller in magnitude than those with respect to jacket temperature. Larger percentage changes can be implemented in inlet initiator concentration manipulation than in jacket temperature manipulation. Therefore, depending on the magnitude of the perturbations, both jacket temperature and inlet initiator concentration are potential control variables for the constant jacket temperature reactor.

Mathematical sensitivities of an isothermal reactor were also studied. The sensitivity coefficients

of the isothermal reactor were similar to those of the constant jacket temperature reactor.

## 4.2 Numerical Sensitivities

In this section the effect of changes in model parameters on the final predictions of the model outputs are calculated. The numerical sensitivity of a model output is defined as the percentage change in a model output from its value at a reference condition, due to a percentage change in a model parameter from its corresponding reference value. The numerical sensitivity coefficents are comparable to the final values of the mathematical sensitivity coefficients only when the same initial conditions are used in the reactor models. The numerical sensitivity method calculates the final effect of a parameter manipulation on an output by solving the nonlinear model of the reactor for two sets of parameters, and calculating the percentage changes in the final predictions. The mathematical method solves a set of linearized sensitivity equations along the entire length of the reactor to find the effect of perturbations in the model parameters.

### 4.2.1 Jacket Temperature Sensitivities

The jacket temperature sensitivities are listed in Table 4.1. Sensitivities at three reference jacket temperatures, 403, 433 and 493 K, are presented. The largest changes in all outputs, due to a one percent change in jacket temperature, occur at the low temperature, 403 K. At this jacket temperature the reaction rates are slow and the initiator does not completely decompose. This is not a desirable mode of operation because the overall conversion is low. A change in jacket temperature significantly changes the reactor temperature and molecular weights.

Over the range of jacket temperatures presented in Table 4.1 the $M_N$ sensitivities are opposite in direction to the jacket temperature change. The $M_W$, polydispersity and conversion sensitivities, however, all increase at low temperatures and decrease at high temperatures due to increases in jacket temperature. Referring to Figure 3.4, this result is expected because $M_N$ is a continuously decreasing function with respect to increasing jacket temperature, whereas $M_W$, polydispersity and conversion all have maxima near 420 K. From a control point of view, the jacket temperature is a useful manipulated variable for the constant jacket

Table 4.1 Jacket Temperature Sensitivities

| Jacket Temperature Sensitivity | $T_o$ K | $C_{IO}$ mol/l | $M_N$ Change % | $M_W$ Change % | PD Change % | $X_M$ Change % | $X_I$ Change % |
|---|---|---|---|---|---|---|---|
| 403 - 1% | 373 | $9.7 \times 10^{-4}$ | + 6.15 | - 4.72 | -18.2 | -28.1 | -38.6 |
| 403 + 1% | 373 | $9.7 \times 10^{-4}$ | -13.4 | +25.2 | +42.8 | +45.9 | +65.8 |
| 433 - 1% | 373 | $9.7 \times 10^{-4}$ | + 4.68 | +16.1 | +11.0 | + 4.70 | 0 |
| 433 + 1% | 373 | $9.7 \times 10^{-4}$ | - 3.61 | -10.6 | - 7.19 | - 3.56 | 0 |
| 493 - 1% | 373 | $9.7 \times 10^{-4}$ | + 1.40 | + 2.63 | + 1.30 | + 1.28 | 0 |
| 493 + 1% | 373 | $9.7 \times 10^{-4}$ | - 0.67 | - 1.35 | - 0.60 | - 0.85 | 0 |

temperature reactor in the range of 420 to 470 K. In this region an increase in jacket temperature will decrease the molecular weights, polydispersity and conversion.

The numerical sensitivities for the 433 K case, agree well with the final result of the mathematical sensitivities with respect to jacket temperature manipulations, shown in Figures 4.1 and 4.2. The numerical sensitivities are more accurate than the mathematical sensitivities because they are derived from the nonlinear model of the reactor. The magnitudes of the numerical sensitivities are different for positive and negative perturbations, reflecting the nonlinearity of the system. The mathematical method, however, provides linearized, average sensitivities valid in the region of the reference conditions.

### 4.2.2. Inlet Initiator Concentration Sensitivities

The inlet initiator concentration sensitivities for the constant jacket temperature reactor are listed in Table 4.2. The three reference conditions are $2.43 \times 10^{-4}$, $9.7 \times 10^{-4}$ and $9.7 \times 10^{-3}$ mol/l. For all cases the molecular weight sensitivities are negative for a positive perturbation in inlet initiator concentration, whereas the corresponding conversion sensitivities are all

Table 4.2 Inlet Initiator Concentration Sensitivities

| Initiator Concentration Sensitivity | $T_J$ K | $T_O$ K | $M_N$ Change % | $M_W$ Change % | PD Change % | $X_M$ Change % | $X_I$ Change % |
|---|---|---|---|---|---|---|---|
| $2.425 \times 10^{-4}$ -1% | 433 | 373 | + 0.65 | + 1.19 | + 0.38 | - 0.51 | - 0.10 |
| $2.425 \times 10^{-4}$ +1% | 433 | 373 | - 0.59 | - 0.73 | - 0.35 | + 0.51 | 0 |
| $9.7 \times 10^{-4}$ -1% | 433 | 373 | + 0.76 | + 1.12 | + 0.42 | - 0.26 | 0 |
| $9.7 \times 10^{-4}$ + 1% | 433 | 373 | - 0.74 | - 1.07 | - 0.29 | + 0.24 | 0 |
| $9.7 \times 10^{-3}$ - 1% | 433 | 373 | + 0.80 | + 0.78 | 0 | - 0.19 | 0 |
| $9.7 \times 10^{-3}$ + 1% | 433 | 373 | - 0.77 | - 0.77 | + 0.03 | + 0.19 | 0 |

positive. These trends were also observed in the corresponding mathematical sensitivities shown in Figures 4.4 and 4.5. These sensitivities follow the trends reported in Figure 3.7; as the inlet initiator concentration increases the product molecular weights decrease and conversion increases. The initiator conversion decreases for a decrease in inlet initiator concentration at the lowest concentration, $2.43 \times 10^{-4}$ mol/l. In this system there is not sufficient initiator to cause a rapid increase in reactor temperature and, hence, complete initiator decompositon.

## 4.3 Choice of Control Variables Based on Sensitivity Analysis

The main reason for investigating the effects of changes in input parameters on the model outputs is to determine suitable control variables for this reactor system.

The results of the mathematical sensitivities for the base case reactor indicate that manipulation of the jacket temperature causes significant changes in the overall conversion and molecular weights. The numerical sensitivity results support those of the mathematical sensitivities. In general, increases in the jacket

temperature decrease the molecular weights and conversion of the final product. However, depending on the choice of model and operating parameters, the sensitivity coefficient can change sign and magnitude.

The second choice of control variable for both the constant jacket temperature reactor is the inlet initiator concentration. Increases in initiator concentration caused decreases in the molecular weights and increases in the monomer conversion. Although the magnitudes of these sensitivity coefficients, both in the mathematical and numerical derivaitions, are less than those of the jacket temperatures, the available range for manipulations, greater than 1000% of the base case concentration, justify its use as a control variable.

## 4.4 Sensitivity of Model Outputs with Respect to Rate Constants

The numerical sensitivities of the model outputs with respect to rate constants are calculated to find the effect of uncertainties in the rate constant parameters on the model outputs. The definition of these sensitivities is similar to those for the model parameters in the previous section.

The rate constant sensitivities investigated are with respect to 10 percent changes in frequency factors and activation energies, wherever possible. These sensitivities are listed in Table 4.3. The sensitivity coefficients with respect to the activation energies for decomposition, $E_d$, and transfer to polymer, $E_{fp}$, were calculated for one and five percent changes, respectively.

The parameter which most significantly affects the model outputs is the activation energy for transfer to polymer. For a five percent increase in $E_{fp}$ the weight average molecular weight increases by 589%, with very little effect on the other variables. The magnitude of this sensitivity is very large and emphasizes the need for an accurate estimate of $k_{fp}$. In Chapter 2 and Chen et.al.'s paper the uncertainty in $k_{fp}$ was addressed.

The activation energy for initiator decomposition significantly affects most of the model predictions. For a one percent increase in $E_d$, $M_W$ increases by 56%, PD by 44%, $M_N$ and $X_m$ both by 9%. These results agree qualitatively with those of Goldstein and Amundson (1965).

All other activation energies, except that for termination by disproportionation, significantly affect the model outputs. The frequency factors, except that for

Table 4.3 Rate Constant Sensitivities

| Rate Constant | Sensitivity | | $M_N$ Change % | $M_W$ Change % | PD Change % | $X_M$ Change % | $X_I$ Change % |
|---|---|---|---|---|---|---|---|
| $k_{do}$ | $6.38 \times 10^{13}$ | -10% | + 2.61 | +12.58 | + 9.71 | + 2.59 | 0 |
| | $6.38 \times 10^{13}$ | +10% | - 2.41 | - 9.16 | - 6.92 | - 2.43 | 0 |
| $E_d$ | 29700 | - 1% | - 7.34 | -25.6 | -19.7 | - 7.44 | 0 |
| | 29700 | + 1% | + 8.61 | +56.0 | +43.7 | + 8.58 | 0 |
| initiator efficiency factor f | 0.50 | -10% | + 8.24 | + 2.55 | + 3.98 | + 7.44 | 0 |
| | 0.50 | +10% | - 6.87 | - 9.59 | - 2.92 | - 8.58 | 0 |
| $k_{po}$ | $2.95 \times 10^{7}$ | -10% | - 5.25 | -11.2 | - 6.22 | - 5.34 | 0 |
| | $2.95 \times 10^{7}$ | +10% | + 4.91 | +12.4 | + 7.10 | + 4.85 | 0 |
| $E_p$ | 8200-.555*P | -10% | +44.2 | +332 | +197 | +44.1 | 0 |
| | 8200-.555*P | +10% | -42.4 | -63.4 | -36.5 | -42.7 | 0 |
| $k_{tco}$ | $1.60 \times 10^{9}$ | -10% | + 2.73 | +15.7 | +12.6 | + 2.75 | 0 |
| | $1.60 \times 10^{9}$ | +10% | - 2.37 | -10.5 | - 8.34 | - 2.43 | 0 |
| $E_{tc}$ | 2400 | -10% | - 6.79 | -25.8 | -20.4 | - 6.80 | 0 |
| | 2400 | +10% | + 7.01 | +55.1 | +44.9 | + 6.96 | 0 |
| $k_{tdo}$ | $2.72 \times 10^{11}$ | -10% | 0 | 0 | 0 | 0 | 0 |
| | $2.72 \times 10^{11}$ | +10% | 0 | 0 | 0 | 0 | 0 |
| $E_{td}$ | 20000 | -10% | 0 | 0 | 0 | 0 | 0 |
| | 20000 | +10% | 0 | 0 | 0 | 0 | 0 |
| $k_{fpo}$ | $9.0 \times 10^{5}$ | -10% | 0 | -11.9 | -12.0 | 0 | 0 |
| | $9.0 \times 10^{5}$ | +10% | 0 | +16.0 | +15.9 | 0 | 0 |
| $E_{fp}$ | 9000 | - 5% | + 0.35 | +589 | +586 | +0.32 | 0 |
| | 9000 | + 5% | 0 | -35.1 | -35.1 | 0 | 0 |

$k_{td}$, also affect the model outputs, but not as strongly as their corresponding activation energies. This is expected due to the exponential dependence of the rate constants on the activation energies. From this study it can be concluded that accurate estimates of the kinetic parameters are necessary for reliable model predictions.

# 5. OPTIMIZATION STUDIES

## 5.1 Definition of the Optimization Problem

The reactor model described in Chapter 2 is a multi-input multi-output model. It can be written concisely as:

$$\frac{d\underset{\sim}{y}}{dt} = f(\underset{\sim}{y},t,\underset{\sim}{u}) \qquad (5.1)$$

where $\underset{\sim}{y}$ is a vector of state variables

$t$ is the reactor coordinate, time

$\underset{\sim}{u}$ is a vector of control variables

The state variables are monomer conversion, $X_M$, initiator conversion, $X_I$, molecular weights, $M_N$ and $M_W$, and reactor temperature, T. The control variables are jacket zone temperatures and locations, and initiator concentrations, types and injection point locations. This model is nonlinear in the state and control variables.

The only state variable of concern along the reactor coordinate is the reactor temperature. This variable must be controlled within its operating limits, or minimum and maximum constraints, along the entire length of the reactor to avoid ethylene decomposition.

The other state variables, molecular weights and conversion, are meaningful at the reactor exit only. However, the final values of the molecular weights and conversions are influenced by the values of the state variables at all points along the reactor co-ordinate.

An ideal optimization of this system would try to maximize the monomer conversion subject to the temperature constraints throughout the reactor and the constraints on final molecular weights. The control variables are simply the inputs to the reactor. The optimization problem in this work can be formulated as a static optimization with the following objective function:

$$J = a_1 \left(\frac{M_N}{M_{Nd}} - 1\right)^2 + a_2\left(\frac{M_W}{M_{Wd}} - 1\right)^2 + a_3\left(\frac{X_M}{X_{Md}} - 1\right)^2 \quad (5.2)$$

where $M_N$ is the final number average molecular weight

$M_{Nd}$ is the desired value of $M_N$

$M_W$ is the final weight average molecular weight

$M_{Wd}$ is the desired value of $M_W$

$X_M$ is the final monomer conversion

$X_{Md}$ is the desired value of $X_M$

$a_1$, $a_2$ and $a_3$ are weighting factors

The desired values of the molecular weights and conversion are predetermined by the designer, or by the quality specifications for a certain type of polymer. The state variables are normalized in the cost function. Their relative importance is determined by the weighting factors $a_1$, $a_2$ and $a_3$.

The mathematical technique used to solve the optimization problem is the IMSL subroutine ZXSSQ. The method employed by this routine minimizes the sum of the squares of a residual function, which is equivalent to minimizing the cost function, J.

In some optimization problems numerical constraints must be placed on the control variables. For an actual reactor operating limits on the jacket temperature and initiator concentration exist. These operating limits are translated into numerical constraints by the use of Box's transformation (1966):

$$x_i = g_i + (h_i - g_i) \sin^2 y_i \quad i = 1,\ldots,N \qquad (5.3)$$

where $g_i$ is the lower limit on $x_i$

$h_i$ is the upper limit on $x_i$

$x_i$ is the control variable

$y_i$ is the transformed control variable

N is the number of constrained variables

Use of the transformed control variable, $y_i$, ensures that the control variable, $x_i$, does not exceed its operating limits throughout the optimization procedures. Constraints may be imposed upon both the jacket temperature and initiator concentration.

## 5.2 Jacket Temperature as the Control Variable

The object of this optimization problem using the jacket temperature as the control variable is to find a range of polymer product qualities that can be produced in a base type reactor by manipulating the jacket temperature. The reactor configuration is a base type model. The initial values for all the control variables are those of the base case simulation, Table 3.1. The only control variable which can be changed by the optimization calculations is the jacket temperature. The results for several optimizations are presented in Table 5.1.

The simplest type of optimization problem involves one control variable, $T_J$, and one desired property, either number average molecular weight, weight average molecular weight or conversion. These simple optimizations are listed as the first four entries in Table 5.1. The results show that using the jacket

Table 5.1 Optimization Results - Jacket Temperature as Control Variable

| Desired Properties | | $T_J$ K | $T_O$ K | $C_{IO}$ mol/l | $M_N$ | $M_W$ | PD | $X_M$ % | $X_I$ % |
|---|---|---|---|---|---|---|---|---|---|
| $M_N$ | 120000 | 453.2 | 373 | $9.7\times10^{-4}$ | 119750 | 422130 | 3.53 | 5.35 | 100 |
| $M_N$ | 100000 | 513.0 | 373 | $9.7\times10^{-4}$ | 99980 | 288650 | 2.89 | 4.40 | 100 |
| $M_W$ | 300000 | 498.7 | 373 | $9.7\times10^{-4}$ | 102990 | 304370 | 2.96 | 4.60 | 100 |
| $X_M$ | 5.0 | 407.0 | 373 | $9.7\times10^{-4}$ | 185060 | 849730 | 4.59 | 5.01 | 60.5 |
| $M_N$<br>$M_W$ | 120000<br>480000 | 445.8 | 373 | $9.7\times10^{-4}$ | 125230 | 471660 | 3.77 | 5.59 | 100 |
| $M_N$<br>$M_W$ | 120000<br>400000 | 457.4 | 373 | $9.7\times10^{-4}$ | 117540 | 402930 | 3.43 | 5.25 | 100 |
| $M_N$<br>$M_W$<br>$X_M$ | 120000<br>480000<br>5.0 | 448.4 | 373 | $9.7\times10^{-4}$ | 123260 | 452750 | 3.67 | 5.50 | 100 |
| $M_N$<br>$M_W$<br>$X_M$ | 100000<br>400000<br>5.5 | 462.2 | 373 | $9.7\times10^{-4}$ | 115070 | 383440 | 3.33 | 5.14 | 100 |
| $M_N$<br>$M_W$<br>$X_M$ | 100000<br>500000<br>6.0 | 447.8 | 373 | $9.7\times10^{-4}$ | 123700 | 456930 | 3.69 | 5.52 | 100 |
| $M_N$<br>$M_W$<br>$X_M$ | 100000<br>600000<br>8.0 | 437.8 | 373 | $9.7\times10^{-4}$ | 132570 | 551370 | 4.16 | 5.92 | 100 |

temperature as the control variable high number average molecular weight polymers with polydispersities of three to five and conversions of approximately five percent are attainable using a fixed amount of initiator ($9.7 \times 10^{-4}$ mol/l) at the reactor entrance. By specifying only one polymer property in the objective function, however, there is very little control over the other properties. The kinetics of the system determine the other property values. Only certain ranges of each property can be attained by manipulating only the jacket temperature. Neither a number average molecular weight of less than 100,000 nor a weight average molecular weight of less than 275,000 nor monomer conversion of greater than 5.6% can be achieved.

The optimization problem with monomer conversion as the desired property is the only one for which the final initiator conversion is less than 100%. The type and concentration of initiator determine the monomer conversion, hence manipulation of the jacket temperature has little effect on monomer conversion.

To achieve better control over the product polymer qualities at least two final properties should be specified in the objective function. Results for such optimizations are listed in Table 5.1.

The specification of more than one polymer property while manipulating only one control variable exceeds the degrees of freedom of the system. Therefore, either the desired properties must be approximately equal to those attained by specifying only one property, or weighting factors must be included in the cost function, equation 5.2.

The fourth to sixth entries in Table 5.1 all have a $M_N$ similar to that of the first entry, 120,000. In these results the weight average molecular weights range from 404,800 to 474,100; polydispersities from 3.44 to 3.78; and monomer conversions from 5.3 to 4.6 percent. The control variable, $T_J$, ranges from 445.8 to 457.4 K, which is a very narrow range. Over this twelve degree range of jacket temperature the number average molecular weight, specified in all cases, is approximately 120,000 and all other properties vary 10% from the single specified property, $M_N$, case. Therefore, the designer has very little freedom when using only one control variable to control more than one property.

The last three entries in Table 5.1 further illustrate this point. In all three cases $M_N$ is specified as 100,000 with $M_W$ and $X_M$ specified at increasing values. As the desired $M_W$ and hence

polydispersity, increases, the final $M_N$ deviates more significantly from its desired values. Thus, a higher penalty is paid with respect to the $M_N$ specification when using only one control variable, jacket temperature, to meet three property specifications.

## 5.3 Inlet Initiator Concentration as the Control Variable

The objective of this optimization study is to find the range of polymer product qualities that can be produced in a base type reactor by manipulating the inlet initiator concentration. The initial values of all variables are those of the base case simulation, Table 3.1. The optimization results are presented in Table 5.2.

In the simple optimizations, with only one final property specified, a broad range of molecular weights and high conversions are obtained. These simple optimizations are the first five entries in Table 5.2. The number average molecular weights range from 49,000 to 104,000 and weight average molecular weights from 163,000 to 416,000. The minimum $M_N$ and $M_w$ are much lower than those obtained using the jacket temperature as the control variable. The conversions attained using initiator concentration as the control variable are between 6.7 and 8.5%, which is higher than those of the jacket temperature

Table 5.2 Optimization Results - Inlet Initiator Concentration as Control Variable

| Desired Properties | | $C_{IO}$ mol/l | $T_J$ K | $T_O$ K | $M_N$ | $M_W$ | PD | $X_M$ % | $X_I$ % |
|---|---|---|---|---|---|---|---|---|---|
| $M_N$ | 100000 | $1.35 \times 10^{-3}$ | 433 | 373 | 107780 | 439100 | 4.02 | 6.70 | 100 |
| $M_N$ | 50000 | $3.67 \times 10^{-3}$ | 433 | 373 | 50040 | 165860 | 3.32 | 8.45 | 100 |
| $M_W$ | 300000 | $1.95 \times 10^{-3}$ | 433 | 373 | 81453 | 301840 | 3.71 | 7.31 | 100 |
| $M_W$ | 200000 | $2.99 \times 10^{-3}$ | 433 | 373 | 58647 | 200190 | 3.41 | 8.07 | 100 |
| $X_M$ | 8.0 | $2.86 \times 10^{-3}$ | 433 | 373 | 60687 | 208630 | 3.44 | 7.99 | 100 |
| $M_N$* | 50000 | $3.42 \times 10^{-3}$ | 433 | 373 | 52845 | 176790 | 3.35 | 8.32 | 100 |
| $M_W$ | 200000 | | | | | | | | |
| $M_N$ | 100000 | $1.56 \times 10^{-3}$ | 433 | 373 | 96570 | 378020 | 3.91 | 6.93 | 100 |
| $M_W$ | 350000 | | | | | | | | |
| $M_N$ | 120000 | $1.16 \times 10^{-3}$ | 433 | 373 | 120870 | 515560 | 4.27 | 6.45 | 100 |
| $M_W$ | 350000 | | | | | | | | |
| $X_M$ | 5.0 | | | | | | | | |

* weighting factors 0.4 for $M_N$, 0.2 for $M_W$

optimizations. Both the lower molecular weights and higher monomer conversions are attributable to the increased initiator concentration in the system.

The optimization problem with monomer conversion as the desired property is easier to solve using inlet initiator concentration as the control variable than using jacket temperature. From the simulation studies in Chapter 3 it is known that monomer conversion is directly related to the inlet initiator concentration. However, the solution of the monomer conversion optimization requires more iterations than that of the molecular weight optimizations. Since problems were encountered in monomer conversion optimization using either jacket temperature or inlet initiator concentration as the control variable this type of optimization is not recommended.

As in the jacket temperature optimizations, the inlet initiator concentration optimization problem is solved with two and three specified final properties. These results are the last three entries in Table 5.2. In the first two of these entries the number average and weight average molecular weights are specified in the optimization problem. The desired number average molecular weights are each the same as in an optimization with only number average molecular weight specified. The

solutions of the two-property specification optimization problem deviate more significantly from the desired values than the single-property optimization results. The reason for this is the reduced flexibility in final property values when specifying two properties and manipulating only one variable. In the case with desired molecular weights of 50,000 ($M_N$) and 200,000 ($M_W$) weighting factors are required in the cost function in order to find the solution.

The last entry in Table 5.2 specified all three final properties of the polymer. The molecular weight result is within 7.4% of the desired value and the conversion result within 29%. Again, by specifying more than one property and manipulating only one control variable the results deviate significantly from the desired values.

## 5.4 Combination of Jacket Temperature and Inlet Initiator Concentration as the Control Variables

To increase the range of the number average and weight average molecular weights attainable by optimization both jacket temperature and inlet initiator concentration are defined as control variables. These control variables are easy to manipulate, either alone or

in combination, in an industrial reactor. The use of two control variables increases the degrees of freedom in the system, therefore, it can be expected that $M_N$ and $M_W$ can be controlled simultaneously. Results for optimizations with several different molecular weight combinations are given in Table 5.3.

The advantage of optimizing both the jacket temperature and initiator concentration over the jacket temperature alone is that lower molecular weights, $M_N$ of 40,000 and $M_W$ of 200,000, and higher conversions, 12.8%, are achieved. The main advantage over the initiator concentration alone is that higher polydispersities, 5.0, can be attained. Also, with two manipulated variables the two-property optimization results are within ten percent of the desired values without any penalties or weighting factors.

The numerical solution of optimization problems with two control variables take longer than that of problems with only one control variable. To produce the same desired polymer, the optimization with two control variables requires an average of twice as many iterations as the single variable optimization.

Table 5.3 Optimization Results - Jacket Temperature and Inlet Initator Concentration as Control Variables

| Desired Properties | | $T_J$ K | $C_{IO}$ mol/l | $T_O$ K | $M_N$ | $M_W$ | PD | $X_M$ % | $X_I$ % |
|---|---|---|---|---|---|---|---|---|---|
| $M_N$ | 100000 | 461.2 | $1.20 \times 10^{-3}$ | 373 | 99942 | 326150 | 3.26 | 5.52 | 100 |
| $M_N$<br>$M_W$ | 100000<br>300000 | 489.7 | $1.05 \times 10^{-3}$ | 373 | 100040 | 300050 | 3.00 | 4.83 | 100 |
| $M_N$<br>$M_W$ | 50000<br>200000 | 411.8 | $4.38 \times 10^{-3}$ | 373 | 49946 | 199610 | 4.00 | 10.1 | 100 |
| $M_N$<br>$M_W$ | 40000<br>200000 | 396.3 | $6.94 \times 10^{-3}$ | 373 | 40013 | 200180 | 5.00 | 12.8 | 100 |
| $M_N$<br>$M_W$ | 150000<br>450000 | 510.6 | $5.16 \times 10^{-4}$ | 373 | 148190 | 441120 | 2.98 | 3.52 | 100 |

## 5.5 Multiple Jacket Temperature Zones as the Control Variables

When using multiple jacket temperature zones as control variables, either the jacket temperatures of specified zones or the lengths of the zones can be manipulated in the optimization problem. In this work the magnitude of the jacket temperatures and the lengths of the zones are treated as separate control variables.

### 5.5.1 Zone Temperatures

To study the effect of the different jacket temperature zones, the jacket is divided into two zones of constant temperature. The first zone extends from the reactor entrance to one-quarter of the total reactor length; the second from this point to the end of the reactor. The results for the two-zone optimization are listed as the first four entries in Table 5.4. For low number average molecular weights a low jacket temperature in the first zone and a high temperature in the second zone is required. For higher polydispersities with constant number average molecular weight the jacket temperature in the first zone should be lower. In all these cases the conversion is low, approximately 5%, due

Table 5.4 Optimization Results - Jacket Zone Temperatures as-Control Variables

| Desired Properties | $T_J$ K | $T_{J2}$ K | $T_{J3}$ K | $C_{IO}$ mol/l | $T_O$ K | $M_N$ | $M_W$ | PD | $X_M$ % | $X_I$ % |
|---|---|---|---|---|---|---|---|---|---|---|
| 2 Zones<br>Zone 1 at 0.0 s<br>Zone 2 at 7.5 s | | | | | | | | | | |
| $M_N$ 120000 | 454.7 | 435.3 | - | $9.7\times10^{-4}$ | 373 | 123240 | 443130 | 3.60 | 5.50 | 100 |
| $M_N$ 120000<br>$M_W$ 480000 | 418.4 | 462.4 | - | $9.7\times10^{-4}$ | 373 | 120830 | 485430 | 4.02 | 5.39 | 100 |
| $M_N$ 120000<br>$M_W$ 600000 | 391.5 | 463.6 | - | $9.7\times10^{-4}$ | 373 | 128430 | 589350 | 4.59 | 5.73 | 100 |
| $M_N$ 100000<br>$M_W$ 350000 | 402.1 | 533.1 | - | $9.7\times10^{-4}$ | 373 | 102530 | 364630 | 3.56 | 4.58 | 100 |
| 3 Zones<br>Zone 1 at 0.0 s<br>Zone 2 at 6.3 s<br>Zone 3 at 16.8 s | | | | | | | | | | |
| $M_N$ 120000<br>$M_W$ 400000 | 457.3 | 446.8 | 378.1 | $9.7\times10^{-4}$ | 373 | 120880 | 424050 | 3.51 | 5.40 | 100 |
| $M_N$ 120000<br>$M_W$ 480000 | 410.7 | 457.3 | 431.4 | $9.7\times10^{-4}$ | 373 | 120680 | 479860 | 3.98 | 5.39 | 100 |
| $M_N$ 100000<br>$M_W$ 350000 | 369.5 | 502.0 | 510.5 | $9.7\times10^{-4}$ | 373 | 105480 | 361890 | 3.43 | 4.71 | 100 |

to the small amount of initiator, $9.7 \times 10^{-4}$ mol/l, injected at the reactor entrance.

For a three-zone reaction, the reactor is divided into heating, reaction and cooling zones, starting at the reactor entrance, 6.3 s and 16.8 s, respectively. These jacket temperature zones correspond to the reactor zone subdivisions for the base case reactor. The results for this type of optimization are listed as the last three entries in Table 5.4. To produce a polymer with a low number average molecular weight the first zone should have a low jacket temperature, and the other zones high jacket temperatures. In this reactor very little reaction occurs in the first zone and polymerization occurs quickly in the second zone. The third zone has no effect on the product polymer qualities. To produce a polymer with higher polydispersity and constant number average molecular weight the jacket temperature in the first zone should be lower and those in the second zone should be the same. Again, the temperature of the third jacket zone has very little effect on the molecular weights.

### 5.5.2 Zone Lengths

The length of the jacket temperature zones, with pre-specified zone temperatures, has been investigated.

Since the cooling zone has very little effect on the polymer properties the objective of this optimization is to find the best position of the second jacket zone. The simplest solution of this problem uses the method of interval halving to search for the starting point of the second zone. The temperatures of both zones are specified. For the results listed in Table 5.5 the heating zone temperature is 433 K, the same temperature as the heating zone in the base case simulation. The second zone temperature is either 373 or 503 K. As shown above, the use of a higher temperature in the second jacket zone yields a product with a lower number average molecular weight.

To decrease the number average molecular weight of the product polymer the beginning of the hotter second zone is moved towards the reactor entrance. Thus, very little reaction occurs in the short, lower temperature heating zone and polymerization occurs rapidly in the hot reaction zone. To increase the polydispersity the beginning of the hot second zone is moved towards the reactor exit. Here, in the longer, lower temperature heating zone the polymerization reactions occur slowly, creating high $M_w$ products.

Table 5.5 Optimization Results - Jacket Zone Lengths as Control Variables

| Desired Properties | | $T_{J1}$, loc K, s | $T_{J2}$, loc K,s | $T_o$ K | $C_{IO}$ mol/l | $M_N$ | $M_W$ | PD | $X_M$ % | $X_I$ % |
|---|---|---|---|---|---|---|---|---|---|---|
| $M_N$ | 200000 | 433, 0 | 373, 7.5 | 373 | $9.7 \times 10^{-4}$ | 215020 | 499260 | 2.32 | 2.19 | 22.8 |
| $M_N$ | 120000 | 433, 0 | 503, 9.0 | 373 | $9.7 \times 10^{-4}$ | 118680 | 454210 | 3.83 | 5.30 | 100 |
| $M_N$ | 100000 | 433, 0 | 503, 3.3 | 373 | $9.7 \times 10^{-4}$ | 106030 | 338300 | 3.19 | 4.73 | 100 |
| $M_N$<br>$M_W$ | 100000<br>300000 | 433, 0 | 503, 3.0 | 373 | $9.7 \times 10^{-4}$ | 105860 | 335160 | 3.17 | 4.73 | 100 |
| $M_N$<br>$M_W$ | 100000<br>400000 | 433, 0 | 503, 6.3 | 373 | $9.7 \times 10^{-4}$ | 109990 | 384650 | 3.50 | 4.91 | 100 |

The use of multiple jacket zones provides more flexibility in the control of molecular weights of the product than the base type reactor with a single jacket temperature. However, for more useful results, the jacket temperature in each zone should be related to the reactor zones. A more complicated jacket configuration and optimization problem would determine the best temperature and length of each jacket zone.

## 5.6 Multiple Initiator Injection Points as the Control Variables

Using multiple initiator injection points as the control variables either the initiator concentrations at the specified injection points or the locations of the injection points can be the control variables in the optimization problem. Two optimization problems are studied separately. In the first the initiator concentrations are determined at the reactor inlet and one injection point. In the second the location of the injection point is determined.

### 5.6.1 Initiator Concentration

In the first case the location of the injection point is at the midpoint of the reactor, t = 15 s. The

initiator which is injected at the reactor entrance is completely consumed by the time it reaches this injection point. An injection of initiator at this point will cause and increase in $M_N$, $M_W$ and conversion. The optimization program finds the initiator concentrations at the reactor inlet, $C_{I0}$ and the injection point, $C_{I1}$, required for producing a desired polymer. Results for several cases are presented in Table 5.6.

These results show an effect similar to that observed for the inlet initiator concentration in Chapter 3: to decrease the number average molecular weight and increase the monomer conversion, the total amount of initiator injected into the system must be higher. To increase the polydispersity while maintaining a constant value for $M_N$, the initiator concentration at the reactor entrance decreases and that at the injection point increases. The polydispersities obtained in this reactor configuration are much higher than those of all other reactors. The additional injection of initiator is the key to increasing the polydispersity of the product.

In Table 5.7 and Figure 5.1 similar reactor configurations with one and two initiator injection points are compared. In both reactors $2.0 \times 10^{-3}$ mol/l of initiator is injected at the reactor entrance. In the

Table 5.6 Optimization Results - Multiple Initiator Injection Concentrations as Control Variables

| Desired Properties | | $C_{IO}$ mol/l | $C_{I1}$ mol/l | $T_J$ K | $T_O$ K | $M_N$ | $M_W$ | PD | $X_M$ % | $X_I$ % |
|---|---|---|---|---|---|---|---|---|---|---|
| $M_N$ | 120000 | $6.34 \times 10^{-4}$ | $7.48 \times 10^{-4}$ | 433 | 373 | 121710 | 1944500 | 16.0 | 7.74 | 100 |
| $M_N$<br>$M_W$ | 100000<br>700000 | $1.43 \times 10^{-3}$ | $5.73 \times 10^{-4}$ | 433 | 373 | 97675 | 703570 | 7.20 | 9.34 | 100 |
| $M_N$<br>$M_W$ | 100000<br>600000 | $1.58 \times 10^{-3}$ | $3.99 \times 10^{-4}$ | 433 | 373 | 97957 | 606690 | 6.19 | 9.25 | 100 |
| $M_N$<br>$M_W$ | 100000<br>500000 | $1.72 \times 10^{-3}$ | $2.37 \times 10^{-4}$ | 433 | 373 | 98949 | 518990 | 5.25 | 8.89 | 100 |
| $M_N$<br>$M_W$ | 100000<br>450000 | $1.70 \times 10^{-3}$ | $5.78 \times 10^{-4}$ | 433 | 373 | 100800 | 490320 | 4.87 | 8.49 | 100 |
| $M_N$<br>$M_W$ | 50000<br>400000 | $2.00 \times 10^{-3}$ | $3.09 \times 10^{-3}$ | 433 | 373 | 49993 | 400290 | 8.01 | 11.7 | 100 |
| $M_N$<br>$M_W$ | 50000<br>350000 | $2.27 \times 10^{-3}$ | $2.89 \times 10^{-3}$ | 433 | 373 | 49454 | 348530 | 7.05 | 11.9 | 100 |
| $M_N$<br>$M_W$ | 50000<br>300000 | $2.65 \times 10^{-3}$ | $2.50 \times 10^{-3}$ | 433 | 373 | 50538 | 301330 | 5.96 | 12.0 | 100 |

$C_{IO}$ injected at 0.0 s, $C_{I1}$ at 15.0 s

Table 5.7 Comparison of Constant Jacket Temperature Reactors with One and Two Injection Points

| $c_{IO}$, loc mol/l, s | $c_{Il}$, loc mol/l, s | $T_J$ K | $T_o$ K | $M_N$ | $M_W$ | PD | $X_M$ % | $X_I$ % |
|---|---|---|---|---|---|---|---|---|
| $2.0 \times 10^{-3}$, 0.0 | 0 | 433 | 373 | 79990 | 294430 | 3.69 | 7.35 | 100 |
| $2.0 \times 10^{-3}$, 0.0 | $3.09 \times 10^{-3}$, 15.0 | 433 | 373 | 49993 | 400290 | 8.01 | 11.7 | 100 |

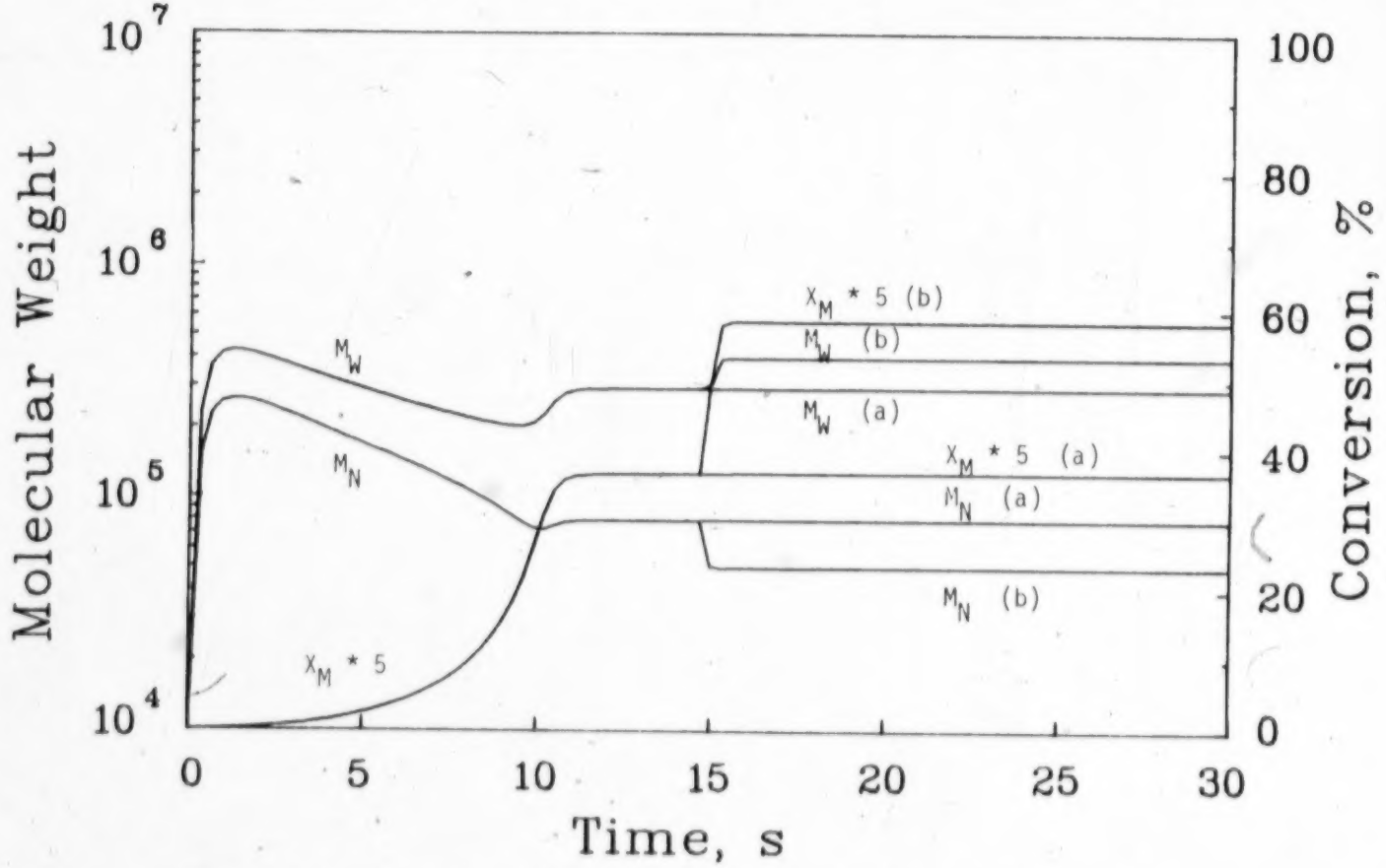


Figure 5.1 Comparison of Reactor Profiles with One and Two Initiator Injection Points (a) one injection (b) two injections

second reactor more initiator, $3.09 \times 10^{-3}$ mol/l, is injected at the midpoint of the reactor. The number average molecular weight of the second case is lower than that of the first due to the higher overall initiator concentration. The polydispersity, weight average molecular weight and conversion are all higher because more initiator is injected into the reactor past the reaction zone, resulting in temperature variations.

### 5.6.2 Injection Point Location

The optimal location of the initiator injection point is investigated using an interval halving method. The initiator concentration at the reactor entrance is pre-specified. In the cases studied the concentration at the injection point is 10% of the inlet initiator concentration. The results for several cases are presented in Table 5.8.

The first three cases, all with initiator concentrations of $.97 \times 10^{-3}$ and $.97 \times 10^{-4}$ mol/l, show that to increase the number average molecular weight, the second injection point must be located near the location of the temperature peak in the base case reactor. As this peak moves away from the entrance the molecular weights of the products increase. This shift in the temperature

Table 5.8 Optimization Results - Location of Initiator Injection Point as Control Variable

| Desired Properties | | $C_{IO}$, loc mol/l, s | $C_{Il}$, loc mol/l, s | $T_J$ K | $T_O$ K | $M_N$ | $M_W$ | PD | $X_M$ % | $X_I$ % |
|---|---|---|---|---|---|---|---|---|---|---|
| $M_N$ | 150000 | $9.7x10^{-4}$,0 | $9.7x10^{-5}$,14.7 | 433 | 373 | 146300 | 898650 | 6.14 | 7.18 | 100 |
| $M_N$ | 140000 | $9.7x10^{-4}$,0 | $9.7x10^{-5}$,13.5 | 433 | 373 | 138710 | 754360 | 5.44 | 6.81 | 100 |
| $M_N$ | 130000 | $9.7x10^{-4}$,0 | $9.7x10^{-5}$,10.5 | 433 | 373 | 128770 | 589070 | 4.58 | 6.32 | 100 |
| $M_N$ | 70000 | $2.5x10^{-3}$,0 | $2.5x10^{-4}$,10.5 | 433 | 373 | 69339 | 280370 | 4.04 | 8.78 | 100 |
| $M_N$<br>$M_W$ | 70000<br>400000 | $2.5x10^{-3}$,0 | $2.5x10^{-4}$,14.7 | 433 | 373 | 75729 | 337480 | 4.46 | 9.58 | 100 |

peak, or the location of the second injection point, also decreases the overall conversion, as in the base case simulations.

Injecting larger total amounts of initiator into the reactor results in decreases in both $M_N$ and $M_W$, and an increase in the overall conversion. This behaviour has already been observed in the multiple injection optimizations and the base case simulations.

The disadvantages of using the interval halving method to find the best injection point location are that the starting interval must be within 3 seconds of the optimal location, and that the numerical solution can easily search in the wrong direction, especially when a multi-objective cost function is used. The interval halving method is an adequate technique for finding the injection point location only if the desired concentration and approximate location are known a priori.

The first type of optimization, finding the initiator concentrations for known injection points, is most useful in an industrial appreciation where the initiator injection points on a reactor are fixed. The second type of optimization, determining the location of the injection point, is useful in the design of the reactor.

## 5.7 Multiple Initiator Types as the Control Variables

An alternative to providing several injection of one initiator along the length of the reactor is to mix several different initiator types together and inject this mixture at the reactor inlet. Industrially, it is easier to mix several initiators together and inject them at the beginning of the reactor than it is to provide a second injection point when none exists. The designer would ideally choose a few initiators that have unique, distinct temperature regions in which they are most reactive.

The objective of the optimization problem is to find the best concentrations of each type of initiator to be injected at the reactor entrance. For this problem the base initiator, benzoyl peroxide, is mixed with t-butyl peroxide. The decomposition rates of these initiators are:

benzoyl peroxide $\quad k_{d1} = 6.30 \times 10^{13} \exp\left(\frac{-29700}{RT}\right)$

t-butyl peroxide $\quad k_{d2} = 3.26 \times 10^{14} \exp\left(\frac{-35100}{RT}\right)$

(Hamielec and Friis, 1972)

The rate constants are shown over the typical reactor temperature range in Figure 5.2. The second initiator, t-butyl peroxide, becomes reactive at approximately 450 K. This temperature is slightly lower than the peak

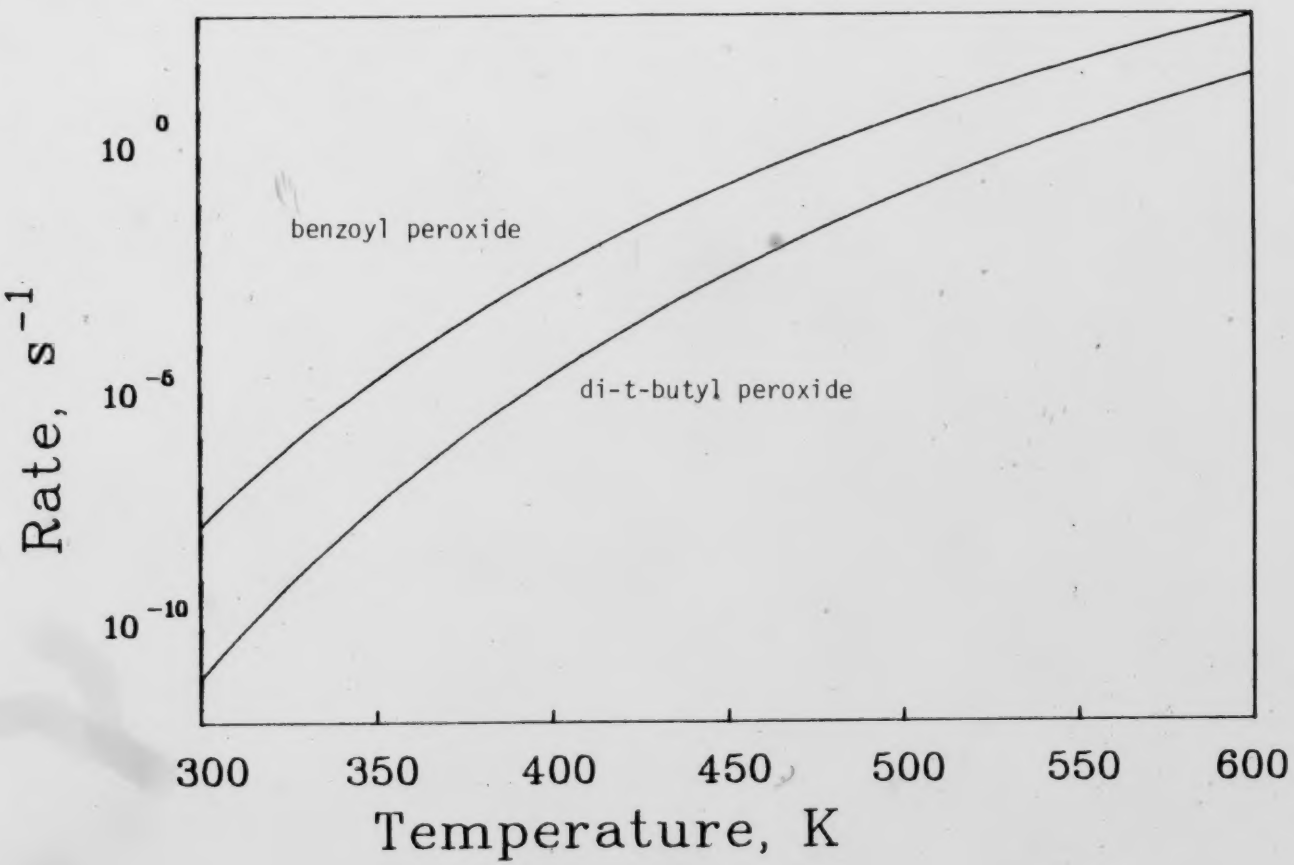


Figure 5.2 Initiator Decomposition Rates

reactor temperature in the base case simulation. Therefore, the second initiator should start to decompose after the first initiator is completely consumed. This second reaction zone will change the product quality and conversion.

The results for several different products are presented in Table 5.9. To produce high molecular weight products small amounts of both initiators are required. For the cases with a desired $M_W$ of 750,000 the benzoyl peroxide concentration is less than $1.2 \times 10^{-3}$ and t-butyl peroxide concentration less than $1.5 \times 10^{-4}$ mol/l. In these cases the second initiator is not completely consumed at the reactor exit. Due to the low peak temperature in the first reaction zone, the second initiator cannot react to its full extent. To produce lower $M_N$ products at constant $M_W$, and increase the polydispersity, more of both initiators must be added to the reactor. This is also consistent with the results of the base case simulations.

In Figure 5.3 and Table 5.10 the two initiator system is compared with a base type reactor under similar conditions. From the figure it can be seen that at the point where the first initiator becomes completely consumed the second initiator maintains the reaction.

Table 5.9 Optimization Results - Multiple Initiator Type Concentrations as Control Variables

| Desired Properties | | $C_{I1}$ mol/l | $C_{I2}$ mol/l | $T_J$ K | $T_o$ K | $M_N$ | $M_W$ | PD | $X_M$ % | $X_{I1}$ % | $X_{I2}$ % |
|---|---|---|---|---|---|---|---|---|---|---|---|
| $M_N$ | 160000 | $8.17\times10^{-4}$ | $9.70\times10^{-7}$ | 433 | 373 | 157580 | 759510 | 4.82 | 5.92 | 100 | 16.2 |
| $M_W$ | 750000 | | | | | | | | | | |
| $M_N$ | 150000 | $9.7\times10^{-4}$ | $6.92\times10^{-5}$ | 433 | 373 | 150010 | 750140 | 5.00 | 6.79 | 100 | 20.6 |
| $M_W$ | 750000 | | | | | | | | | | |
| $M_N$ | 140000 | $1.18\times10^{-3}$ | $1.52\times10^{-4}$ | 433 | 373 | 139990 | 749760 | 5.36 | 7.89 | 100 | 28.2 |
| $M_W$ | 750000 | | | | | | | | | | |
| $M_N$ | 100000 | $2.09\times10^{-3}$ | $1.55\times10^{-4}$ | 433 | 373 | 100020 | 500280 | 5.02 | 10.0 | 100 | 57.7 |
| $M_W$ | 500000 | | | | | | | | | | |
| $M_N$ | 90000 | $2.72\times10^{-3}$ | $2.14\times10^{-4}$ | 433 | 373 | 90026 | 500430 | 5.56 | 12.0 | 100 | 86.4 |
| $M_W$ | 500000 | | | | | | | | | | |
| $M_N$ | 80000 | $3.26\times10^{-3}$ | $3.62\times10^{-4}$ | 433 | 373 | 79968 | 499960 | 6.25 | 13.3 | 100 | 100 |
| $M_W$ | 500000 | | | | | | | | | | |
| $M_N$ | 70000 | $3.75\times10^{-3}$ | $2.41\times10^{-4}$ | 433 | 373 | 69345 | 350230 | 5.05 | 12.7 | 100 | 100 |
| $M_W$ | 350000 | | | | | | | | | | |

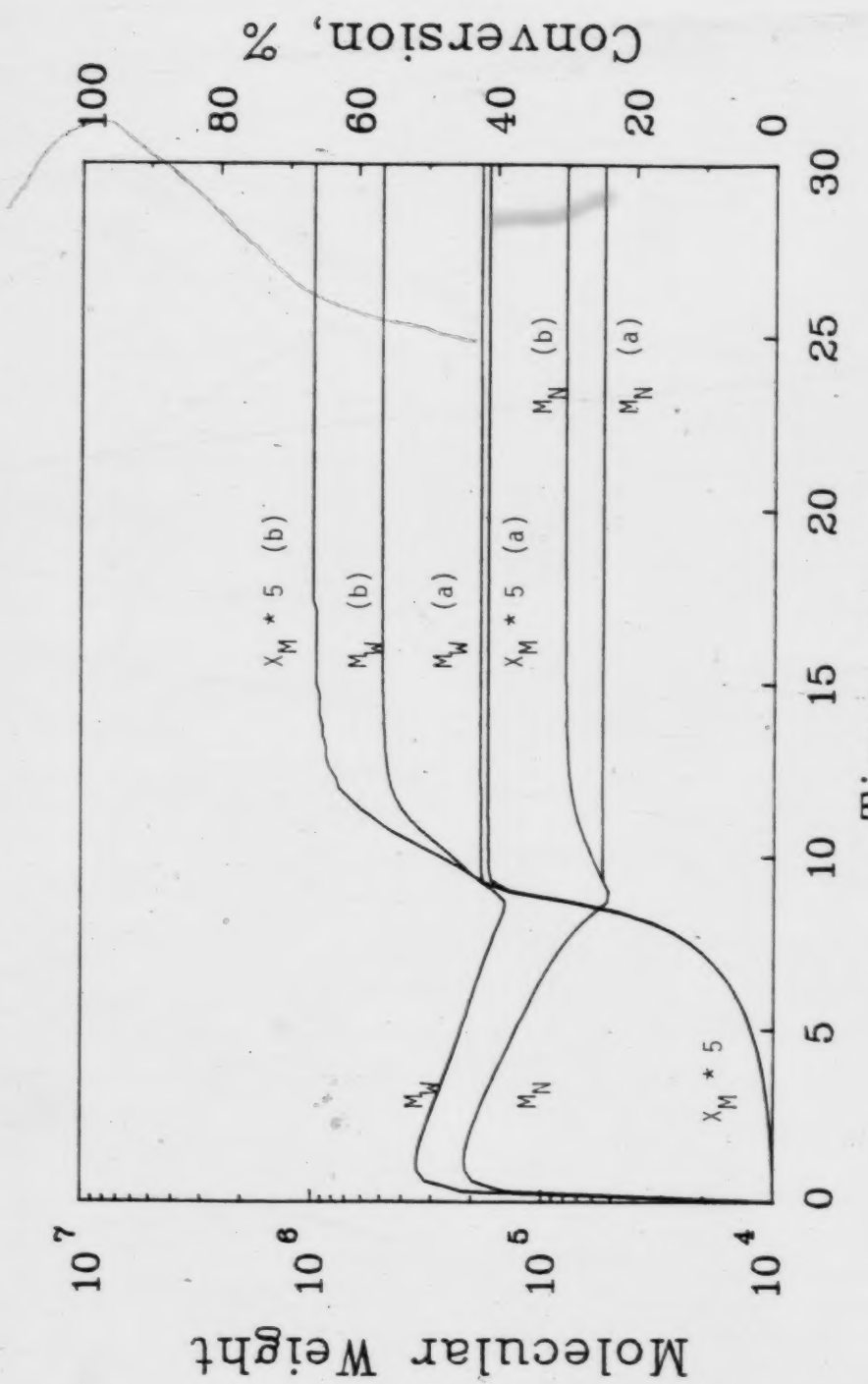


Figure 5.3 Comparison of Reactor Profiles with Single and Mixed Initiators

(a) single initiator (b) mixed initiators

Table 5.10 Comparison of Constant Jacket Temperature Reactors Outputs with Single and Multiple Initiators

| $C_{I1}$ mol/l | $C_{I2}$ mol/l | $T_J$ K | $T_o$ K | $M_N$ | $M_W$ | PD | $X_M$ % | $X_{I1}$ % | $X_{I2}$ % |
|---|---|---|---|---|---|---|---|---|---|
| $2.26 \times 10^{-3}$ | 0 | 433 | 373 | 54800 | 185000 | 3.38 | 8.23 | 100 | - |
| $3.26 \times 10^{-3}$ | $3.62 \times 10^{-4}$ | 433 | 373 | 79968 | 499960 | 6.25 | 13.3 | 100 | 100 |

Thus, a higher temperature peak is reached and the monomer conversion increases. The increased activity leads to an increase in $M_N$, $M_W$ and polydispersity. This effect is similar to that of a second injection of the same initiator at the end of the reaction zone, as presented in Figure 5.1 The above results indicate that the use of several types of initiators can improve the conversion of a given reactor, and significantly alters the properties of the polymer product.

The use of different initiators in the optimization program causes many numerical problems. The range of concentrations for the second initiator has to be constrained between 0 and 40% of the base initiator concentration. Above 40% the reactor temperature exceeds the upper safety limit of ethylene polymerization.

## 5.8 Significance of Optimization Results

The results of the optimization studies can be used to determine the appropriate control strategies for this reactor. The polymer engineer studying polyethylene reactors would be interested in the results of the multiple initiator injection studies and the multiple initiator type studies. The polymer engineer would determine the amounts and types of each initiator injected

at as many points as desirable along the reactor length, and the effects of these variables on the polymer product. The results of the optimization studies will be incorporated into the overall reactor control scheme discussed in Chapter 6.

# 6. REACTOR CONTROL TO IMPROVE CONVERSION

## 6.1 Overall Control Objective

The main control objective of this study is to improve the overall conversion of monomer to polymer per pass in the reactor. The secondary control objective is to increase the degree of branching in the polymer product, indicated by the polydispersity. Typically, low density polyethylene has a polydispersity between 3 and 20. (Romanini, 1982) To increase both conversion and polydispersity in a single pass through the reactor, more initiator should be added, either via multiple injections of one initiator type or via multiple types of initiators injected at the reactor inlet. Owing to the lack of data on commercial initiators, the first alternative was studied in detail.

In the optimization studies of Chapter 5 only one extra initiator injection point, beyond the injection point at the reactor entrance, was studied. In practice, a reactor could have more than one injection point. A constant initiator injection rate simulation was carried out for the tubular polyethylene reactor. The results of this simulation are presented in Figure 6.1. The constant initiator injection begins at t = 3 s. At each 0.3 s,

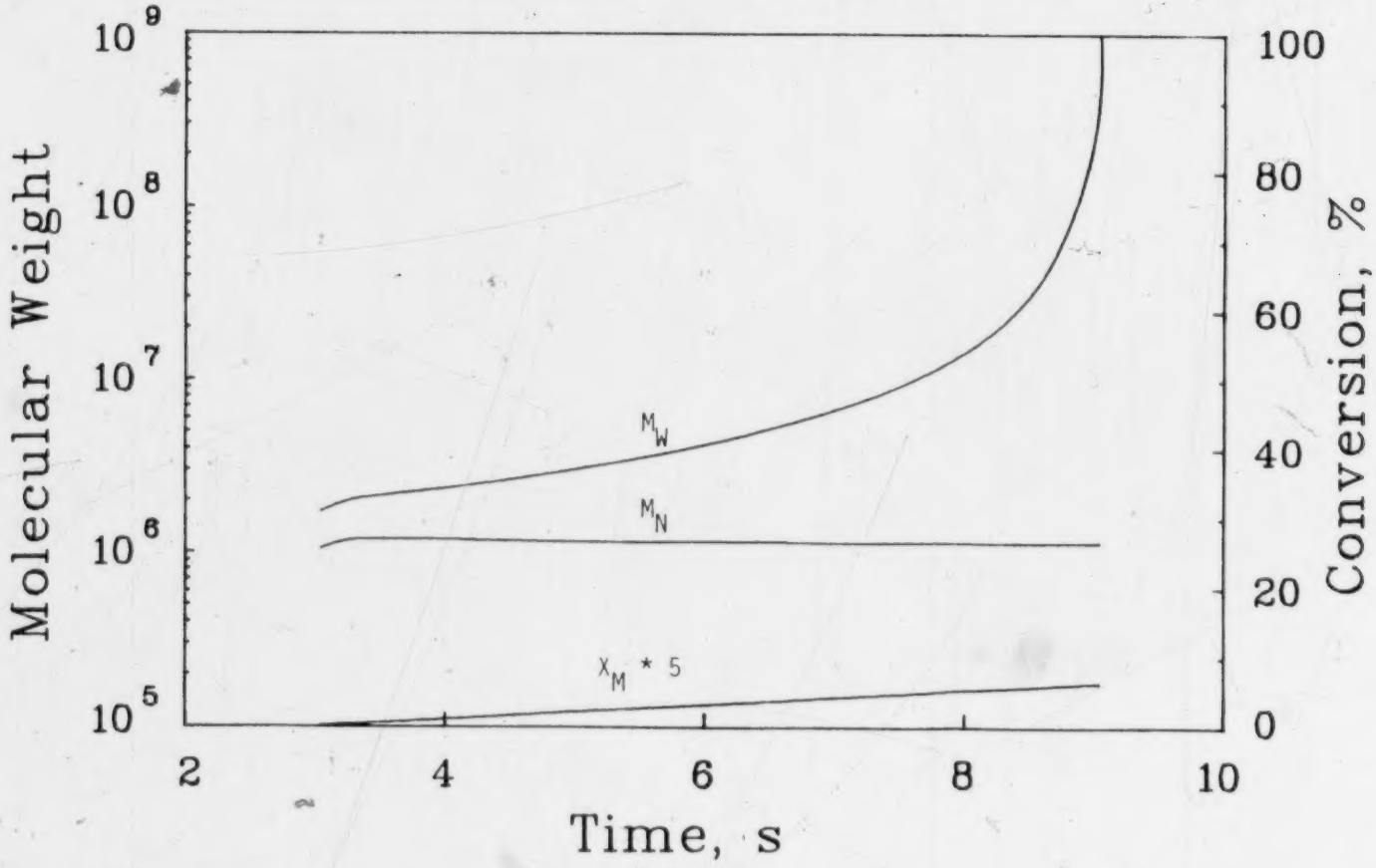


Figure 6.1 Molecular Weight and Conversion Profiles for Constant Initiator Injection

$9.7 \times 10^{-7}$ mol/l of initiator is injected into the reactor, for a total of 26 injections. In Figure 6.1 it is shown that the monomer conversion increases linearly with the number of injections of initiator. The number average molecular weight is approximately constant and the weight average molecular weight, and hence polydispersity, increase exponentially. Since this simulation study has shown that many injections of small concentrations of initiator increase both the conversion and polydispersity of the product, the conversion improvement schemes should incorporate some features of this scheme.

## 6.2 Conversion Improvement Schemes

The proposed overall conversion improvement scheme is based on three preliminary schemes, described in Table 6.1. These are referred to as the constant temperature reaction zone, constant jacket temperature and high temperature injection reactors. In each scheme, a large amount of initiator is injected at the reactor inlet and several smaller amounts of initiator are injected in the reaction zone. These reactors differ mainly in the criteria for choosing the location of the injection points.

Table 6.1 Features of Conversion the Preliminary Improvement Schemes

| Scheme | Jacket Temperature | Reactor Temperature | Initial Initiator Injection | Subsequent Initiator Injections |
|---|---|---|---|---|
| Constant Temperature Reaction Zone | variable, to absorb heat of polymeri-zation | constant | at reactor inlet large amount | at location where previous injecion is 99% decomposed small amount |
| Constant Jacket Temperature | constant | variable, as in base case | at reator inlet large amount | at location where reactor temperature falls below a prespecified value small amount |
| High Temperature Injection | constant | variable, as in base case | at reactor inlet large amount | at locations immediately beyond each temperature peak small amount |

The results of the three schemes are presented in Table 6.2. All schemes produce similar polymers, with $M_N$ of 100,000 and $M_W$ of approximately 1,000,000, under slightly different conditions. The monomer conversions range from 10.2 to 10.4 %. The constant jacket temperature scheme has the fastest increases in molecular weights and conversion because the reaction temperature decreases between injection points. The rate of increase of molecular weights and conversion is slower in the high temperature injection and the constant temperature reaction zone reactors because the injections occur at subsequently higher temperatures, where incremental molecular weight effects are less.

The proposed overall conversion improvement consists of a constant jacket temperature reactor with multiple initiator injections after the heating zone. It is comparable to a base type reactor with multiple injections. The unique feature of this reactor is the fixed injection interval, chosen by the designer. Fixed injection intervals enable an easier construction, by not having to provide as many injection points as required for varied injection point locations. This also reduces the complexity of the control system required to synchronize the initiator injections. Provision is also made in this reactor model for multiple jacket temperature zones. As

Table 6.2 Comparison of the Preliminary Conversion Improvement Schemes

| $T_J$* K | $T_O$ K | $T_{ISO}$ K | $C_{IO}$ mol/l | $C_I$ per injection mol/l | Number of Injections | $M_N$ | $M_W$ | PD | $X_M$ % | $X_I$ % |
|---|---|---|---|---|---|---|---|---|---|---|
| Constant Temperature Reaction Zone | | | | | | | | | | |
| 433 | 373 | 485 | $1.7 \times 10^{-3}$ | $8.5 \times 10^{-5}$ | 7 | 101760 | 982000 | 9.65 | 10.7 | 100 |
| Constant Jacket Temperature | | | | | | | | | | |
| 433 | 373 | - | $1.7 \times 10^{-3}$ | $8.5 \times 10^{-5}$ | 4 | 108580 | 843470 | 7.77 | 10.2 | 100 |
| High Temperature | | | | | | | | | | |
| 373 | 433 | - | $1.7 \times 10^{-3}$ | $8.5 \times 10^{-5}$ | 5 | 106210 | 938330 | 8.84 | 10.4 | 100 |

* at beginning of reactor if $T_J$ varies

shown in the optimization studies it may be desirable to divide the jacket into heating, reaction and cooling zones of different temperatures or multiple hot reaction and cool quench zones.

The molecular weight and conversion profiles for this scheme are presented Figure 6.2. This scheme produces a polymer with an $M_N$ of 96,800, $M_W$ of 997,000 and 13.6% conversion. Seven injections of $1.5 \times 10^{-5}$ mol/l of initiator are injected with a spacing of 1.2 s, starting at 4.2 s. The maximum reaction temperature reached in this reactor is 493 K, after the first initiator injection point. The hot injection zones provide large reaction rates without violating any temperature constraints.

To verify that the proposed scheme for initiator injection does meet the objectives, this scheme was compared with a similar constant jacket temperature reactor with only one injection of initiator at the reactor entrance. The results are presented in Table 6.3 and Figure 6.3. In both reactors the same total amount of initiator is injected. However, in the base type reactor all of the initiator is injected at the inlet, whereas in the conversion improvement reactor a large amount is injected at the inlet, followed by smaller amounts at the

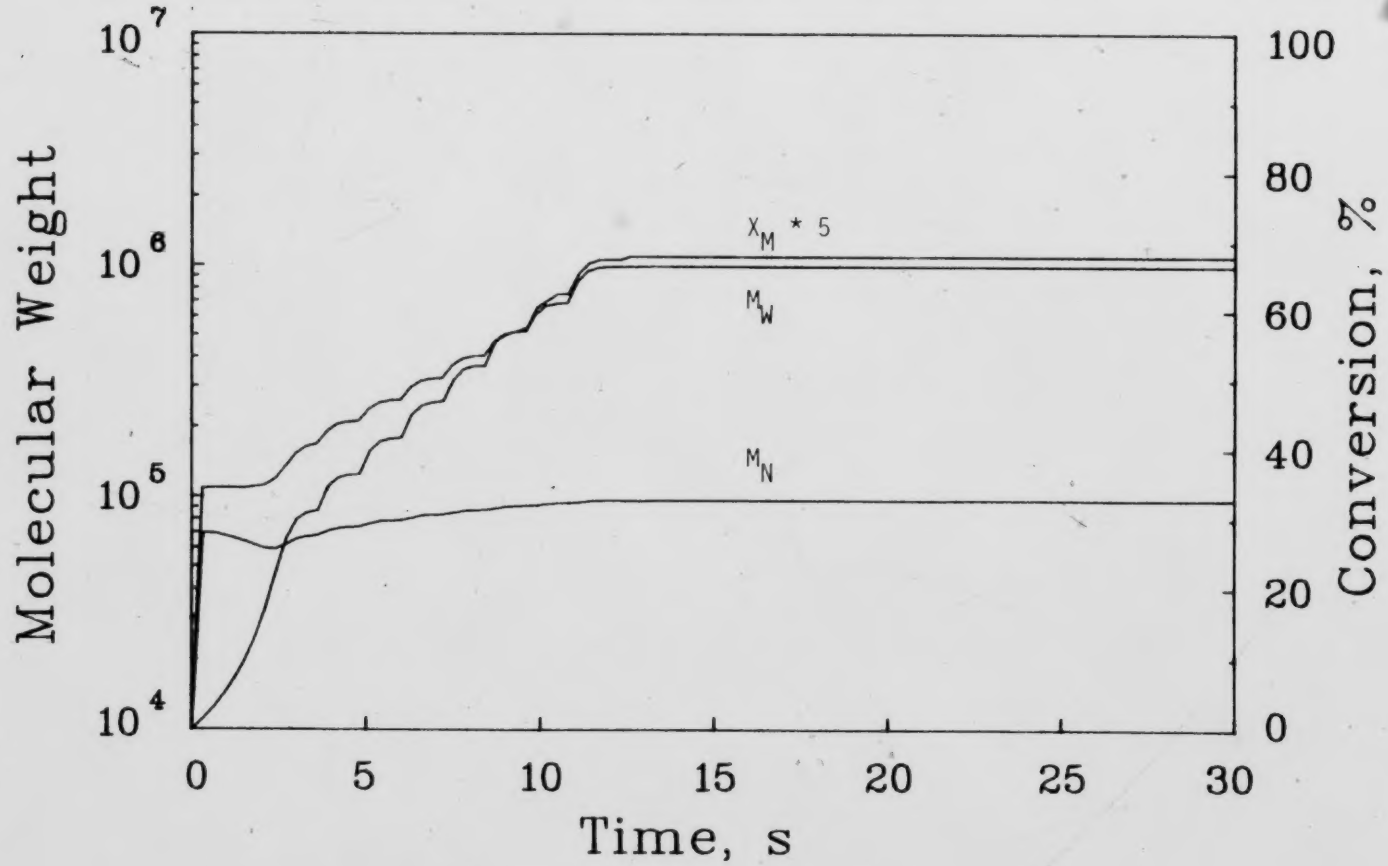


Figure 6.2 Overall Conversion Improvement Scheme

Table 6.3 Comparison of Conversion Improvement and Base Type Reactors

| $T_J$ K | $T_o$ K | $C_{IO}$ mol/l | $C_I$ per injection mol/l | Total $C_I$ mol/l | $M_N$ | $M_W$ | PD | $X_M$ % | $X_I$ % |
|---|---|---|---|---|---|---|---|---|---|
| 413 | 433 | $2.0 \times 10^{-3}$ | $1.5 \times 10^{-4}$ | $3.05 \times 10^{-3}$ | 96823 | 997330 | 10.3 | 13.6 | 100 |
| 413 | 433 | $3.05 \times 10^{-3}$ | - | $3.05 \times 10^{-3}$ | 48693 | 115920 | 2.38 | 6.83 | 100 |

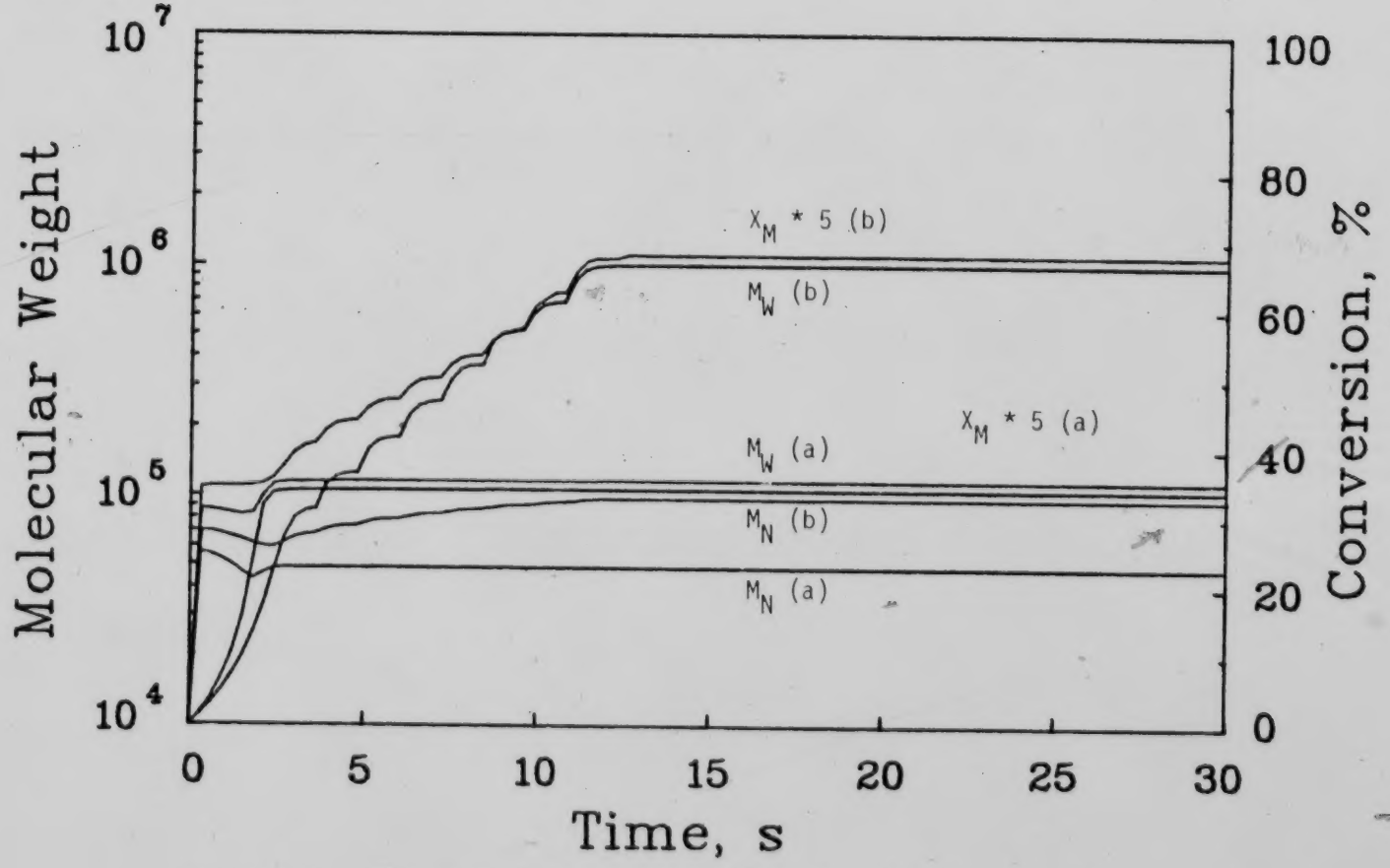


Figure 6.3 Conversion Improvement and Base Type Reactor Comparison

(a) base type (b) conversion improvement

injection points. The overall increase in conversion for the proposed scheme is from 6.8 to 13.6 %, and in polydispersity from 2.4 to 10.3. Therefore, this proposed reaction injection scheme has truly fulfilled its objectives of increasing conversion and polydispersity.

The effect of initiator injection concentration on product quality is presented in Table 6.4. As the injection concentration increases the number of injections required to produce the desired product decreases. The rate of increase of $M_W$ and $X_M$ increases with increasing concentration; however, the rate of increase of $M_N$ does not follow a clear trend.

The effect of injection spacing on product quality is presented in Table 6.5. Increasing the injection spacing increases the rate of increase of $M_N$, $M_W$ and conversion per injecton. Also, fewer injections are required to produce the desired product.

In the simulation and optimization studies it was shown that the jacket temperature affects conversion and molecular weights. The effects of jacket temperature on molecular weight are presented in Table 6.6. In this reactor the best jacket temperature is determined by the maximum reactor temperature constraint, and the molecular

Table 6.4 Effect of Initiator Injection Concentration on Conversion Improvement

| $T_J$ K | $T_o$ K | $C_{IO}$ mol/l | $C_I$ per injection mol/l | Number of Injections | $M_N$ | $M_W$ | PD | $X_M$ % | $X_I$ % |
|---|---|---|---|---|---|---|---|---|---|
| 433 | 433 | $2.0 \times 10^{-3}$ | $2.0 \times 10^{-5}$ | 18 | 120380 | 1013900 | 8.42 | 13.1 | 100 |
| 433 | 433 | $2.0 \times 10^{-3}$ | $1.0 \times 10^{-4}$ | 9 | 98279 | 905740 | 9.22 | 13.1 | 100 |
| 433 | 433 | $2.0 \times 10^{-3}$ | $1.5 \times 10^{-4}$ | 9 | 91317 | 1165100 | 12.76 | 14.1 | 100 |

Table 6.5 Effect of Injection Spacing on Conversion Improvement

| $T_J$ K | $T_O$ K | $C_{IO}$ mol/l | $C_I$ per injection mol/l | Number of Injections | Injection Spacing s | $M_N$ | $M_W$ | PD | $X_M$ % | $X_I$ % |
|---|---|---|---|---|---|---|---|---|---|---|
| 413 | 433 | $2.0 \times 10^{-3}$ | $1.0 \times 10^{-4}$ | 8 | 1.2 | 104180 | 1010700 | 9.70 | 13.4 | 100 |
| 413 | 433 | $2.0 \times 10^{-3}$ | $1.0 \times 10^{-4}$ | 6 | 2.4 | 108910 | 828700 | 7.61 | 13.0 | 100 |
| 413 | 433 | $2.0 \times 10^{-3}$ | $2.0 \times 10^{-4}$ | 5 | 2.4 | 98594 | 853050 | 8.65 | 13.6 | 100 |

Table 6.6 Effect of Jacket Temperature on Conversion Improvement

| $T_J$ K | $T_0$ K | $C_{I0}$ mol/l | $C_I$ per injection mol/l | Number of Injections | $M_N$ | $M_W$ | PD | $X_M$ % | $X_I$ % | $T_J$ max K |
|---|---|---|---|---|---|---|---|---|---|---|
| 373 | 433 | $2.0 \times 10^{-3}$ | $1.0 \times 10^{-4}$ | 10 | 99726 | 398370 | 4.00 | 10.1 | 73.5 | 444.1 |
| 413 | 433 | $2.0 \times 10^{-3}$ | $1.0 \times 10^{-4}$ | 8 | 104180 | 1010700 | 9.70 | 13.4 | 100 | 493.8 |
| 423 | 433 | $2.0 \times 10^{-3}$ | $1.0 \times 10^{-4}$ | 9 | 102410 | 1110300 | 10.84 | 13.7 | 100 | 497.8 |
| 433 | 433 | $2.0 \times 10^{-3}$ | $1.0 \times 10^{-4}$ | 9 | 98279 | 905740 | 9.22 | 13.1 | 100 | 499.3 |
| 453 | 433 | $2.0 \times 10^{-3}$ | $1.0 \times 10^{-4}$ | 11 | 93429 | 976950 | 10.46 | 13.1 | 100 | 505.1 |
| 473 | 433 | $2.0 \times 10^{-3}$ | $1.0 \times 10^{-4}$ | - | - | - | - | - | - | > 510 |

weight and conversion development. In the high temperature region, above 400 K, in which the injected initiator decomposes completely between injections, higher jacket temperatures lead to smaller increases in molecular weights and conversion. This effect, per injection, is similar to the overall temperature effect in the base case reactor in Chapter 3. For the initiator concentrations listed in Table 6.6 the jacket temperature must be below 470 K to provide sufficient cooling to maintain the reactor temperature below 510 K and prevent runaway reactions.

This conversion improvement reactor is designed with provision for multiple jacket temperature zones. With the freedom to provide as many jacket temperature zones as desired a designer might consider alternating heating and cooling zones at each initiator injection point. A low temperature cooling zone begins at the point where the reactor temperature reaches its maximum for the previous initiator injection. This will quickly stop the polymerization reactions. At the next initiator injection point the jacket temperature is raised to enable initiator decomposition. These heating and cooling zones are repeated for each injection point. A simulation with such heating and cooling zones is compared with a constant temperature zone reactor in Table 6.7. The increase in

Table 6.7 Effect of Multiple Heating and Cooling Zones

| $C_{IO}$ mol/l | $C_I$ $C_I$ per Injection mol/l | No. Injections | $T_O$ K | $T_J$ K | $M_N$ | $M_W$ | PD | $X_M$ % | $X_I$ % |
|---|---|---|---|---|---|---|---|---|---|
| $2.0 \times 10^{-3}$ | $9.7 \times 10^{-4}$ | 7 | 433 | 483 | 91512 | 546650 | 5.35 | 11.4 | 100 |
| $2.0 \times 10^{-3}$ | $9.7 \times 10^{-4}$ | 7 | 433 | 533/373 | 93657 | 591410 | 6.31 | 11.6 | 100 |

conversion for the multiple zone reactor is less than two percent over that of the constant jacket temperature reactor. Logistically, control of the multiple heating and cooling zones and co-ordination of these zones with the initiator injection points is a difficult task. For such a small increase in conversion the use of multiple heating and cooling zones is not worthwhile.

## 6.3 Recommendations for Reactor Control to Improve Conversion

The proposed scheme, a constant jacket temperature reactor with multiple initiator injections at fixed locations, meets the objectives of increasing conversion and polydisperity. Compared to a similar base type reactor, this scheme doubles the conversion and increases the polydispersity five-fold. Using such a scheme to improve conversion should increase the profit margin of polyethylene production by reducing the operating cost per unit produced.

Other modifications to this scheme might enhance its profitability and should also be investigated. These include variable injection concentrations and the use of multiple initiator types, in addition to the variables investigated in section 6.2.

The concentration of initiator at each injection point need not be fixed. In most multiple injection point simulations the molecular weights increase when additional initiator is injected. However, in Chapter 5, one case was reported in which $M_N$ decreased and $M_W$ increased when a large concentration of initiator was injected. Therefore, by varying the amount of initiator injected at each injection point it may be possible to get opposing trends in molecular weight developments. For the most efficient use of initiator and maximum conversion an optimization strategy should be developed to determine the initiator concentrations at each injection point. This type of optimization is basically an extension of the multiple initiator optimization studied in Chapter 5. It would be most useful to a plant engineer who must determine the initiator concentrations required for making a specific product.

The use of multiple initiators is a common method of conversion improvement in industrial reactors. As shown in Chapter 5, multiple initiators, if selected properly, also increase the conversion and polydisperity of the polymer product. The use of multiple initiators in the conversion improvement reactor could help to increase the monomer conversion even further. For an industrial application multiple initiator types should be investigated.

# 7. RELATIONSHIPS BETWEEN TEMPERATURE PROFILES AND MOLECULAR WEIGHTS

The objective of finding a numerical relationship between the molecular weights and the temperature profile is to aid in final molecular weight prediction. In a high pressure tubular polymerization reactor it is difficult to determine the polymer molecular weights online. Reactor temperatures, however, can be measured or calculated online. By establishing a numerical relationship between the molecular weights and the temperature profile it is hoped that molecular weights, or trends in molecular weights, can be predicted online.

## 7.1 Definition of Moments of a Temperature Profile

For each reactor simulation the reactor temperature can be recorded at each point along the reactor coordinate, giving a temperature profile. As shown in Figures 3.5 and 3.8, the temperature profile has a characteristic peak indicating the point at which polymerization occurs at the maximum rate. The magnitude and location of this peak is a function of initiator concentration and jacket temperature, as well as other reactor variables.

A statistical method of quantifying the location and magnitude of the temperature peak is to calculate the moments of the temperature profile. The first and second moments, or the average and standard deviation, of the temperature profile are calculated for the constant jacket temperature reactor as follows:

average

$$T_{AV} = \frac{\sum_{K=n_i}^{n_f} (T_K * t_K - T_f * t_f)}{N} \qquad (7.1)$$

standard deviation

$$T_{SD} = \frac{\sum_{K=n_i}^{n_f} (T_K * t_K - T_f * t_f)^2}{N(N-1)} \qquad (7.2)$$

where: $n_i$ is the beginning point of the reaction zone,

$$\frac{d^2T}{dt^2} = 0, \quad \frac{dT}{dt} > 0$$

$n_f$ is the endpoint of the reaction zone

$$\frac{d^2T}{dt^2} = 0, \quad \frac{dT}{dt} < 0$$

N is the number of points in the reaction zone,

$$n_f - n_i + 1$$

$T_K$ is the reactor temperature at point K

$T_f$ is the reactor temperature at the endpoint

$t_K$ is the reactor coordinate at point K

$t_f$ is the reactor coordinate at the endpoint

This calculation region, $n_i$ to $n_f$, is shown schematically for the base case temperature profile in Figure 7.1

The molecular weight and temperature profiles for the base case reactor simulation are shown in Figure 7.2. At the beginning of the reaction zone the molecular weights are decreasing while the reactor temperature increases. Near 10 s the molecular weights reach their minima. Here, the initiator decomposition rate is sufficiently fast enough to initiate the polymerization reactions and the molecular weights begin to increase.

The overall relationship between the temperature and molecular weight profiles is not a simple one. But, for the constant jacket temperature reactor, the reactor temperature is related to the rate of polymerization in the reaction zone. Therefore, the temperature profile is an indication of the molecular weight development. Since the polymerization rate affects the temperature profile, the magnitude and breadth of the temperature peak should give an indication of the product molecular weights.

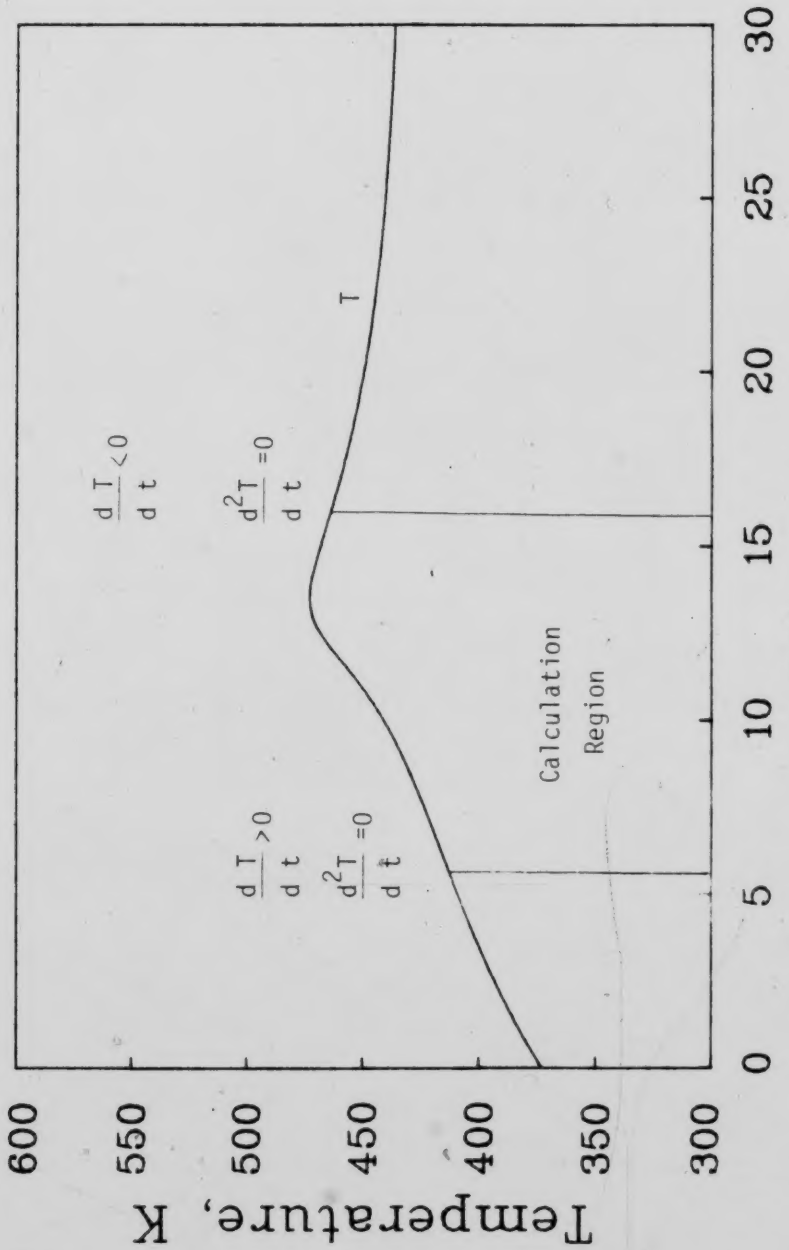


Figure 7.1 Definition of Temperature Moments for Base Case Reactor

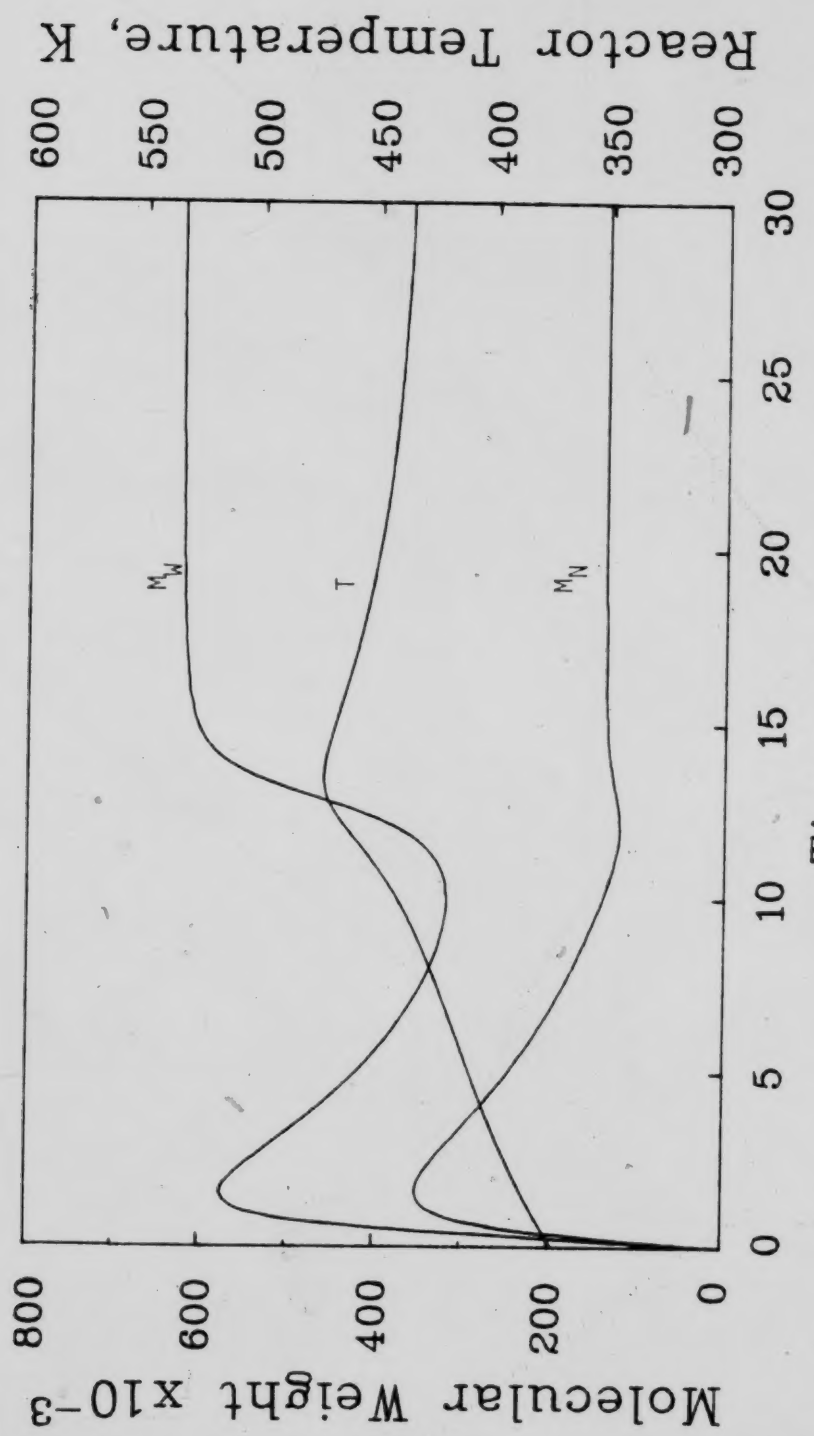


Figure 7.2 Relationship Between Temperature and Molecular Weight Profiles

## 7.2 Effect of Jacket Temperature on Temperature Moments

In Chapter 3 it was shown that increases in the jacket temperature caused decreases in the molecular weights (Figure 3.4). Figure 3.5 shows that at higher jacket temperatures the reactor temperature peak increases and moves towards the reactor entrance.

From the preceding definition of the temperature moments, one would also expect the temperature moments to decrease with increasing jacket temperature. The effect of jacket temperature on the temperature moments is presented in Table 7.1 and Figure 7.3. In general, the temperature profile average and standard deviation decrease with increasing jacket temperature.

The temperature moments predict the molecular weight trends correctly in the typical operating temperature ranges of the constant jacket temperature reactor. The temperature moments are valid for jacket temperatures ranging from 420 to 470 K.

## 7.3 Effect of Inlet Initiator Concentration on Moments

In the simulation studies in Chapter 3 it was shown that for most cases, increases in the inlet

Table 7.1 Effect of Jacket Temperature on Moments

| MODEL INPUTS | | | MODEL OUTPUTS | | MOMENTS | | | |
|---|---|---|---|---|---|---|---|---|
| Jacket Temperature K | $T_o$ K | $C_{IO}$ mol/l | $M_N$ | $M_W$ | Average | Standard Deviation | Reaction Zone Beginning s | Reaction Zone Length s |
| 403 | 373 | $9.7 \times 10^{-4}$ | 213930 | 676450 | - | - | - | - |
| 423 | 373 | $9.7 \times 10^{-4}$ | 155760 | 956610 | 6452 | 1801 | 8.4 | 12.3 |
| 433 | 373 | $9.7 \times 10^{-4}$ | 138290 | 625420 | 4967 | 1466 | 6.3 | 9.6 |
| 443 | 373 | $9.7 \times 10^{-4}$ | 127550 | 495230 | 4120 | 1268 | 5.1 | 8.1 |
| 450 | 373 | $9.7 \times 10^{-4}$ | 122140 | 442370 | 3654 | 1145 | 4.5 | 7.2 |
| 453 | 373 | $9.7 \times 10^{-4}$ | 120170 | 424910 | 3526 | 1063 | 4.5 | 6.6 |
| 463 | 373 | $9.7 \times 10^{-4}$ | 114690 | 380590 | 3132 | 978 | 3.9 | 6.0 |
| 473 | 373 | $9.7 \times 10^{-4}$ | 110470 | 350320 | 2717 | 890 | 3.3 | 5.4 |
| 490 | 373 | $9.7 \times 10^{-4}$ | 105190 | 316880 | 1713 | 1001 | 0.6 | 6.6 |
| 553 | 373 | $9.7 \times 10^{-4}$ | 91616 | 248590 | 8336 | 4837 | 0.6 | 29.7 |

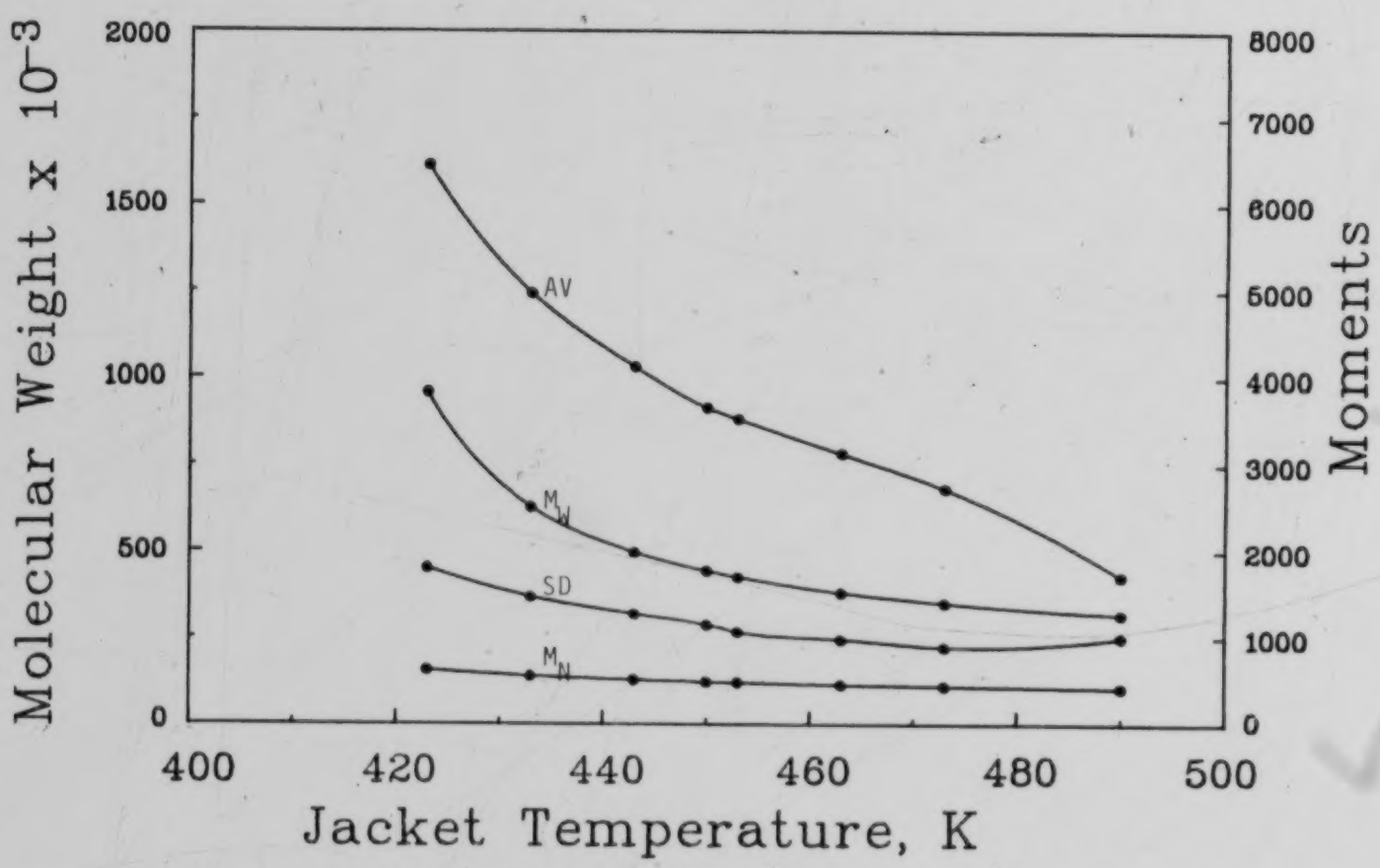


Figure 7.3 Effect of Jacket Temperature on Moments

initiator concentration caused decreases in the product molecular weights. These results are shown in Figure 3.7. Because an increase in the initiator concentration leads to an increase in the polymerization rate, the temperature profiles of the reactor fluid in the constant jacket temperature reactor and the jacket fluid in the isothermal reactor should change with changes in initiator concentration. Figure 3.8 shows that with higher initiator concentrations the temperature peak is larger in magnitude and located closer to the reactor inlet.

The shift in temperature profiles due to increased initiator concentrations should be observed as a change in magnitude of the temperature profile moments. The moment results for the constant jacket temperature reactor are presented in Table 7.2 and Figure 7.4.

In the constant jacket temperature reactor the expected results are confirmed. With increases in the inlet initiator concentration both the average and standard deviation of the temperature profile decrease. The average decreases sharply at low concentrations, $10^{-3}$ mol/l, similar to the $M_w$ trend. The standard deviation, or measure of the width of the profile, decreases slightly over the entire range of

Table 7.2 Effect of Inlet Initiator Concentration on Moments

| MODEL INPUTS | | | MODEL OUTPUTS | | MOMENTS | | | |
|---|---|---|---|---|---|---|---|---|
| $T_J$ K | $T_o$ K | Initiator Concentration mol/l | $M_N$ | $M_W$ | Average | Standard Deviation | Reaction Zone Beginning s | Reaction Zone Length s |
| 433 | 373 | $1.0 \times 10^{-4}$ | 575175 | 5423800 | - | - | - | - |
| 433 | 373 | $2.425 \times 10^{-4}$ | 355470 | 2824900 | - | - | - | - |
| 433 | 373 | $4.85 \times 10^{-4}$ | 228760 | 1360900 | 6405 | 1691 | 8.4 | 12.0 |
| 433 | 373 | $9.7 \times 10^{-4}$ | 138290 | 625420 | 4967 | 1466 | 6.3 | 9.6 |
| 433 | 373 | $1.455 \times 10^{-3}$ | 101820 | 406160 | 4222 | 1301 | 5.4 | 8.1 |
| 433 | 373 | $1.94 \times 10^{-3}$ | 81772 | 303360 | 3733 | 1189 | 4.8 | 7.2 |
| 433 | 373 | $4.85 \times 10^{-3}$ | 40262 | 129470 | 2768 | 952 | 3.6 | 5.4 |
| 433 | 373 | $9.7 \times 10^{-3}$ | 23259 | 72313 | 2324 | 932 | 2.7 | 5.1 |
| 433 | 373 | $1.455 \times 10^{-2}$ | 16819 | 52701 | 1969 | 872 | 2.1 | 4.8 |
| 433 | 373 | $1.94 \times 10^{-2}$ | 13340 | 42484 | 1848 | 875 | 1.8 | 6.3 |

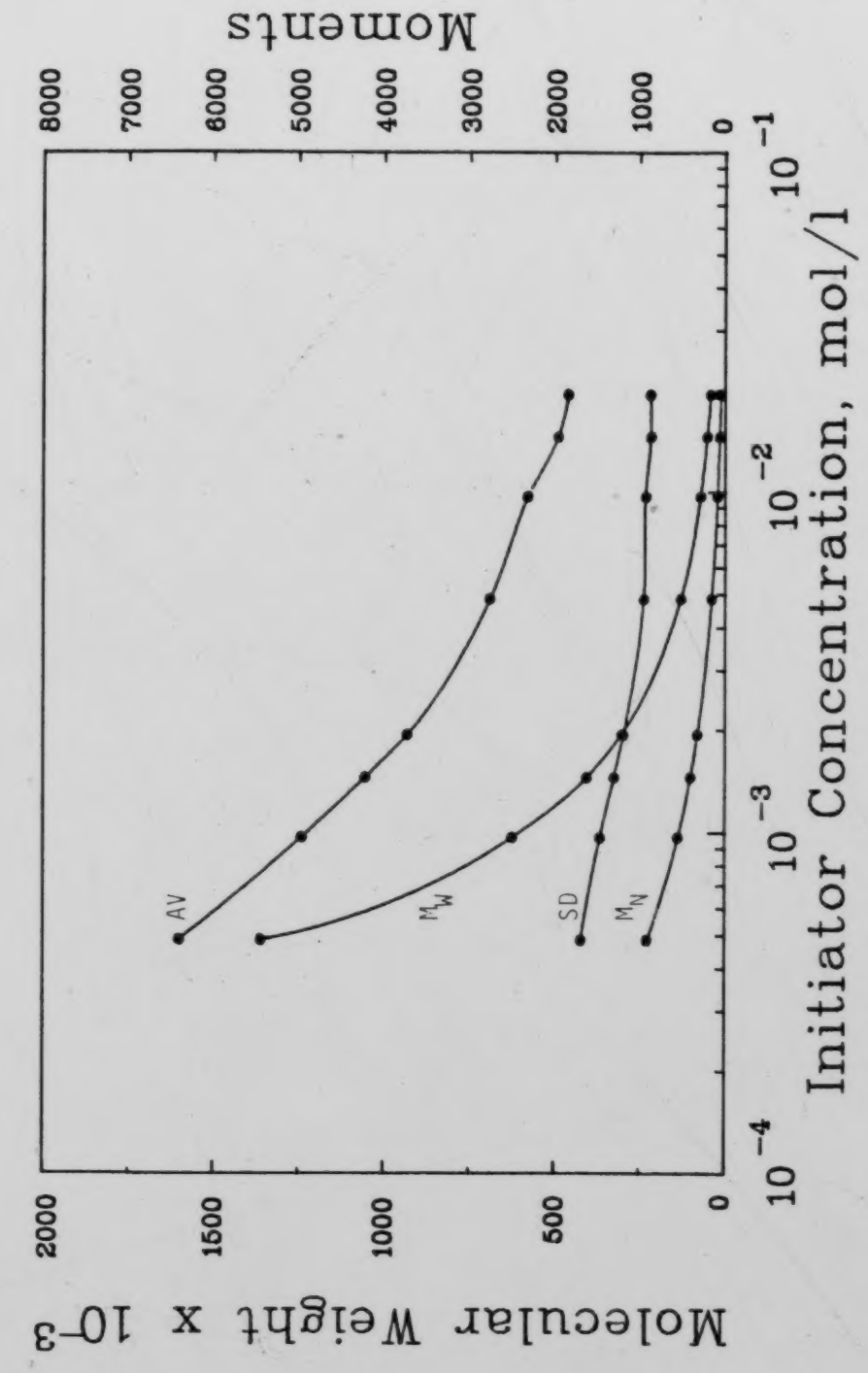


Figure 7.4 Effect of Inlet Initiator Concentration on Moments

concentrations. This trend is similar to that of the $M_N$. Therefore, in this reactor the temperature profile average is indicative of changes in molecular weights, especially changes in $M_W$.

## 7.4 Implications of Temperature Profile Moments

The temperature profile moments described in this chapter are useful tools in predicting changes in molecular weights under certain conditions. Changes in the average and standard deviation of the reactor temperature profile are indicative of changes in the polymer molecular weights due to jacket temperature or initiator concentration changes in the constant jacket temperature reactor. The primary use of these moments is to predict molecular weight changes online. Using temperature measurements at as many locations as possible along the reactor length, the simple moment calculations can be performed by a mini-computer or by hand. By observing the trends in the temperature profile average, an operator or controller can predict changes in molecular weights and can initiate corrective action, if necessary. Hence, the moment calculations can be used for supervisory control of the polymer molecular weight.

# 8. CONCLUSIONS

The steady state model of a tubular polyethylene reactor presented in this study predicts changes in outputs due to changes in initiator concentration, jacket temperature or inlet feed temperature. As the initiator concentration increases the product molecular weights decrease and conversion increases. With increases in inlet or jacket temperatures the molecular weights increase and conversion decreases. From the studies presented in this work and reported in the literature, the most useful control variables are initiator concentration and type, and reactor temperature.

A simple feedback control scheme would adjust the jacket temperature or initiator concentration in order to change the product quality. More complex control schemes would adjust the jacket temperatures in predetermined zones of the reactor or multiple initiator concentrations. In an industrial reactor the heat capacities of the reactor and jacket fluids and the heat transfer characteristics of the reactor wall may change during the reactor operation. A control scheme which adjusts the jacket temperature to control the reactor products must incorporate these changes in heat transfer properties during operation. The more complex reactor

control schemes would adjust both initiator concentration and jacket temperature simultaneously to control the product quality. Before implementing such control schemes on an industrial reactor the combined effects of changes in these control variables should be investigated. Areas of operation in which these changes best control the product quality should be determined.

The mathematical and analytical sensitivity studies provided better understanding of the effects of initiator concentration and jacket temperature on the model outputs. The sensitivity studies of the model with respect to the rate constants pointed out a need for more accurate kinetic data, especially for the transfer to polymer reaction. The rate constants reported in the literature should be verified for the conditions used in simulation, and the model should be validated with either an experimental or an industrial reactor.

The optimization studies determined the operating conditions for producing a desired polymer. Multiple initiator injection points, initiator types and jacket temperature zones increased the complexity of the optimization problem and the range of product qualities that could be produced. The conversion improvement schemes used multiple initiator injections to increase the conversion and polydispersity of the polymer product.

The temperature profile moments were used to develop a relationship between molecular weights and temperature profiles. The temperature profile moment gives an indication of the direction of change of the product molecular weights, reflecting changes in jacket temperature and inlet initiator concentration. A simple steady state control scheme can incorporate these temperature moments. The temperature moments can be calculated online using several thermocouple outputs from the reactor. The trends in temperature moments with real time can be analyzed and corrective action implemented, if necessary. The computing effort that would be required for the temperature moment calculations is negligible in comparison to the model-based control schemes. The temperature moment control scheme can easily be added to the control software of any reactor unit.

In conclusion, this work was a preliminary study of a tubular polyethylene reactor model. The model developed is useful in predicting the effects of changes in operating conditions and kinetic parameters on the product polymer quality. The results of this study indicate that polyethylene reactor modelling and control is an area which could benefit from more research.

## REFERENCES


Agrawal, S. and Han, C.D., AIChE J., 21, No. 3, pp 449-465 (1975).

Atherton, R.W., Schainker, R.B. and Ducot, E.R., AIChE J., 21, No. 3, pp 441-448 (1975).

Beck, J.V. and Arnold, K.J., Parameter Estimation in Engineering and Science, Wiley, New York (1977).

Billmeyer, F.W. Jr., J. Amer. Chem. Soc., 75, pp 6118-6122 (1953).

Chen, C.H., Vermeychuk, J.G., Howell, J.A. and Ehrlich, P., AIChE J., 22, No. 3, pp 463-471 (1976).

Cintron-Cordero, R., Mostello, R.A. and Biesenberger, J.A., Can. J. of Chem. Eng., 46, pp 434-443 (1968).

Donati, G., Marini, L., Marziano, G., Mazzaferri, C., Spampinato, M. and Langianni, E., Advan. Chem. Series, Am. Chem. Soc., pp 579-590 (1982).

Ehrlich, P. and Mortimer, G.A., Adv. Polym. Sci., 7, pp 386-448 (1970).

Goldstein, R.P. and Amundson, N.R., Chem. Eng. Sci., 20, pp 195-236 (1965).

Goto, S., Yamamoto, K., Furui, S. and Sugimoto, M., J. Appl. Polym. Sci., 36, pp 21-40 (1981).

Hamielec, A.E. and Friis, N., Introduction to Chain Polymerization Kinetics, McMaster University (1975).

Hellwege, K.H., Knoppf, W. and Wetzel, W., Koll Z., 180, p 126 (1962).

Hoftyzer, P.J. and Zwietering, Th. N., Chem. Eng. Sci., 14, pp 241-250 (1961).

Hwu, M.C. and Foster, R.D., Chem. Eng. Prog., 78, pp 62-68 (1982).

IMSL Library, subroutines DVERK and ZXSSQ, MTS, University of Alberta.

Lee, K.H. and Marano, J.P. Jr., in Polymerization Reactors and Processes, Amer. Chem. Soc. (1979).

Mulliken, R.V. and Mortimer, G.A., J. Macromol. Sci.-Chem. A4 (7), pp 1495-1505 (1970).

Mulliken, R.V. and Mortimer, G.A., J. Macromol. Sci.-Chem. A6 (7), pp 1301-1310 (1972).

Romanini, D., Polym.-Plast. Technol. Eng., 19, No. 2, pp 201-226 (1982).

Sage, A.P., Optimum Systems Control, Prentice-Hall Englewood Cliffs, N.J. (1968).

Sittig, M., Polyolefin Production Processes-Latest Developments, Noyes Data Corporation (1976).

Thies, H., AIChE meeting on Modelling of Polymerization Reactors, Houston (1979).

Thomas, I.M. and Kiparissides, C., 'Sensitivity Analysis of a Batch Polymerization Reactor', unpublished.

Volter, B.V., Second Intern. Fed. of Automatic Control Congress, Basel (1963).

## Appendix A
## Derivation of Kinetic Equations

The mechanism of free radical polymerization of ethylene is described by the following elementary reactions:

(i) initiator decomposition

$$I \xrightarrow{k_d} 2\ R_o \longrightarrow 2\ f\ R_o^*$$

(ii) chain initiation

$$R_o^* + M \xrightarrow{k_I} R_1^*$$

(iii) propagation

$$R_x^* + M \xrightarrow{k_p} R_{x+1}^* \qquad x \in [1,\infty)$$

(iv) transfer to polymer

$$R_x^* + P_y \xrightarrow{k_{fp}} P_x + R_y^* \qquad x \in [1,\infty),\ y \in [1,\infty)$$

(v) termination by combination

$$R_x^* + R_y^* \xrightarrow{k_{tc}} P_{x+y} \qquad x,y \in [1,\infty)$$

(vi) termination by disproportionation

$$R_x^* + R_y^* \xrightarrow{k_{td}} P_x + P_y \qquad x,y \in [1,\infty)$$

where:

I represents the initiator molecules

$R_o$: the initiator radicals

$R_o^*$: the activated initiator radicals

M: monomer molecules

f: initiator efficiency

$R_x^*$: live radical of chain length x

$P_x$: dead polymer of chain length x

$k_d$: initiator decomposition rate constant

$k_I$: chain initiation rate constant

$k_p$: propagation rate constant

$k_{tc}$: termination by combination rate constant

$k_{fp}$: transfer to polymer rate constant

$k_{td}$: termination by disproportionation rate constant

Material balances are derived for each species in the reactor to give the overall kinetic model.

Initiator

The rate of initiator disappearance is expressed as:

$$\frac{d[I]}{dt} = - 2 k_d[I] \qquad (A.1)$$

where:

[I] is the initiator concentration

t is the reactor coordinate

$k_d$ is the initiator decomposition rate

The chain initiator rate is:

$$\frac{d[R_o^*]}{dt} = 2\, f\, k_d[I] - k_I[M][R_o^*] \qquad (A.2)$$

where:

f is the initiator efficiency factor

If the quasi-steady state approximation is assumed to be valid for radicals of chain length zero then:

$$\frac{d[R_o^*]}{dt} = 0 \qquad (A.3)$$

and

$$2\, f\, k_d[I] = k_I[M][R_o^*] \qquad (A.4)$$

Monomer

Monomer is consumed in the propagation and initiation in reactions and generated in the termination by disproportionation reaction:

$$\frac{d[M]}{dt} = -k_p[M] \sum_{x=1}^{\infty} [R_1^*] - k_I[M][R_o^*] + k_{td}[R_1^*] \sum_{x=1}^{\infty} [R_x^*] \qquad (A.5)$$

where:

[M] is the monomer concentration

$k_p$ is the propagation rate constant

$k_{td}$ is the termination by disproportionation rate constant

$[R_x^*]$ is the concentration of live radicals of chain length x

Radicals are classified in two categories: those with chain length one and those with chain length greater than one. Different mass balances are derived for each radical type.

radicals of chain length one

$$\frac{d[R_1^*]}{dt} = 2 f k_d[I] - k_p[M][R_1^*] - k_t[R_1] \sum_{y=1}^{\infty} [R_y^*]$$

$$- k_{fp}([R_1^*] \sum_{y=1}^{\infty} y[P_y] - P_1 \sum_{y=1}^{\infty}[R_y^*]) \qquad (A.6)$$

where:

$k_t$ is the sum of the termination rate constants ($k_{tc} + k_{td}$)

$k_{fp}$ is the transfer to polymer rate constant

$[P_x]$ is the concentration of dead polymer chains of length x

radicals of chain length greater than one

$$\frac{d[R_x^*]}{dt} = k_p[M][R_{x-1}^*] - k_p[M][R_x^*] - k_t[R_x^*] \sum_{y=1}^{\infty}[R_y^*]$$

$$- k_{fp}([R_x^*] \sum_{y=1}^{\infty} y[P_y] - x[P_x] \sum_{y=1}^{\infty}[R_y^*]) \qquad (A.7)$$

$$x \varepsilon [2,\infty)$$

Polymer Molecules

Polymer molecules are divided into two classes: those of chain length one and greater than one. Mass balances for these two classes of polymer molecules are given below:

polymer of chain length one

$$\frac{d[P_1]}{dt} = k_{td}[R_1^*] \sum_{x=1}^{\infty}[R_x^*] + k_{fp}([R_1^*] \sum_{x=1}^{\infty} x[P_x] - [P_1] \sum_{x=1}^{\infty}[R_x^*]) \quad (A.8)$$

polymer of chain length greater than one

$$\frac{d[P_x]}{dt} = \frac{1}{2} k_{tc} \sum_{y=1}^{x-1}[R_y^*][R_{x-y}^*] + k_{td}[R_x^*] \sum_{y=1}^{\infty}[R_y^*]$$

$$+ k_{fp}([R_x^*] \sum_{y=1}^{\infty} y[P_y] - [P_x] \sum_{y=1}^{\infty}[R_y^*]) \quad (A.9)$$

$$x \varepsilon [2,\infty)$$

The use of radical and polymer moments simplifies the mass balance equations. In this model the moments are defined as:

Radical Moments

zeroth moment: $G(1,t) = \sum_{x=1}^{\infty}[R_x^*]$ (A.10)

first moment $G'(1,t) = \sum_{x=1}^{\infty} x[R^*]$ (A.11)

second moment $G''(1,t) = \sum_{x=1}^{\infty} x(x-1)[R_x^*]$

$$= \sum_{x=1}^{\infty} (x^2[R_x^*] - x[R_x^*]) \quad (A.12)$$

Polymer Moments

zeroth moment $$H(1,t) = \sum_{x=1}^{\infty} ([R_x^*] + [P_x]) \tag{A.13}$$

first moment $$H'(1,t) = \sum_{x=1}^{\infty} x([R_x^*] + [P_x]) \tag{A.14}$$

second moment $$H''(1,t) = \sum_{x=1}^{\infty} x(x-1)([R_x^*] + [P_x]) \tag{A.15}$$

Material balances for the moments of the molecular weights are obtained by differentiating equations (A.10) to (A.15). The material balances for the radical and polymer molecules are substituted into the differential equations. The following expressions for the radical and polymer moments are obtained:

$$\frac{dG(1,t)}{dt} = 2 f k_d[I] - k_t G(1,t) G(1,t) \tag{A.16}$$

$$\begin{aligned}\frac{dG'(1,t)}{dt} = {} & 2 f k_d[I] + k_p[M] G(1,t) - k_t G'(1,t) G(1,t) \\ & - k_{fp} \{G'(1,t)[H'(1,t) - G'(1,t) - G(1,t)] \\ & - G(1,t)[H''(1,t) + H'(1,t) - G''(1,t) - G'(1,t)]\}\end{aligned} \tag{A.17}$$

$$\begin{aligned}\frac{dG''(1,t)}{dt} = {} & 2 k_p[M] G'(1,t) - k_t G''(1,t) G(1,t) \\ & - k_{fp} [G''(1,t)(H'(1,t)) - G(1,t)) \\ & - G(1,t)(H'''(1,t) - G'''(1,t) + 2 \{H''(1,t) - G''(1,t)\})]\end{aligned} \tag{A.18}$$

$$\frac{dH(1,t)}{dt} = 2 f k_d[I] - \frac{1}{2} k_{tc} G^2(1,t) \tag{A.19}$$

$$\frac{dH'(1,t)}{dt} = 2 f k_d[I] + k_p[M] G(1,t) \tag{A.20}$$

$$\frac{dH''(1,t)}{dt} = 2\, k_p[M]\, G'(1,t) + k_{tc}\, G'(1,t)\, G'(1,t) \qquad (A.21)$$

where $G'''(1,t)$ is the third radical moment

$H'''(1,t)$ is the third polymer moment.

According to Lee and Marano:

$$H'(1,t) - G'(1,t) \approx H'(1,t) \qquad (A.22)$$

$$H''(1,t) - G''(1,t) \approx H''(1,t) \qquad (A.23)$$

$$H'''(1,t) - G'''(1,t) \approx H'''(1,t) \qquad (A.24)$$

Thus, the first and second radical moments are:

$$\frac{dG'(1,t)}{dt} = 2\, f\, k_d[I] + k_p[M]\, G'(1,t) - k_t\, G'(1,t),\, G(1,t) - k_{fp}[G'(1,t)\, H'(1,t) - G(1,t)(H''(1,t) + H'(1,t))] \qquad (A.25)$$

$$\frac{dG''(1,t)}{dt} = 2\, k_p[M]\, G'(1,t) - k_t\, G''(1,t)\, G(1,t) - k_{fp}[G''(1,t)\, H'(1,t) - G(1,t)(H'''(1,t) + 2\, H''(1,t))] \qquad (A.26)$$

In Lee and Marano's model the mass balance for the second moment of the radical concentration (A.26) is used only for the derivation of the second moment of the polymer concentration. It is not explicitly required for the molecular weight determination. Therefore, the rate expression for the second radical moment is not included in this model.

The monomer balance equation (A.5) is simplified by the use of the radical moments and the long chain approximation to become:

$$\frac{d[M]}{dt} = - k_p[M]\, G(1,t) \qquad (A.27)$$

The overall disappearance rate of monomer is equal to the formation rate of radicals and polymers of all sizes, ie $\frac{d}{dt} H'(1,t)$.

$$\frac{-d[M]}{dt} = + \frac{dH'(1,t)}{dt} \qquad (A.28)$$

In summary, the overall kinetic model consists of the following rate equations:

Initiator

$$\frac{d[I]}{dt} = - 2\, k_d[I] \qquad (A.1)$$

Monomer

$$\frac{d[M]}{dt} = - k_p[M]\, G(1,t) \qquad (A.27)$$

Radical Moments

$$\frac{dG(1,t)}{dt} = 2\, f\, k_d[I] - k_t\, G(1,t)\, G(1,t) \qquad (A.16)$$

$$\frac{dG'(1,t)}{dt} = 2\, f\, k_d[I] + k_p[M]\, G(1,t) - k_t\, G'(1,t)\, G(1,t)$$

$$- k_{fp}[G'(1,t)\, H'(1,t) - G(1,t)(H''(1,t) + H'(1,t))] \qquad (A.25)$$

Polymer Moments

$$\frac{dH(1,t)}{dt} = 2\, f\, k_d[I] - \frac{1}{2}\, k_{tc}\, G(1,t)\, G(1,t) \qquad (A.19)$$

$$\frac{dH''(1,t)}{dt} = 2\, k_p[M]\, G'(1,t) + k_{tc}\, G'(1,t)\, G'(1,t) \qquad (A.21)$$

## Appendix B
## Derivation of Sensitivity Equations

The reactor model developed in chapter 2 can be represented by the following equation:

$$\frac{d\underset{\sim}{y}}{dt} = \underset{\sim}{f}(\underset{\sim}{y},\underset{\sim}{p},t) \tag{B.1}$$

and a set of initial conditions

$$\underset{\sim}{y}\,|_{t=0} = \underset{\sim}{y}_0 \tag{B.2}$$

where $\underset{\sim}{y}$ is the output vector and $\underset{\sim}{p}$ is the parameter vector. For the the constant jacket temperature reactor the output and parameter vectors are:

$$\underset{\sim}{y} = (X_M,\ X_I,\ G,\ G',\ H,\ H'',\ \frac{T}{T_0})^T \tag{B.3}$$

$$\underset{\sim}{p} = (T_J,\ C_{I0}) \tag{B.4}$$

In this appendix the steps required to calculate the sensitivity coefficients for the outputs with respect to the parameters will be derived.

The sensitivity coefficient for the parameter $p_j$ and the output $y_i$ is defined as the first partial derivative of $y_i$ with respect to $p_j$:

$$\phi_{ij} = \frac{\delta y_i}{\delta p_j} \quad \begin{matrix} i=1,\ldots,7 \\ j=1,2 \end{matrix} \tag{B.5}$$

The sensitivity matrix is a matrix of these coefficients

$$\Phi_{ij} = \frac{\delta y_i}{\delta p_i} = \frac{\delta \underset{\sim}{y}}{\delta \underset{\sim}{p}} \tag{B.6}$$

The information provided by the model is used to determine $\frac{\delta \underset{\sim}{y}}{\delta \underset{\sim}{p}}$.

Since the model is a set of differential equations the sensitivity coefficients cannot be calculated analytically from equation (B.6). Using the sensitivity analysis method (Atherton et al (1975), Beck and Arnold (1977)), a differential equation for the sensitivity matrix may be derived.

The first step in the derivation of the sensitivity matrix is to interchange the order of differentiation in the expression below and substitute equation (B.1) to obtain:

$$\frac{d}{dt}\left(\frac{\delta \underset{\sim}{y}}{\delta \underset{\sim}{p}}\right) = \frac{\delta}{\delta \underset{\sim}{p}}\left(\frac{d \underset{\sim}{y}}{dt}\right) = \frac{\delta}{\delta \underset{\sim}{p}} \underset{\sim}{f}(\underset{\sim}{y}, \underset{\sim}{p}, t) \tag{B.7}$$

Since $\underset{\sim}{y}$ is a function of $\underset{\sim}{p}$

$$\frac{d}{dt}\left(\frac{\delta \underset{\sim}{y}}{\delta \underset{\sim}{p}}\right) = \frac{\delta \underset{\sim}{f}}{\delta \underset{\sim}{y}}\Bigg|_{\underset{\sim}{p}} \frac{\delta \underset{\sim}{y}}{\delta \underset{\sim}{p}} + \frac{\delta \underset{\sim}{f}}{\delta \underset{\sim}{p}}\Bigg|_{\underset{\sim}{y}} \tag{B.8}$$

The matrix of derivatives is defined by equation (B.6). By introducing the sensitivity coefficient $\Phi_{ij}$ as defined in equation (B.5), equation (B.8) may be rewritten in the following form:

$$\frac{d\Phi_{ij}}{dt} = \sum_{k=1}^{7} \frac{\delta f_i}{\delta y_k} \Phi_{kj} + \frac{\delta f_i}{\delta p_j} \quad \begin{matrix} i=1,\ldots,7 \\ j=1,2 \end{matrix} \tag{B.9}$$

To determine the initial conditions for equation (B.8), note that:

$$\frac{\delta\, y_i(0)}{\delta\, p_j} = \delta_{ij} \text{ if } p_j \text{ is an initial conditions} \quad (B.10)$$

$$(\text{ie } p_2 = C_{I0})$$

$$\frac{\delta\, y_i(0)}{\delta p_j} = 0 \text{ is } p_j \text{ is not an initial condition}$$

The initial conditions are summarized as:

$$\Phi_{ij}(0) = \begin{cases} 0 \text{ if } p_j \text{ is not an initial condition} \\ \delta_{ij} \text{ if } p_j \text{ is an initial condition} \end{cases} \quad (B.11)$$

Equations (B.9) and (B.11) give a set of differential equations whose solution determines the numerical value of the sensitivity matrix as a function of time. The number of equations is the product of the number of state variables and the number of parameters (ie 7x2 = 14). Each sensitivity equation (B.9) is linear in the $\Phi_{ij}$'s and has variable coefficients which are determined by the state $\underset{\sim}{y}$.

The equation (B.1) describing the polymerization has been derived in Appendix A. It is:

$$\frac{dy_1}{dt} = k_p(1 - y_1)y_3$$

$$\frac{dy_2}{dt} = 2\, k_d(1 - y_2) \quad (B.12)$$

$$\frac{dy_3}{dt} = 2\, f\, k_d C_{I0}(1 - y_2) - k_T y_3^2$$

$$\frac{dy_4}{dt} = 2 f k_d C_{IO}(1 - y_2) + k_p C_{mo}(1 - y_1)y_3$$

$$- k_T y_3 y_4 - k_{fp}\left[C_{mo} y_1 y_4 - y_3(y_6 + C_{mo} y_1)\right]$$

$$\frac{dy_5}{dt} = 2 f k_d C_{IO}(1 - y_2) - \frac{1}{2} k_{tc} y_3^2$$

$$\frac{dy_6}{dt} = 2 k_p C_{mo}(1 - y_1)y_4 + k_{tc} y_4^2$$

$$\frac{dy_7}{dt} = \frac{-\Delta H C_{mo}}{\rho C_p T_o} \frac{dy_1}{dt} - \frac{4 U \tau}{\rho C_p D}\left(y_7 - \frac{T_J}{T_o}\right)$$

Application of the sensitivity equations (B.9) and (B.11) to the model (B.12) yields the following set of differential equations for the sensitivity coefficients:

<u>jacket temperature</u>, $T_J$ (j=1)

$$\frac{d \Phi_{11}}{dt} = - k_p y_3 \Phi_{11} + k_p(1 - y_1) \Phi_{31}$$

$$+ (1 - y_1)y_3 \frac{\delta k_p}{\delta y_7} \Phi_{71}$$

$$\frac{d \Phi_{21}}{dt} = -2 k_d \Phi_{21} + 2(1 - y_2) \frac{\delta k_d}{\delta y_7} \Phi_{71}$$

$$\frac{d \Phi_{31}}{dt} = -2 f k_d C_{IO} \Phi_{21} - 2 k_T y_3 \Phi_{31}$$

$$+ \left(2 f C_I \frac{\delta k_d}{\delta y_7} - y_3^2 \frac{\delta k_T}{\delta y_7}\right) \Phi_{71}$$

$$\frac{d\,\Phi_{41}}{dt} = \left[y_3\, C_{mo}(k_{fp} - k_p) - y_4\, C_{mo}\, k_{fp}\right] \Phi_{11}$$

$$- 2\, f\, k_d\, C_{IO}\, \Phi_{21} + (k_p C_m - k_T y_4 + k_{fp} y_6 + k_{fp} y_1 C_{mo})\, \Phi_{31}$$

$$- (k_T y_3 + K_{fp} C_{mo} y_1)\, \Phi_{41} + k_{fp} y_3\, \Phi_{61}$$

$$+ \left[2\, f C_I \frac{\delta k_d}{\delta y_7} + C_m y_3 \frac{\delta k_p}{\delta y_7} - y_3 y_4 \frac{\delta k_T}{\delta y_7}\right.$$

$$\left. - (C_{mo} y_1 y_4 - y_3(y_6 + y_1 C_{mo})) \frac{\delta k_{fp}}{\delta y_7}\right] \Phi_{71}$$

$$\frac{d\,\Phi_{51}}{dt} = - 2\, f\, k_d\, C_{IO}\, \Phi_{21} - k_{tc} y_3\, \Phi_{31}$$

$$+ \left(2\, f\, C_I \frac{\delta k_d}{\delta y_7} - \frac{1}{2} y_3^2 \frac{\delta k_{tc}}{\delta y_7}\right) \Phi_{71} \qquad \text{(B.13)}$$

$$\frac{d\,\Phi_{61}}{dt} = - 2\, k_p C_{mo} y_4\, \Phi_{11} + (2\, k_p C_m + 2\, k_{tc} y_4)\, \Phi_{41}$$

$$+ \left(2 C_m y_4 \frac{\delta k_p}{\delta y_7} + y_4^2 \frac{\delta k_{tc}}{\delta y_7}\right) \Phi_{71}.$$

$$\frac{d\,\Phi_{71}}{dt} = \frac{1}{\rho C_p}\left[\frac{\Delta H\, k_p}{T_o} (C_{mo} y_3\, \Phi_{11} - C_m\, \Phi_{31})\right.$$

$$\left. - \left(\frac{\Delta H\, C_m y_3}{T_o} \frac{\delta k_p}{\delta y_7} + \frac{4\, U}{D}\right) \Phi_{71} + \frac{4\, U}{T_o D}\right]$$

$$\Phi_{11}(0)=0;\ \Phi_{21}(0)=0;\ \Phi_{31}(0)=0;\ \Phi_{41}(0)=0;\ \Phi_{51}(0)=0;$$

$$\Phi_{61}(0)=0;\ \Phi_{71}(0)=0 \qquad \text{(B.14)}$$

where all variables are defined in Appendix A.

inlet initiator concentration, $C_{IO}$(j=2)

$$\frac{d\,\Phi_{12}}{dt} = -k_p y_3\,\Phi_{12} + k_p(1-y_1)\,\Phi_{32} + (1-y_1)y_3\frac{\delta k_p}{\delta y_7}\,\Phi_{72}$$

$$\frac{d\,\Phi_{22}}{dt} = -2\,k_d\,\Phi_{22} + 2\,(1-y_2)\,\frac{\delta k_d}{\delta y_7}\,\Phi_{72} - 2\,\frac{k_d}{C_{IO}}\,(1-y_2)$$

$$\frac{d\,\Phi_{32}}{dt} = -2\,f\,k_d\,C_{IO}\,\Phi_{22} - 2\,k_T y_3\,\Phi_{32}$$

$$+ \left(2\,f\,C_I\,\frac{\delta k_d}{\delta y_7} - y_3^2\,\frac{\delta k_T}{\delta y_7}\right)\Phi_{72} + 2\,f\,k_d(1-y_2)$$

$$\frac{d\,\Phi_{42}}{dt} = \left[y_3 C_{mo}(k_{fp}-k_p) - y_4 C_{mo} k_{fp}\right]\Phi_{12}$$

$$- 2\,f\,k_d C_{IO}\,\Phi_{22} + (k_p C_m - k_T y_4 + k_{fp} y_6 + k_{fp} y_1 C_{mo})\,\Phi_{32}$$

$$- (k_T y_3 + k_{fp} C_{mo} y_1)\,\Phi_{42} + k_{fp} y_3\,\Phi_{62}$$

$$+ \left[2\,f\,C_I\,\frac{\delta k_d}{\delta y_7} + C_m y_3\,\frac{\delta k_p}{\delta y_7} - y_3 y_4\,\frac{\delta k_T}{\delta y_7}\right.$$

$$\left. -(C_{mo} y_1 y_4 - y_3(y_6 + y_1 C_{mo}))\frac{\delta k_{fp}}{\delta y_7}\right]\Phi_{72} + 2\,f\,k_d(1-y_2) \qquad \text{(B.15)}$$

$$\frac{d\Phi_{52}}{dt} = -2\,f\,k_d\,C_{IO}\,\Phi_{22} - k_{tc} y_3\,\Phi_{32}$$

$$+ \left(2\,f\,C_I\,\frac{\delta k_d}{\delta y_7} - \frac{1}{2}\,y_3^2\,\frac{\delta k_{tc}}{\delta y_7}\right)\Phi_{72} + 2\,f\,k_d\,(1-y_2)$$

$$\frac{d\,\Phi_{62}}{dt} = -2\,k_p C_{mo} y_4\,\Phi_{12} + 2(k_p C_m + k_{tc} y_4)\,\Phi_{42}$$

$$+ \left(2\,C_m y_4\,\frac{\delta k_p}{\delta y_7} + y_4^2\,\frac{\delta k_{tc}}{\delta y_7}\right)\Phi_{72}$$

$$\frac{d\,\Phi_{72}}{dt} = \frac{1}{\rho C_p}\left[\frac{\Delta H\, C_{mo} k_p y_3}{T_o}\,\Phi_{12} - \frac{\Delta H\, C_m k_p}{T_o}\,\Phi_{32} - \left(\frac{\Delta H C_m y_3}{T_o}\,\frac{\delta k_p}{\delta y_7} + \frac{4\,U}{D}\right)\right]\Phi_{72}$$

$$\Phi_{12}(0)=0;\ \Phi_{22}(0)=1.0;\ \Phi_{32}(0)=0;\ \Phi_{42}(0)=0;\ \Phi_{52}(0)=0;$$

$$\Phi_{62}(0)=0;\ \Phi_{72}(0)=0 \qquad \text{(B.16)}$$

These sensitivity equations provide the sensitivity of the model states with respect to the model inputs. It is also desirable to calculate the sensitivities of the molecular weights with respect to the model inputs.

The molecular weights are calculated from the model states as follows:

$$M_N = \frac{M_{C_2H_4}\, C_{mo} y_1}{y_5} \qquad \text{(B.17)}$$

$$M_W = \frac{M_{C_2H_4}\, y_6}{C_{mo} y_1} \qquad \text{(B.18)}$$

Using the quotient rule of differentiation the sensitivity coefficients for $M_N$ and $M_W$ are:

$$\frac{\delta M_N}{\delta p_j} = M_{C_2H_4}\, C_{mo}\ \frac{y_5\,\frac{\delta y_1}{\delta p_j} - y_1\,\frac{\delta y_5}{\delta p_j}}{y_5^2} \qquad \text{(B.19)}$$

$$\frac{\delta M_W}{\delta p_j} = \frac{M_{C_2H_4}}{C_{mo}}\ \frac{y_1\,\frac{\delta y_6}{\delta p_j} - y_6\,\frac{\delta y_1}{\delta p_j}}{y_1^2} \qquad \text{(B.20)}$$

Thus, the molecular weight sensitivities can be calculated analytically at each point along the reactor coordinate.

The sensitivity coefficients for all model states are calculated by integrating equations (B.13) and (B.15) numerically along with the reactor model. The molecular weight sensitivities are calculated analytically.

In order to show the relative influence of the parameters on the output variables, a normalized sensitivity coefficient was used in place of the true sensitivity coefficient. The normalized sensitivity coefficient is defined as:

$$\psi_{ij} = \phi_{ij} \times \frac{p_j}{y_i} \qquad (B.21)$$

The normalized sensitivity coefficients for the constant jacket temperature reactor are plotted in Figures 4.1 to 4.6.

# Appendix C

## Computer Program

```
C     PROGRAM TO CALCULATE TEMPERATURE, CONVERSION AND MOMENT
C      PROFILES FOR HIGH PRESSURE TUBULAR PE REACTOR.
C      BASED ON MODEL OF LEE AND MARANO.  CHEN RATE CONSTANTS.
C     BENZOYL PEROXIDE INITIATOR
C      WRITTEN BY PEGGY HOWLEY NOV. 30, 1983.
C
      INTEGER N,IND,NW,IER,K
      REAL Y(7),C(24),W(7,10),X,TOL,XEND
      EXTERNAL FCN1
      COMMON /B1/ TO,TEMP,REST,TJ,CIO,CMO
      COMMON /B2/ CP,HR,U,RHOF,D,P
C
C     DATA FOR IMSL SUBROUTINE DVERK
      NW = 7
      N = 7
      TOL = .0010
      WRITE (5,1) TOL
    1 FORMAT (1X, 'RUNGE KUTTA SOLUTION WITH TOL =',F5.4)
      C(1)=3.00
      C(2)=1.0E-5
      C(3)=1.0E-20
      DO 5 I=4,9
      C(I)=0.00
    5 CONTINUE
      READ(4,10) CP
      READ (4,10) HR
      READ (4,10) U
      READ (4,10) RHOF
      READ (4,10) REST
      READ (4,10) D
      READ (4,10) P
      READ (4,10) TO
      WRITE (5,11)
      WRITE (5,12)
      WRITE (5,13) CP,HR,U,RHOF,REST,D,P,TO
   10 FORMAT(14X,F10.2)
   11 FORMAT(10X,'MODEL DATA',/)
   12 FORMAT(5X,'CP',8X,'HR',9X,'H',8X,'RHOF',6X,'REST',7X,'D',9X,'P',9X,
     & 'TO')
   13 FORMAT (1X,8F10.2,/)
      READ (3,20) TJ
      READ (3,20) CIO
      READ (3,20) CMO
      WRITE (5,21)
      WRITE (5,22) TJ
      WRITE (5,23) CIO,CMO
   20 FORMAT (15X,E10.4)
   21 FORMAT(10X,'INITIAL DATA',/)
   22 FORMAT(5X,'JACKET TEMPERATURE = ',F7.1)
   23 FORMAT(5X,'CIO = ',E10.5,' CMO = ',E10.5,/)
C     DEPENDENT VARIABLES
C     Y(1) = MONOMER CONVERSION   (CMO-CM)/CMO
C     Y(2) = INITIATOR CONVERSION   (CIO-CI)/CIO
C     Y(3) = G(1,Z)
C     Y(4) = G'(1,Z)
C     Y(5) = H(1,Z)
C     Y(6) = H''(1,Z)
C     Y(7) = DIMENSIONLESS REACTOR TEMPERATURE
C     INITIAL CONDITIONS
      X = 0.000
```

```
      Y(1) = 0.000
      Y(2) = 0.000
      Y(3) = 0.000
      Y(4) = 0.000
      Y(5) = 0.000
      Y(6) = 0.000
      Y(7) = 1.000
      SUMT=0.0
      SUMT2=0.0
      TMAX=0.0
      TM1=T0
      DT1=500.0
      DT2=1000.0
      ZR=1.0
      ZF=1.0
C
C     PRINT OUT INITIAL CONDITIONS
      WN=0.0
      WW=0.0
      XEND = X
      WRITE (5,50)
      WRITE (5,60) XEND,T0,(Y(I),I=1,4),WN,WW,Y(5),Y(6)
C
C     INTEGRATE WITH RESPECT TO TIME ALONG REACTOR LENGTH USING  DVERK
C
      XF=1.00
      J0=1
      K0=1
      JMAX=100
      STEP=1.0/FLOAT(JMAX)
      KMAX=10
      ZKMAX=FLOAT(KMAX)
      ZMAX=FLOAT(JMAX*KMAX)
      ZJ=FLOAT(J0-1)
      DO 110 J=J0,JMAX
      ZJ=ZJ+1.0
      ZK=FLOAT(K0-1)
      DO 100 K=K0,KMAX
      ZK=ZK+1.0
      ZEND = ((ZJ-1.00)*ZKMAX+ZK)/ZMAX
      XEND=1.0/ZMAX
      X=0.00
      C(20)=0.00
      IND=2
      CALL DVERK(N,FCN1,X,Y,XEND,TOL,IND,C,NW,W,IER)
      WN=28.0*CMO*Y(1)/Y(5)
      WW=28.0*Y(6)/(CMO*Y(1))
C
C     CHECK FOR ERROR MESSAGES
C
      IF (IND.LT.0.OR.IER.GT.0) GO TO 150
  100 CONTINUE
      WRITE (5,60) ZEND,TEMP,(Y(I),I=1,4),WN,WW,Y(5),Y(6)
   50 FORMAT (2X,'X',6X,'T',7X,'XM',8X,'X1',8X,'Y3',8X,'X4',8X,
     & 'MN',8X,'MW')
   60 FORMAT (1X,F6.3,F7.2,8E10.3)
      IF(J.GT.1) GO TO 104
      TM2=TM1
      TM1=TEMP
      GO TO 110
```

```
  104 CONTINUE
      IF (ZEND GT ZF) GO TO 110
      IF(TEMP LE TMAX) GO TO 105
      TMAX=TEMP
      ZTMAX=ZEND
  105 CONTINUE
      DTDX=(TM2-4.0*TM1+3.0*TEMP)/(2.0*STEP)
      CHANGE=DTDX-DT1
      TM2=TM1
      TM1=TEMP
      IF(ZR.LT.1.0) GO TO 106
      IF((DT1.LE.DT2).AND.(DT1.LE.DTDX).AND.(CHANGE.GE.0.0))
     & ZR=ZEND
  106 CONTINUE
      IF((DTDX.LT.0.0).AND.(CHANGE.GE.0.0).AND.(ZF.GT.0.99)) ZF=ZEND
      DT2=DT1
      DT1=DTDX
      IF(ZEND.LT.ZR) GO TO 110
      SUMT=TEMP*ZEND*REST + SUMT
      SUMT2=(TEMP*ZEND*REST)**2 + SUMT2
  110 CONTINUE
  111 CONTINUE
      PD=WW/WN
      WRITE (5,140) WN,WW,PD
  140 FORMAT (1X,'MN = ',E10.5,' MW = ',E10.5,' PD = ',F8.3,/)
      Z=(ZF-ZR)*100.0+1.0
      TAV=SUMT/Z
      TVAR=(Z*SUMT2-SUMT**2)/(Z*(Z-1.0))
      SDT=SQRT(TVAR)
      WRITE (5,145)
      WRITE (5,146) TMAX,ZTMAX,TAV,SDT
  145 FORMAT(10X,'MAX TEMP',2X,'LOCATION ',2X,'AVG TEMP',2X,'STD DEV')
  146 FORMAT(10X,F6.2,F9.2,F11.2,F10.3)
      WRITE(5,147)
      WRITE(5,148)
      WRITE(5,149) ZR,ZF,Z
  147 FORMAT(10X,'REACTION ZONE')
  148 FORMAT(8X,'START',6X,'END',5X,'LENGTH')
  149 FORMAT(8X,F4.2,5X,F4.2,5X,F5.0)
      STOP
  150 CONTINUE
C
C     ERRORS HAVE OCCURRED IN RUNNING 'DVERK'
C
      WRITE (5,160)
      IF (IND.LT.0) WRITE (5,170) IND
      IF (IER.GT.0) WRITE (5,180) IER
      IF (IER.EQ.131) WRITE (5,190) C(20),C(21)
  160 FORMAT (1X,'ERROR DIAGNOSTICS')
  170 FORMAT (1X,'IND = ',I4)
  180 FORMAT (1X,'IER = ',I4)
  190 FORMAT(1X,'C(20) = ',E12.5,' C(21) = ',E12.5)
      WRITE(5,60) ZEND,TEMP,(Y(I),I=1,4),WN,WW
      STOP
      END
      SUBROUTINE FCN1(N,X,Y,YPRIME)
C
C     SUBROUTINE TO CALCULATE TEMPERATURE, CONVERSION AND CHAIN LENGTH
C      MOMENTS ACCORDING TO LEE AND MARANO MODEL
C
```

```
      INTEGER N
      REAL Y(7),YPRIME(7),X,TEMP,CIO,CMO
      COMMON /B1/ TO,TEMP,REST,TJ,CIO,CMO
      COMMON /B2/ CP,HR,U,RHOF,D,P
C
C     SYSTEM PARAMETERS
C
C     CMO = INLET MONOMER CONCENTRATION  MOLE/L
C     CIO = INLET INITIATOR CONCENTRATION  MOLE/L
C     TO = INLET REACTOR TEMPERATURE  K
C     CP = HEAT CAPACITY  CAL/MOLE K
C     D = DIAMETER  M
C     EP,EI,ETC,... ACTIVATION ENERGY / R  K
C     FKPO,FKIO,... FREQUENCY FACTOR FOR RATE CONSTANTS  L/MOLE SEC
C     FKP,FKI,... RATE CONSTANT AT GIVEN TEMPERATURE  L/MOLE SEC
C     F = INITIATOR EFFICIENCY
C     U = HEAT TRANSFER COEFFICIENT  CAL/M2 SEC K
C     HR = HEAT OF REACTION  CAL/MOLE
C     REST = RESIDENCE TIME OF REACTOR  SEC
C     RHOF = FLUID DENSITY  MOLE/L
C     TJ = COOLING JACKET TEMPERATURE  K
C
C     RATE CONSTANT DATA
C
      F =0.50
      FKDO = 6.38E13
      ED =29700.0/1.987
      FKPO = 2.95E7
      EP =(8200.0-0.555*P)/1.987
      FKTCO = 1.60E9
      ETC = 2400.0/1.987
      FKTDO= 2.72E11
      ETD = 20000.0/1.987
      FKFPO = 9.0E5
      EFP = 9000.0/1.987
C
C     REACTION RATES
C
      TEMP=TO*Y(7)
      FKP=FKPO*EXP(-EP/TEMP)
      FKD=FKDO*EXP(-ED/TEMP)
      FKTC=FKTCO*EXP(-ETC/TEMP)
      FKTD=FTDO*EXP(-ETD/TEMP)
      FKT=FKTC+FKTD
      FKFP=FKFPO*EXP(-EFP/TEMP)
C
C     DIFFERENTIAL EQUATIONS
      OMEGA=2.0*F*FKD*CIO*(1.0-Y(2))
      YPRIME(1)=FKP*(1.0-Y(1))*Y(3)*REST
      YPRIME(2)=2.0*FKD*(1.0-Y(2))*REST
      YPRIME(3)=(OMEGA-FKT*Y(3)*Y(3))*REST
      YPRIME(4)=(OMEGA+FKP*CMO*(1.0-Y(1))*Y(3)
     & -FKT*Y(3)*Y(4)-FKFP*(CMO*Y(1)*Y(4)-Y(3)*(Y(6)+Y(1)*CMO)))
     & *REST
      YPRIME(5)=(OMEGA-0.5*FKTC*Y(3)*Y(3))*REST
      YPRIME(6)=(2.0*FKP*CMO*(1.0-Y(1))*Y(4)+FKTC*Y(4)*Y(4))*REST
      YPRIME(7)=-HR*YPRIME(1)*CMO/(RHOF*CP*TO)
     & -4.0*U*REST/(RHOF*CP*D*1000.)*(Y(7)-TJ/TO)
      RETURN
      END
```